The Development of Snow Multi-Bands in High-Resolution Idealized Baroclinic Wave Simulations

Nicholas Leonardo and Brian A. Colle

Acknowledgment: Phillip Yeh (grad student)

[1]School of Marine and Atmospheric Sciences, Stony Brook Univ.

27 February 2024

The Challenge of Snowbands in Winter Storms

- Bands make Quantitative Precipitation Forecasts (QPF) difficult
  - Localized heavy precipitation
  - Extreme gradients
  - Evolution

12 Feb 2006

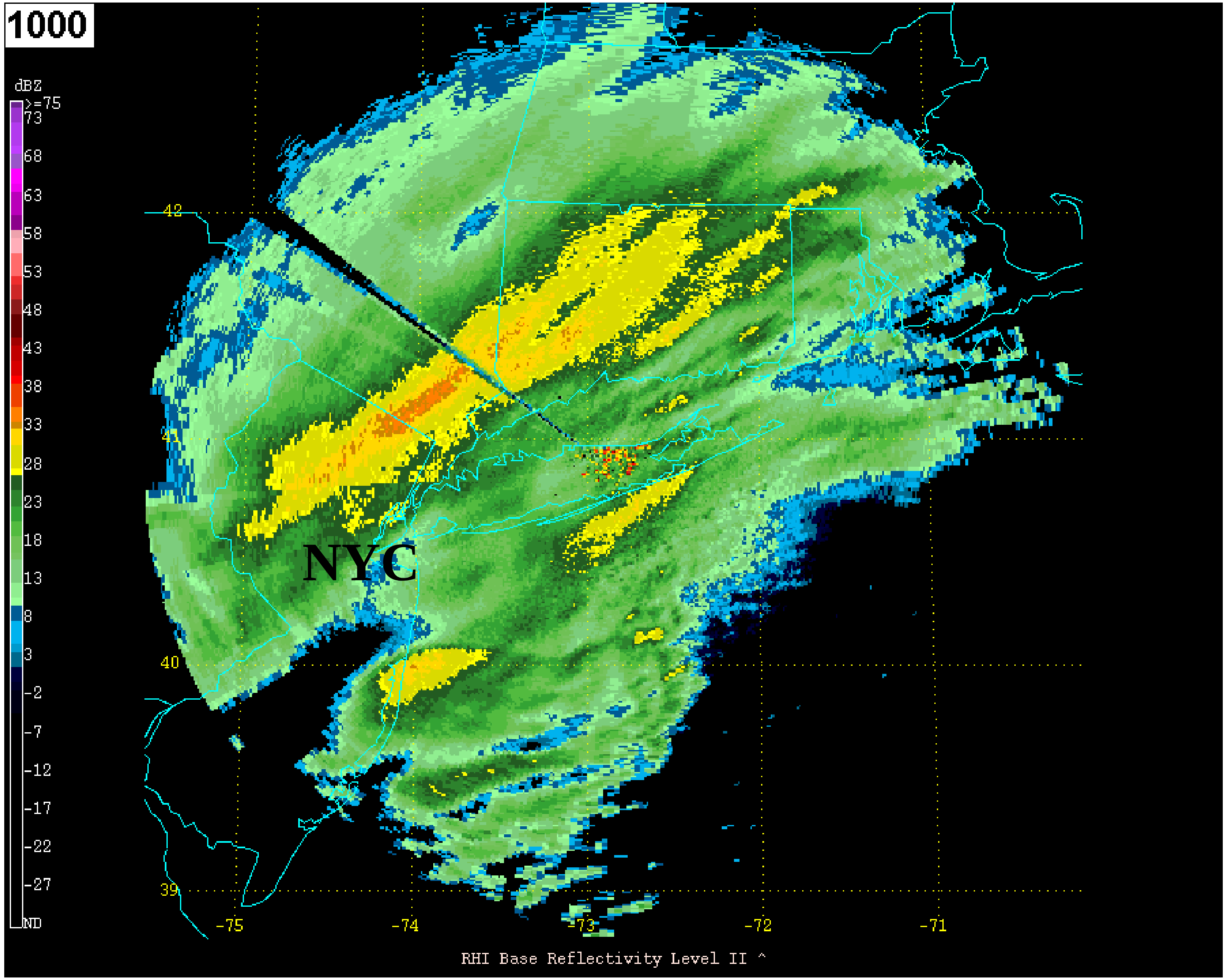

Conceptual Model for "Primary" Band

Plan-view

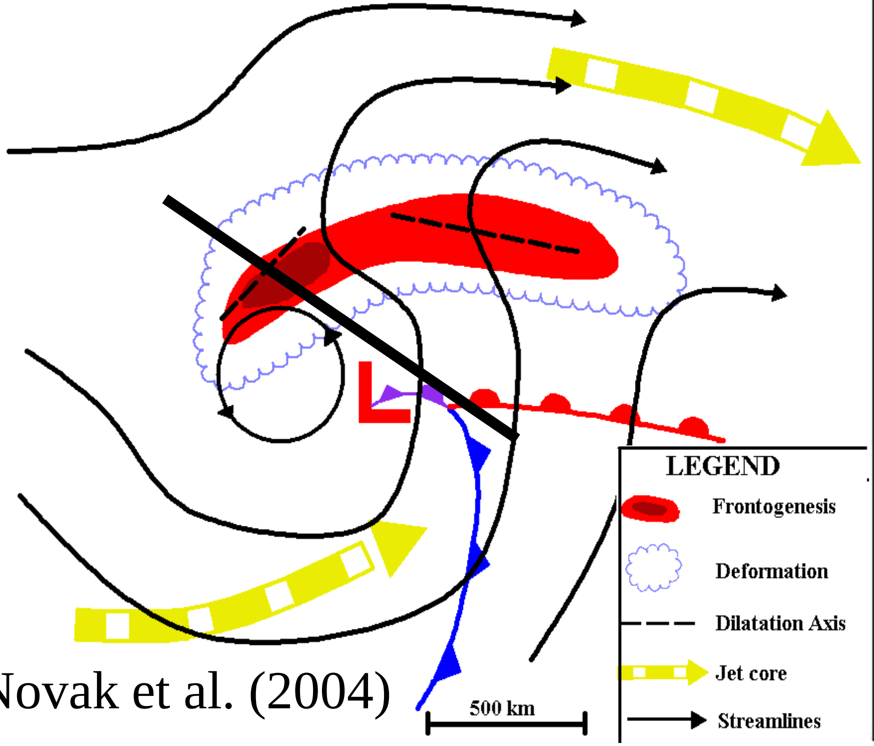

Novak et al. (2004)

Cross Section

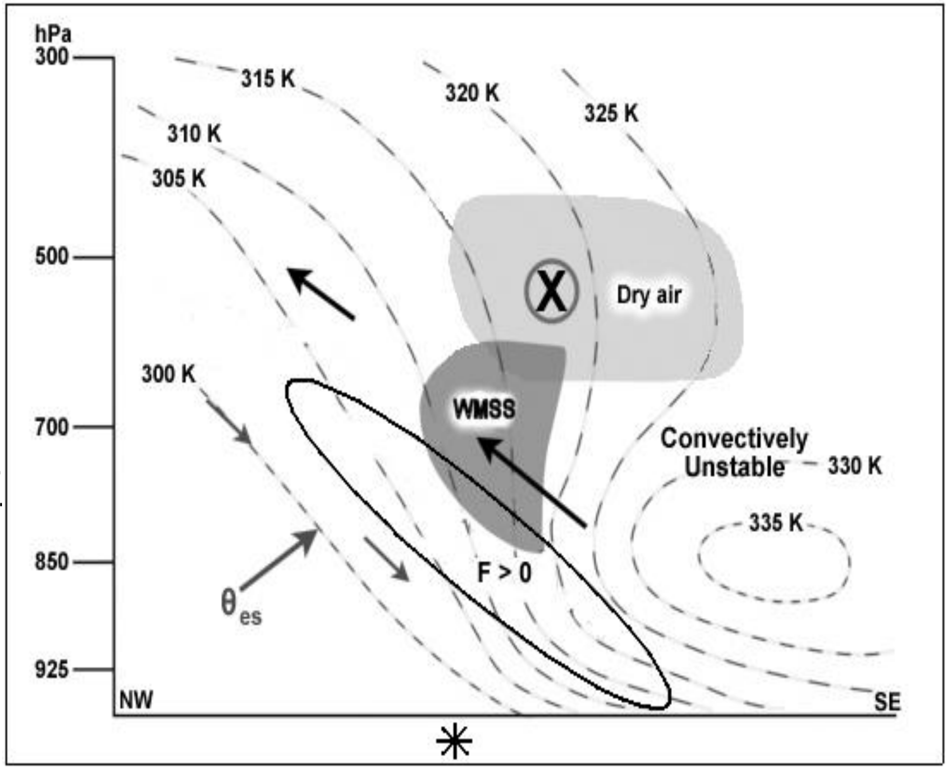

Novak et al. (2006)
(adapted from Moore et al. 2005)

Frontogenesis in the presence of weak moist symmetric stability and sufficient moisture

Band Ingredients and Transition to Multi-Bands

Lift – Frontogenesis

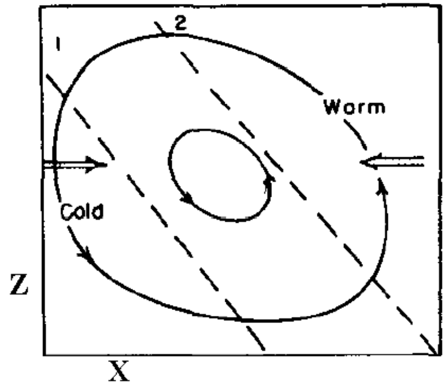

Sanders and Bosart (1985)

Instability – weak moist (conditional or potential) symmetric stability

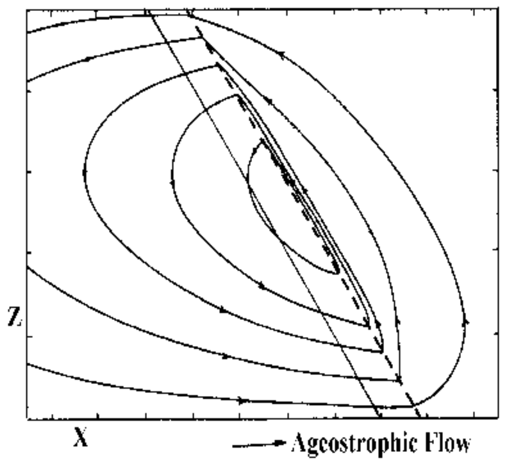

Emanuel (1985)

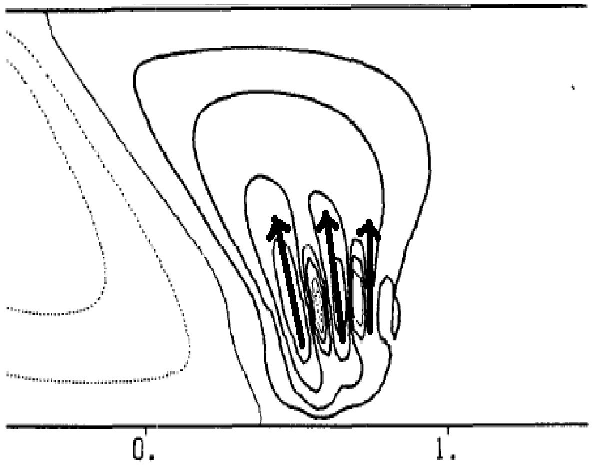

Xu (1992)

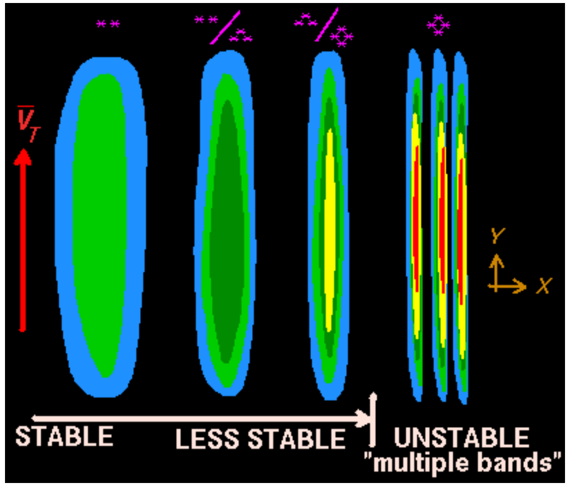

Courtesy Peter Banacos (BTV)

Moisture

Many Smaller-Bands Have Weak or No Frontogenesis

700-800 hPa Frontogenesis vs Instability (neg MPV*)

Ganetis et al. (2018)

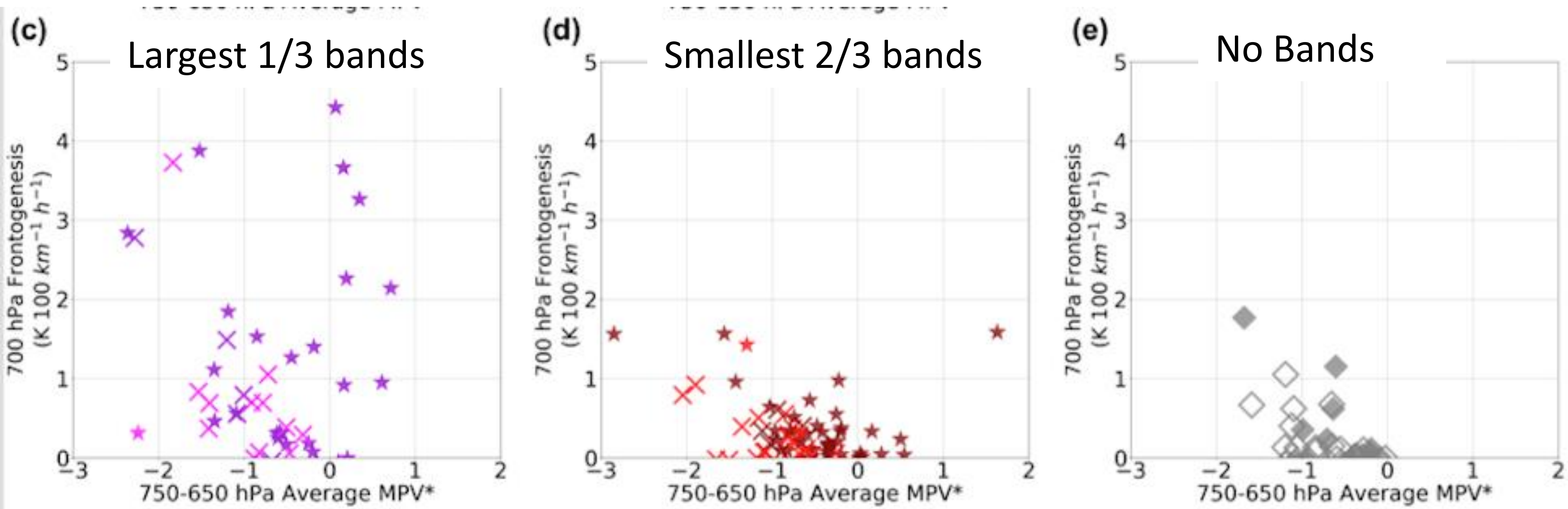

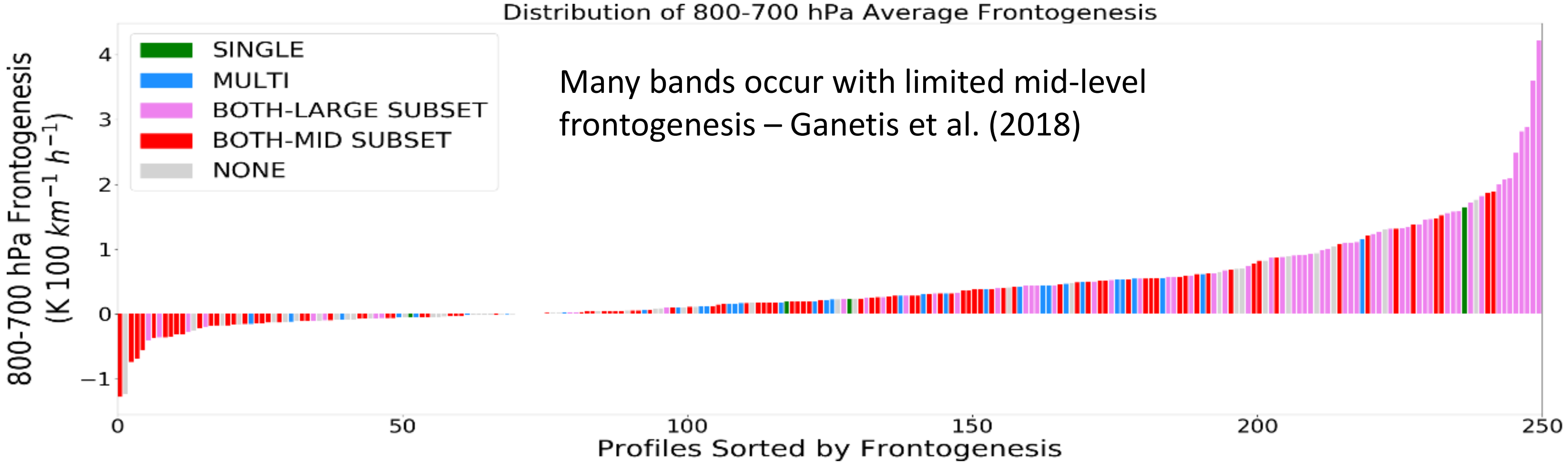

Importance of Vertical Shear for Multi-bands?

TABLE 3. Environmental banding ingredients for each classification type.

	700-hPa frontogenesis [K $(100\,km)^{-1}\,h^{-1}$]	700-hPa MPV* (PVU)	750–650-hPa dT/dP ($\times10^{-4}$ °C Pa^{-1})	750–650-hPa $d\theta_e^*/dP$ ($\times10^{-4}$ K Pa^{-1})	950–750-hPa wind speed difference ($m\,s^{-1}$)
SINGLE	0.90	−0.77	−4.98	4.84	3.71
MULTI	0.13	−0.53	−4.71	5.04	5.84
BOTH–Large bands	0.99	−0.75	−3.08	8.04	3.01
BOTH–Midsized bands	0.14	−0.54	−4.55	5.36	5.67
NONE	0.12	−0.63	−4.68	5.32	10.51

Ganetis et al. 2018

- Multibands & BOTH-Midsized were found to exist in weak frontogenesis
  - Frontogenesis is theorized origin of primary/single snowbands
- Enhanced vertical wind shear (hereafter referred to as “shear”) was observed to exist in environments with multibands & BOTH-Midsized

Other Possible Mechanisms? "Snowbands" with Elevated Cells and Fallout; Organization from Vertical Shear and Deformation?

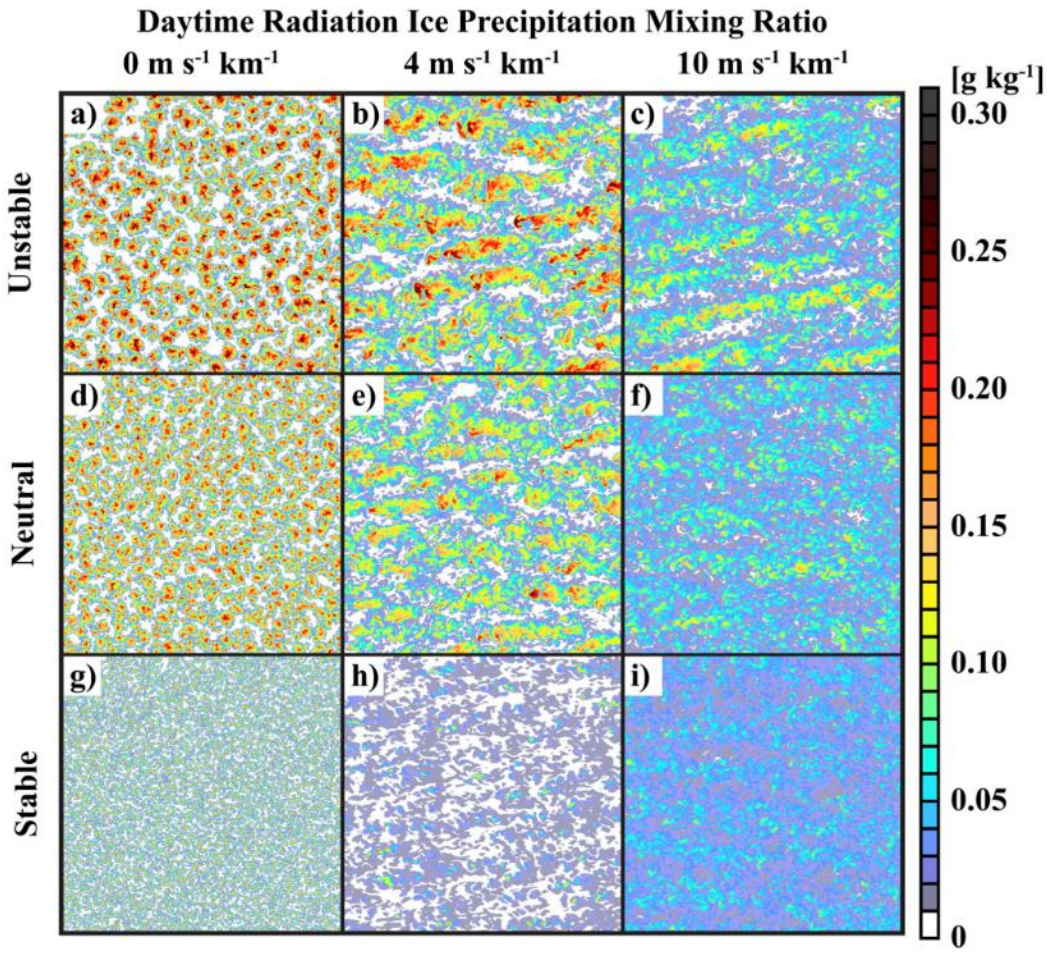

FIG. 13. As in Fig. 9, but for the daytime radiation simulations.

Keeler et al. 2017

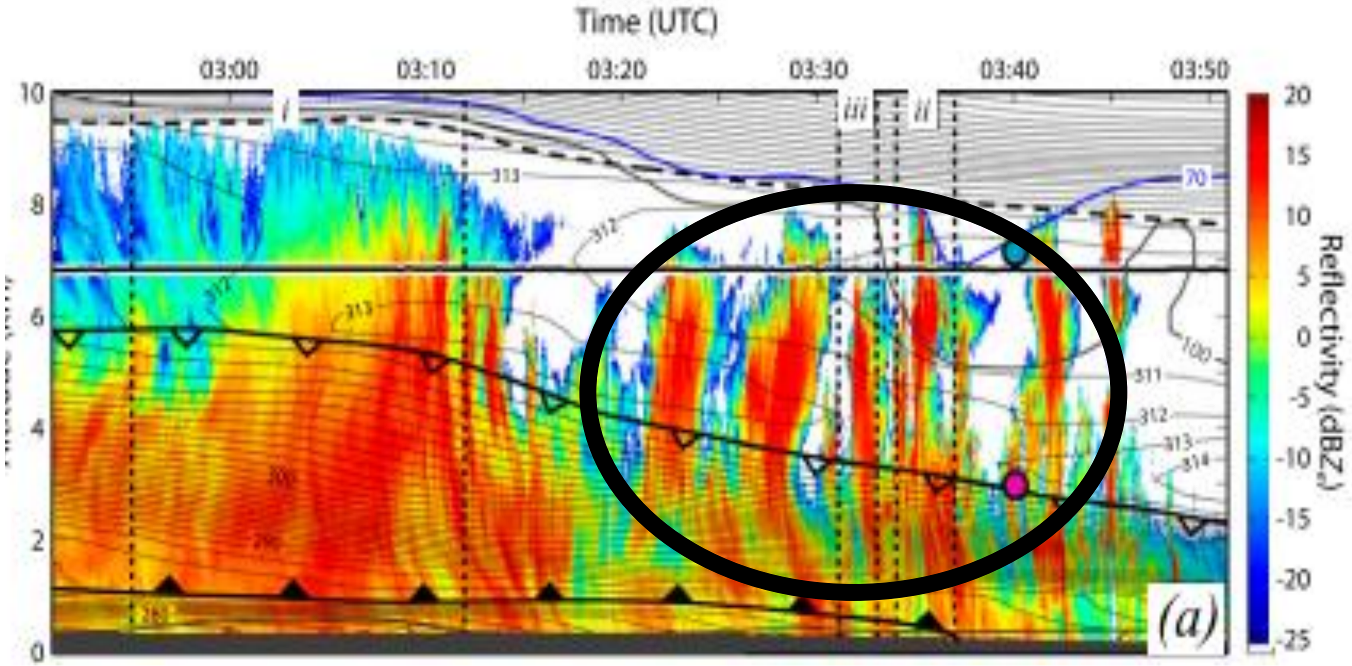

Rosenow et al. 2014; Keeler et al. 2016

17 Feb 2022

Band Evolution

- Precipitation structures become band-like over time
- Sloping region of frontogenesis (purple contours)
- Cloud-top instability
- 2-km WRF section: possible fallout from generating cells

IMPACTS Case: 1930~2330 UTC 17 Feb

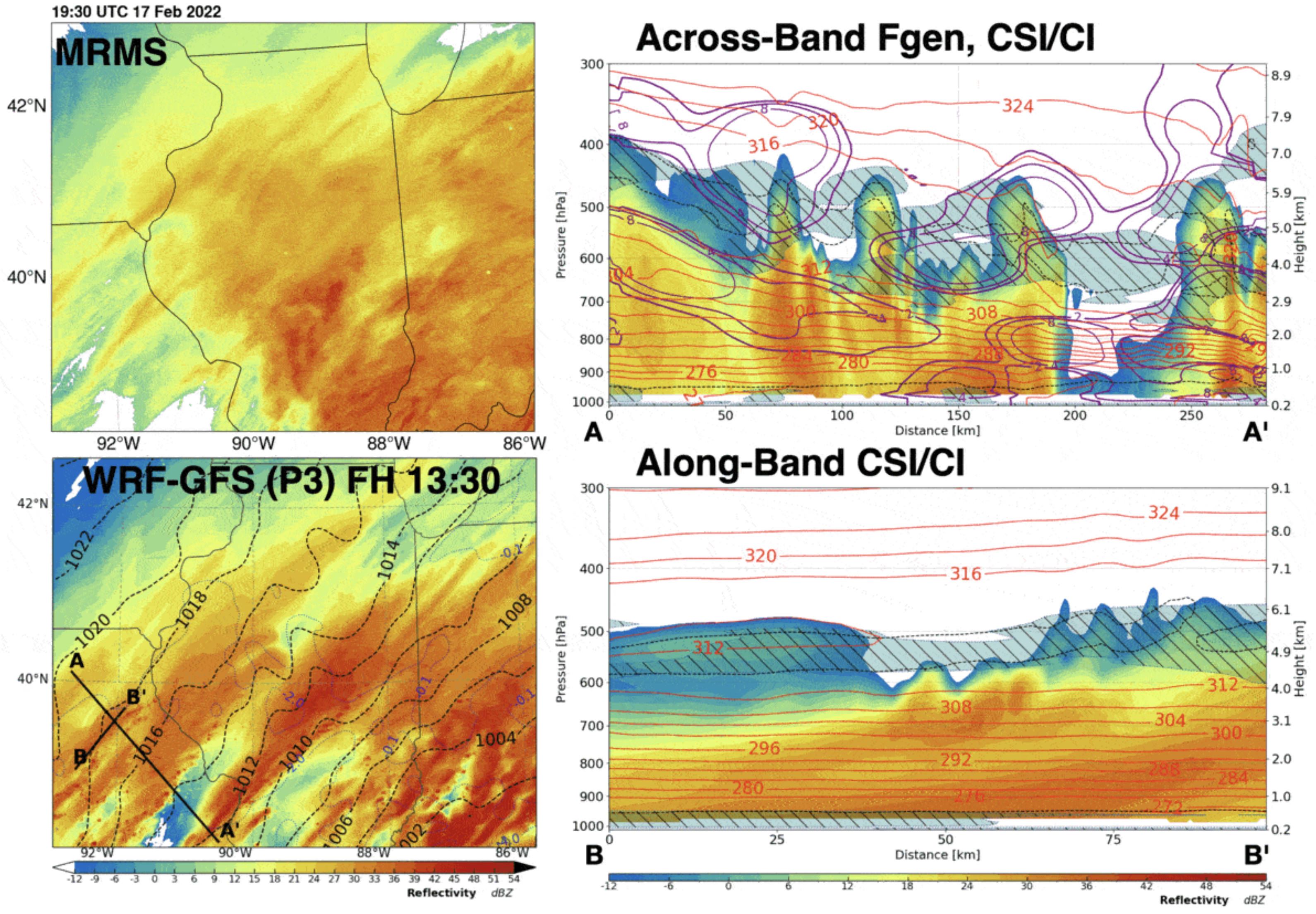

Predictability Challenges – Convective Resolving Models

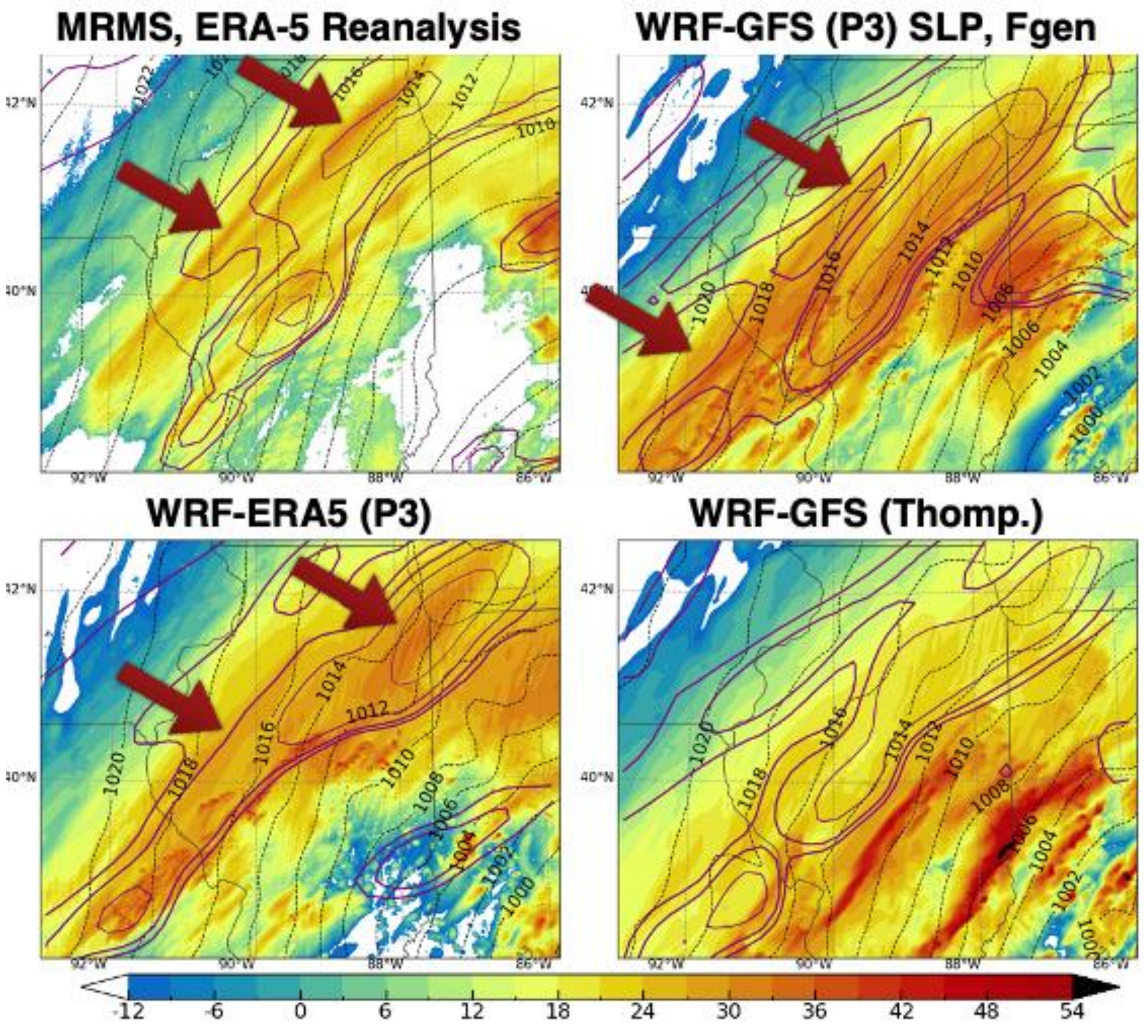

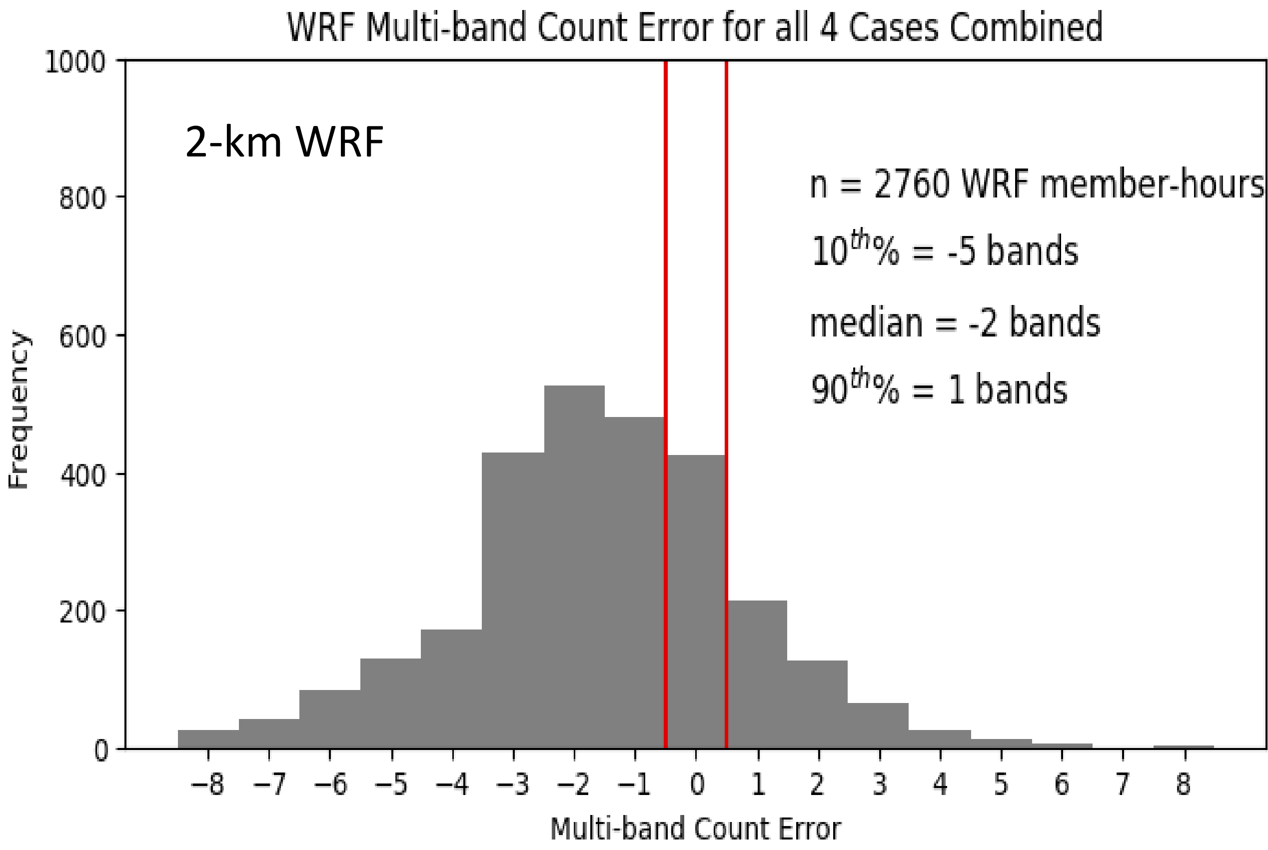

Connelly and Colle (2019 WAF)

More Convective-Plume Multi-bands Along Sloping Baroclinic Zone

1500 UTC 16 Jan 2022

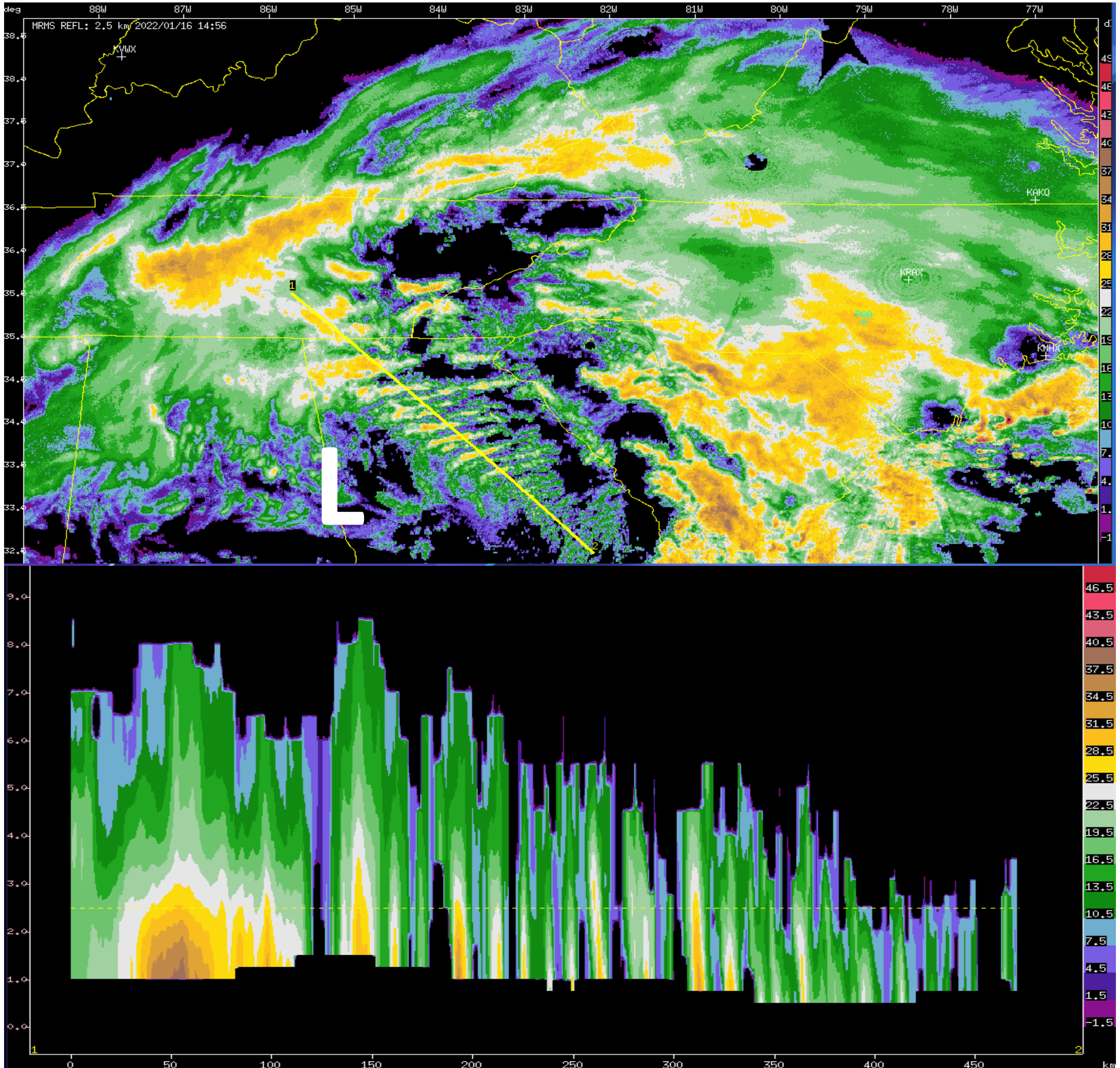

Multi-bands and PV Dipoles

MRMS Composite Reflectivity

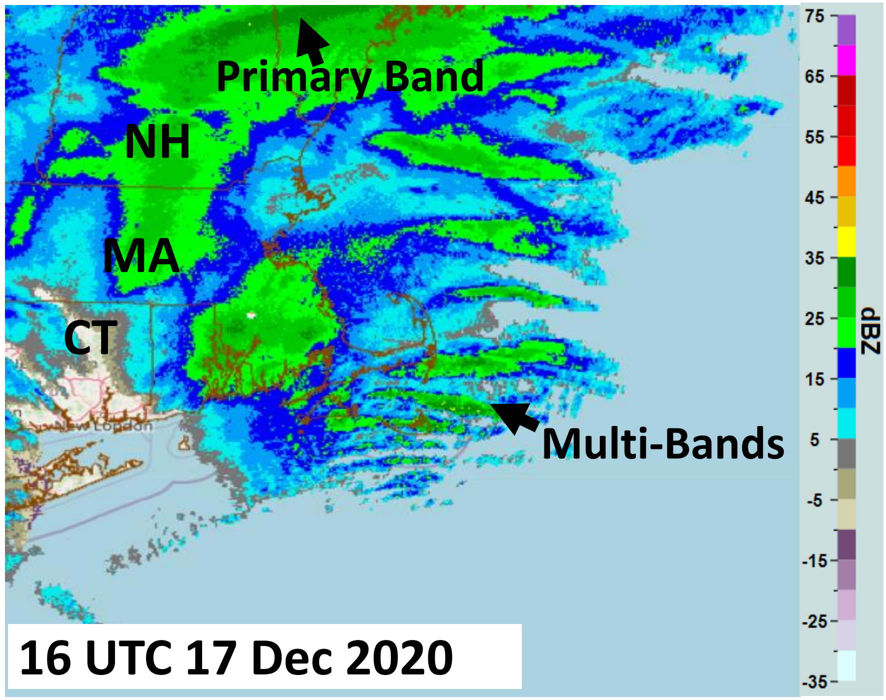

2-km WRF 800-hPa Reflect. (shade), 700-hPa hgt. (black; dam) and θ (blue; K)

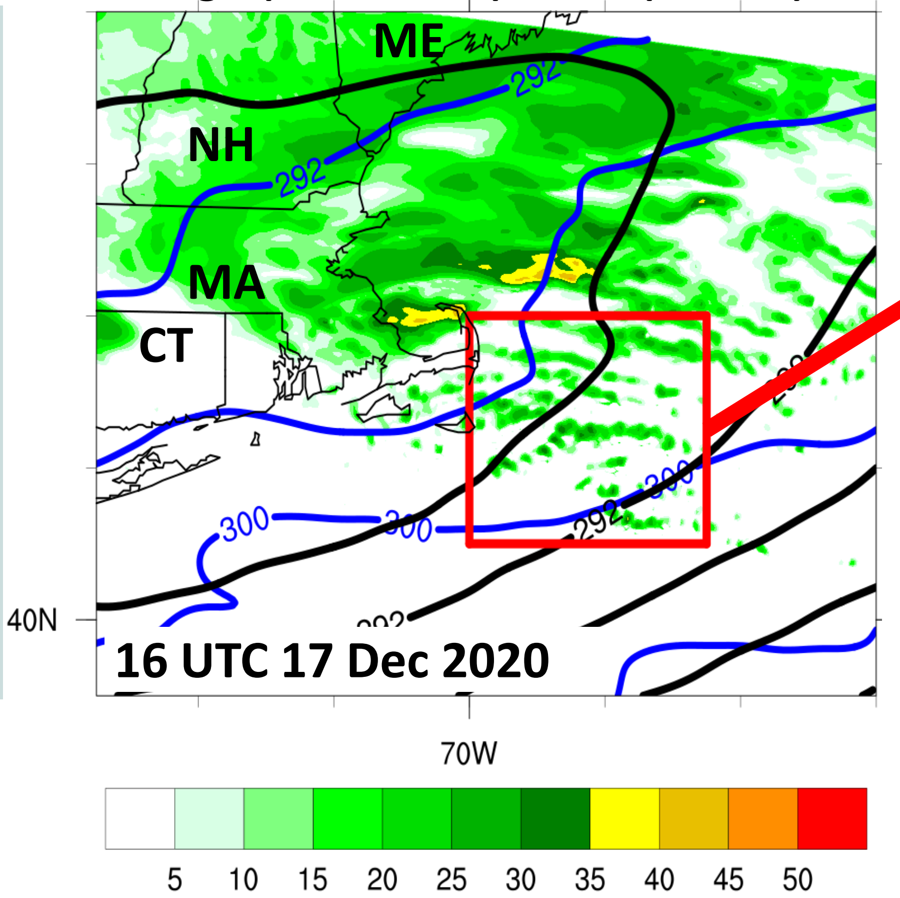

WRF 800-750-hPa PV (shade), w>0.5 m·s^{-1} (green), Wind Vectors

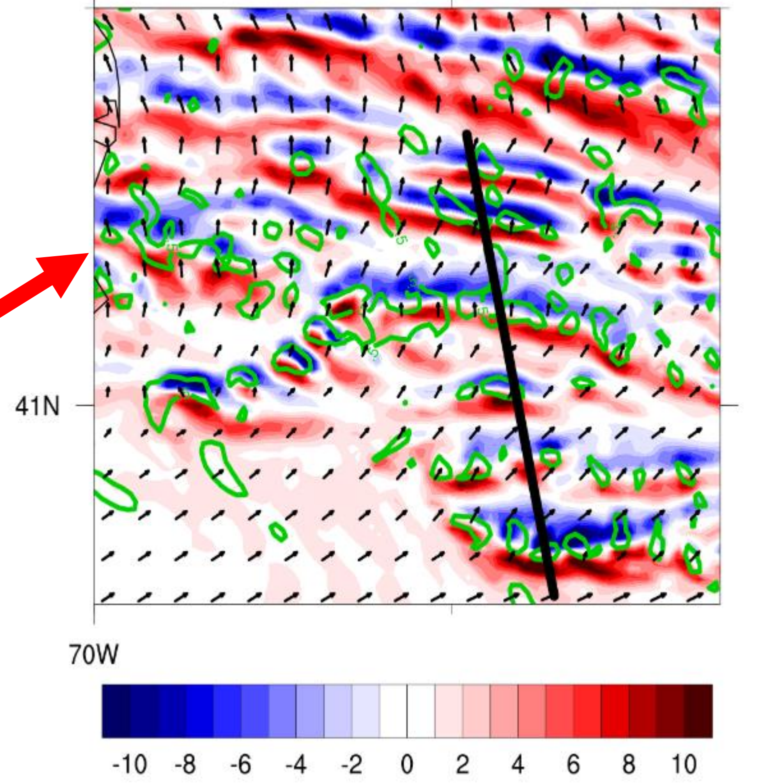

- Multi-bands in some cases are accompanied by PV dipoles
- Use idealized models to better isolate processes

Objectives

- Nested runs of an idealized baroclinic wave model are used to answer the following questions:
  1. How do the precipitation structures in the comma head evolve as the cyclone develops?
  2. How do changes in the ambient frontogenesis (forcing), vertical shear, and instability around the cyclone relate to changes in the precipitation structures.
  3. What mechanisms cause the bands to elongate and persist?
  4. How sensitive is the development of the multi-bands to small changes in the initial conditions?

Idealized Baroclinic Wave Model Setup

700-hPa Snow, 500-hPa Heights, and SLP of the 100-km Grid

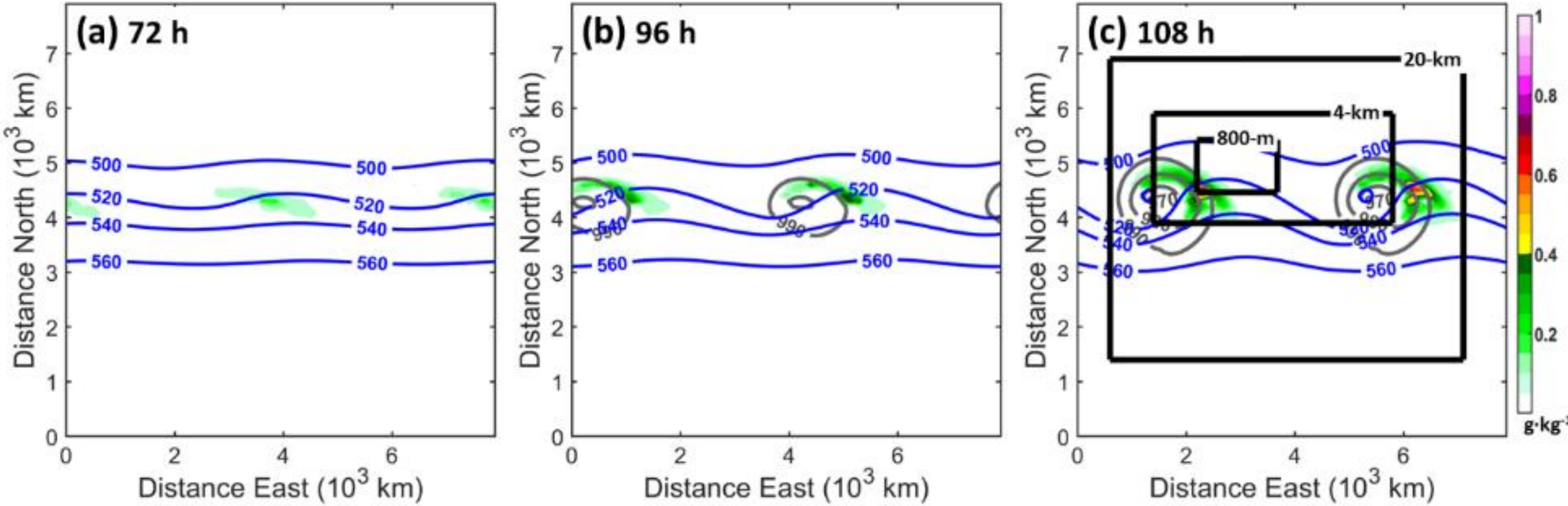

- Ran the baroclinic wave test case of WRF v3.4.1. Used physics consistent with Norris et al. 2014 and 2017: Thompson microphysics, YSU PBL, and Kain-Fritsch convection.
- 20-km and 4-km nests added at 108 h (panel c).
- 800-m added between 114 h and 132 h to capture the peak in band activity. There are similarities between the 4-km and 800-m, such that the 4-km will primarily be shown.

Idealized Band Activity and Evolution: Band Structures

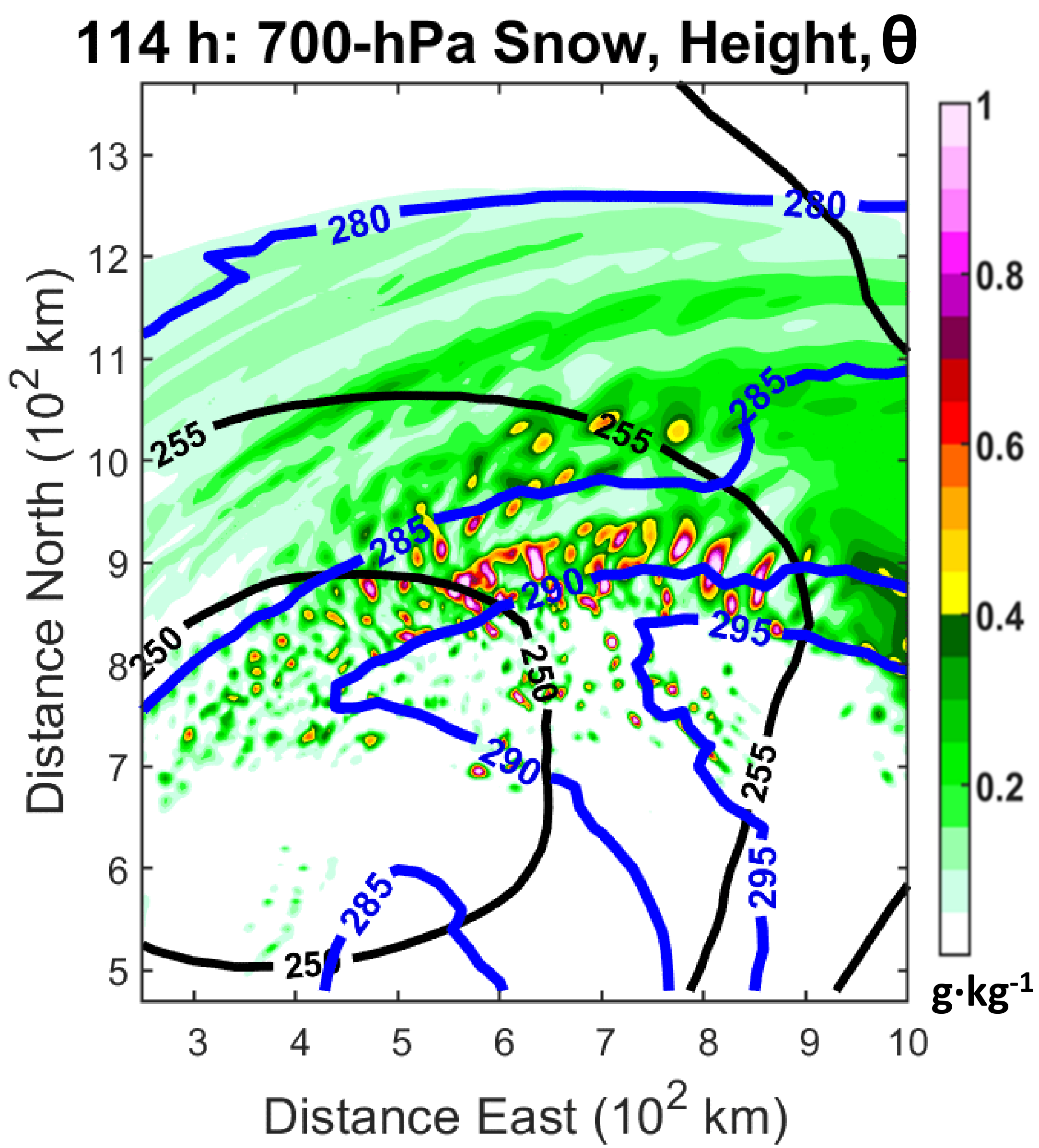

Idealized Band Activity and Evolution: Band Structures

Pre-genesis Stage: 114 h

700-hPa Snow, Heights, and θ

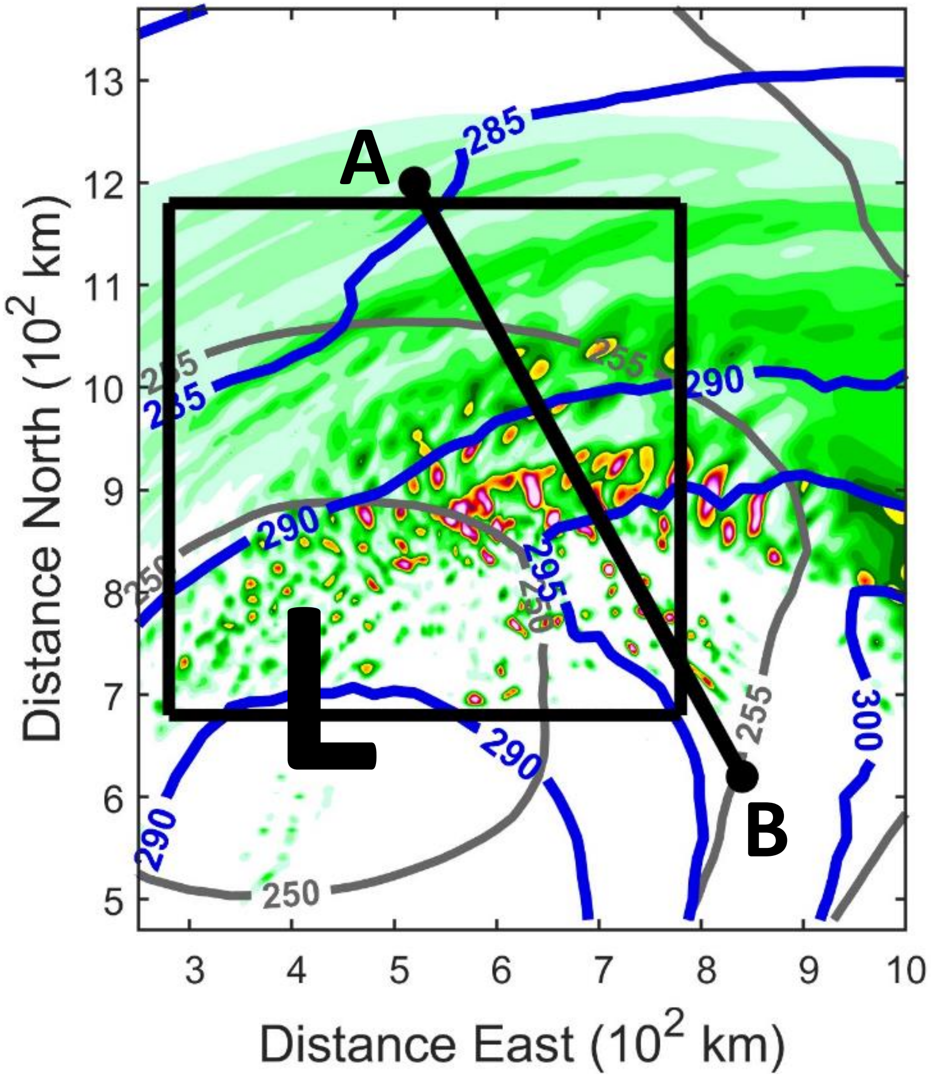

Cross-section Snow, θ, and Circulation Vectors

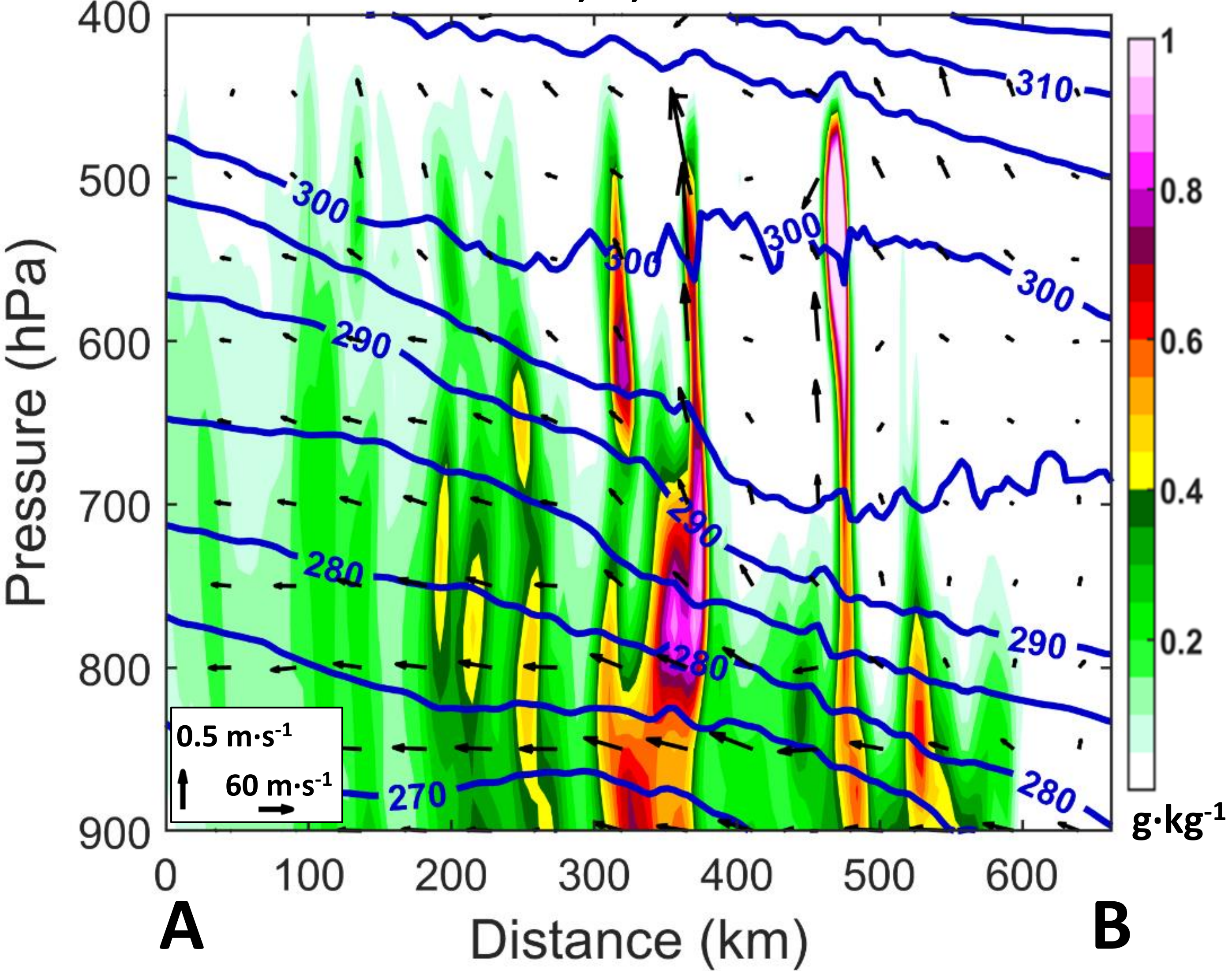

Idealized Band Activity and Evolution: Band Structures

Genesis Stage: 120 h

700-hPa Snow, Heights, and θ

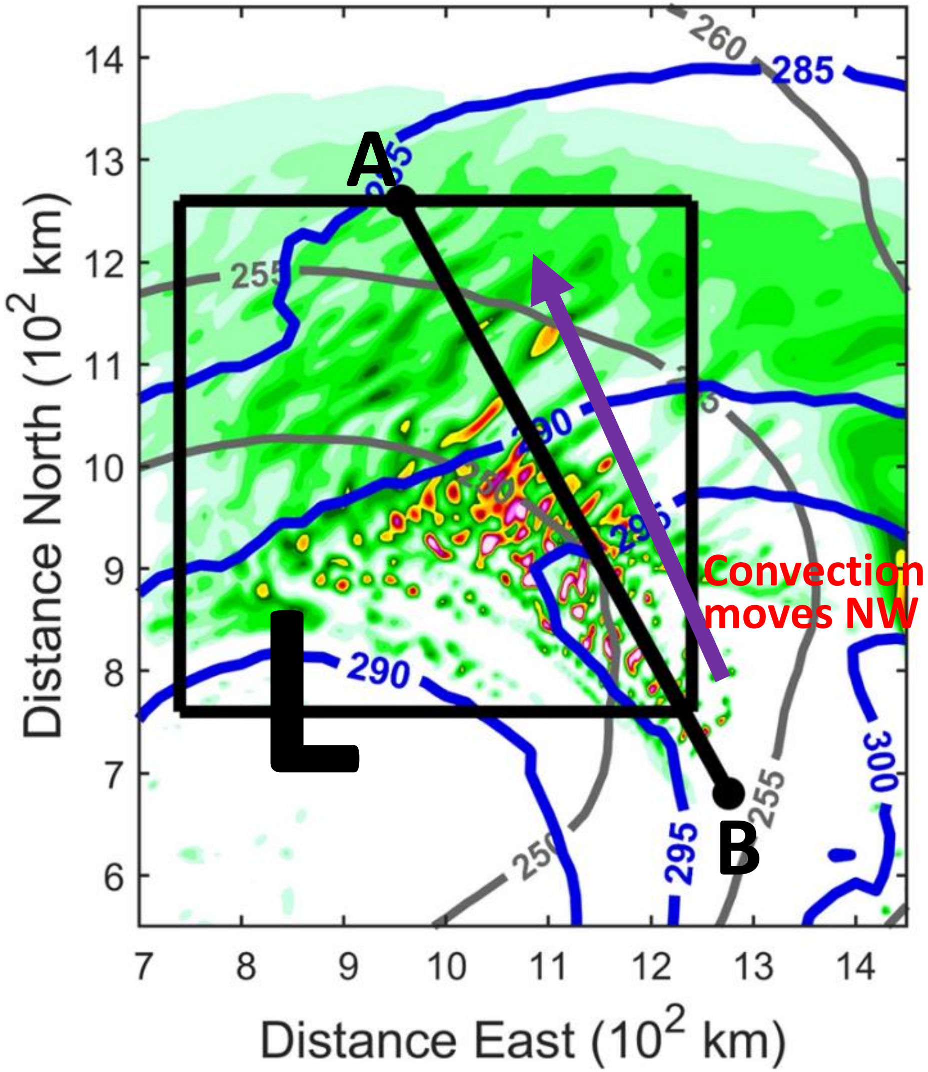

Cross-section Snow, θ, and Circulation Vectors

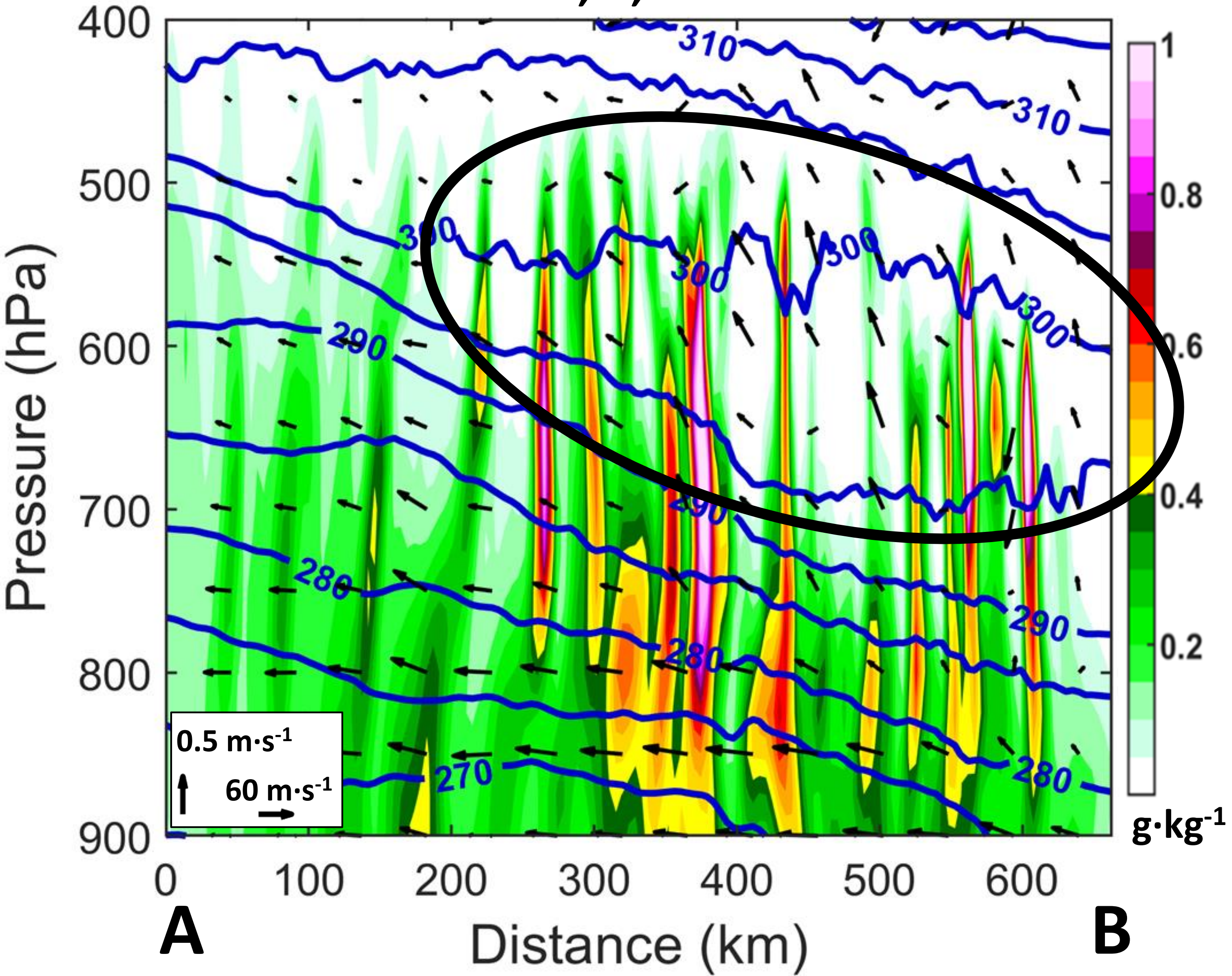

Idealized Band Activity and Evolution: Band Structures

Mature Stage: 129 h

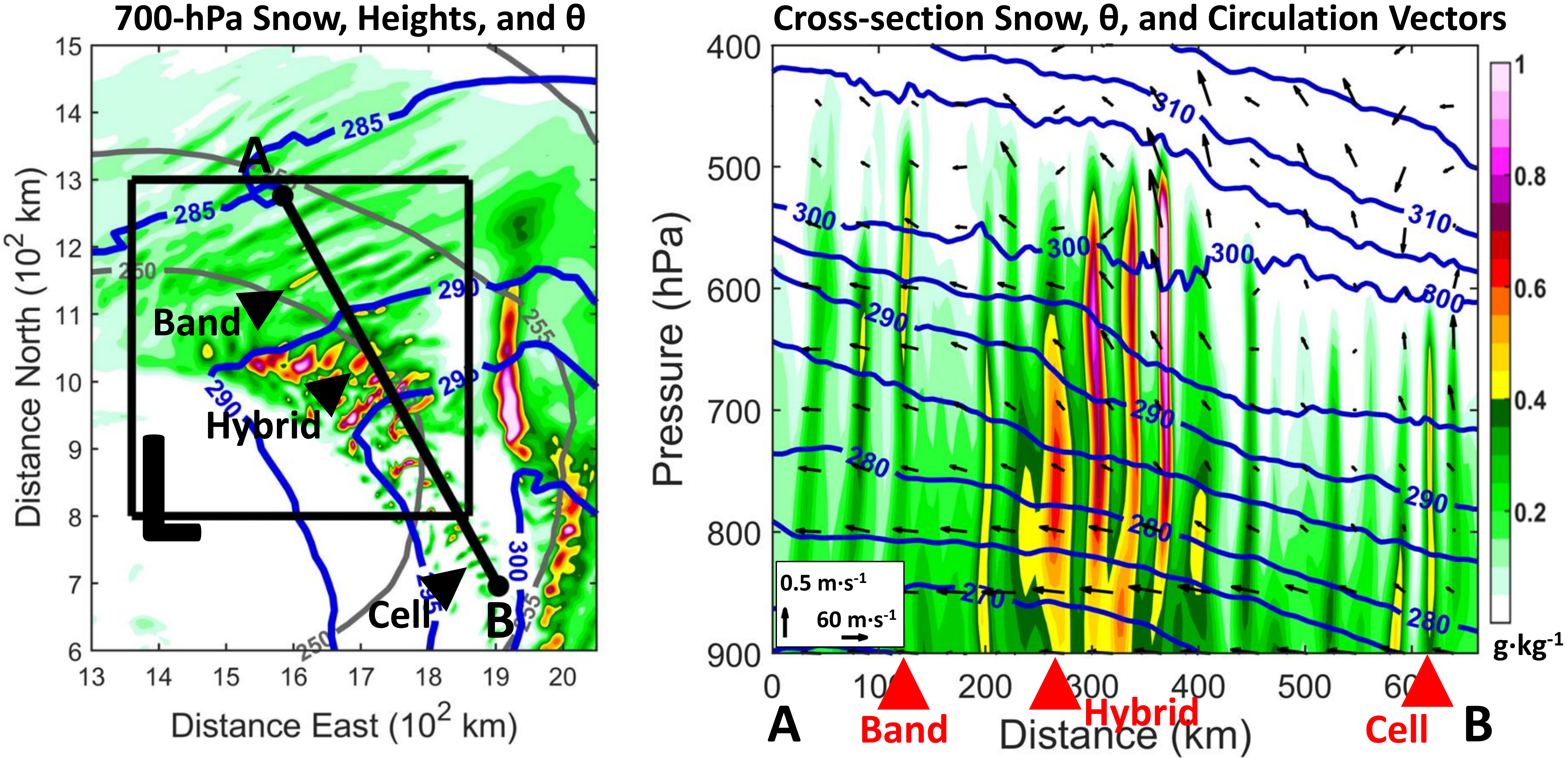

Idealized Band Activity and Evolution: Band Structures

Decay Stage: 138 h

700-hPa Snow, Heights, and θ

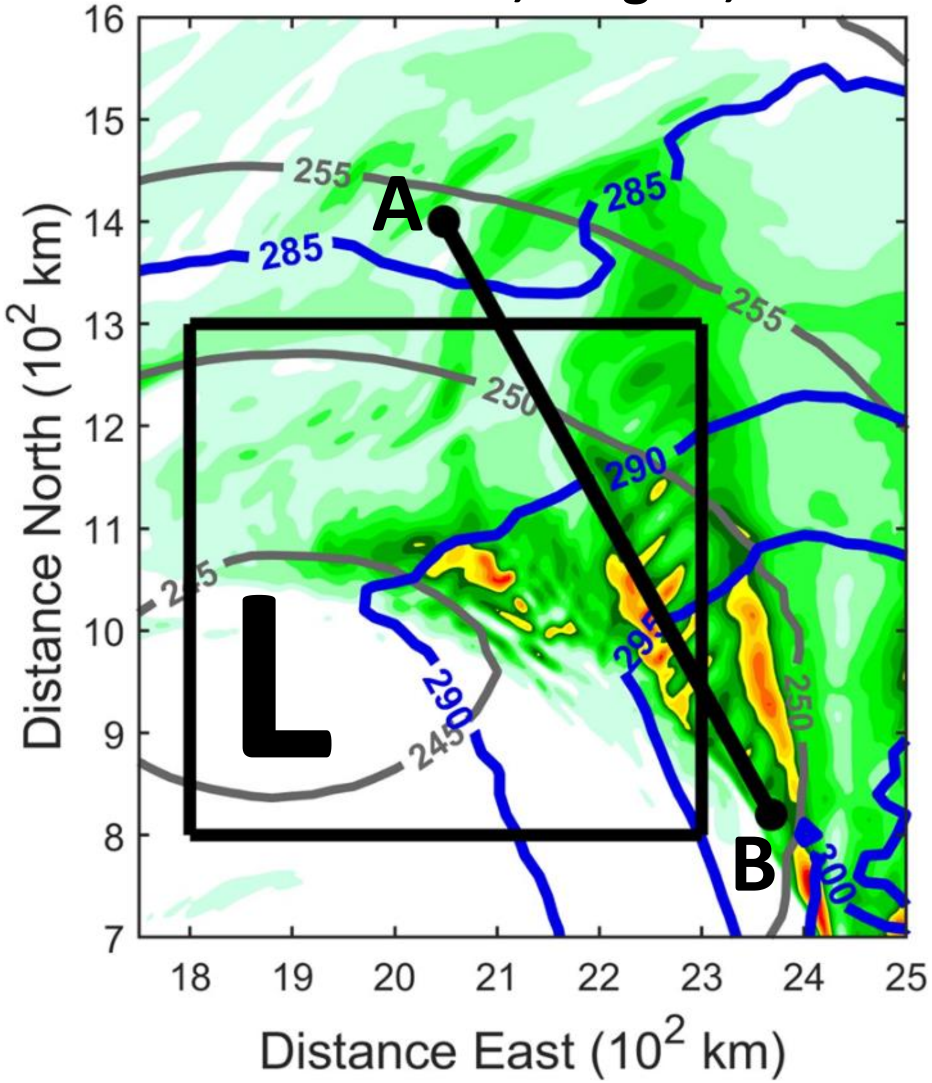

Cross-section Snow, θ, and Circulation Vectors

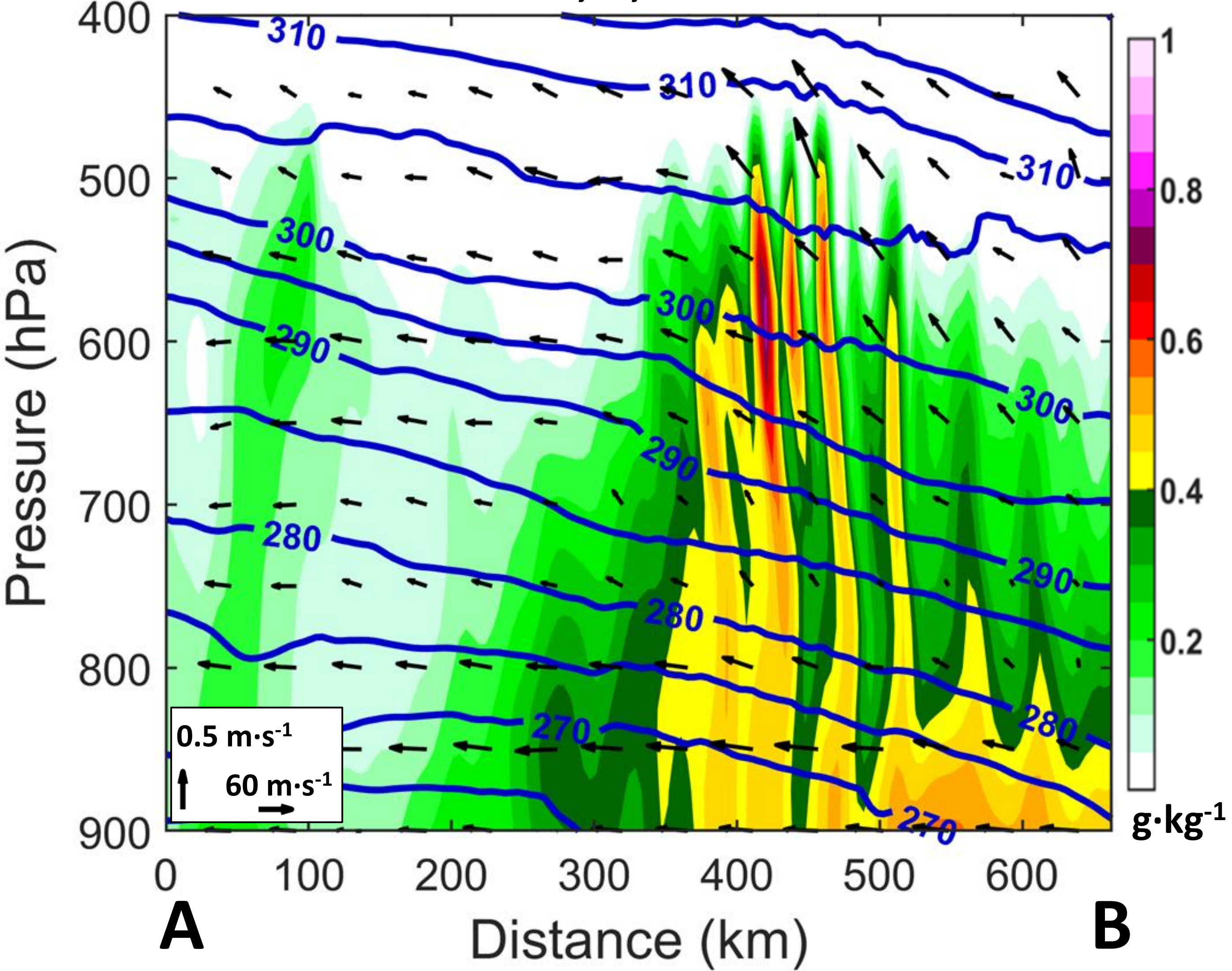

Evolution of Large-Scale Environment and Forcing

Leonardo and Colle (MWR in press 2024)

Evolution of Large-Scale Environment and Forcing

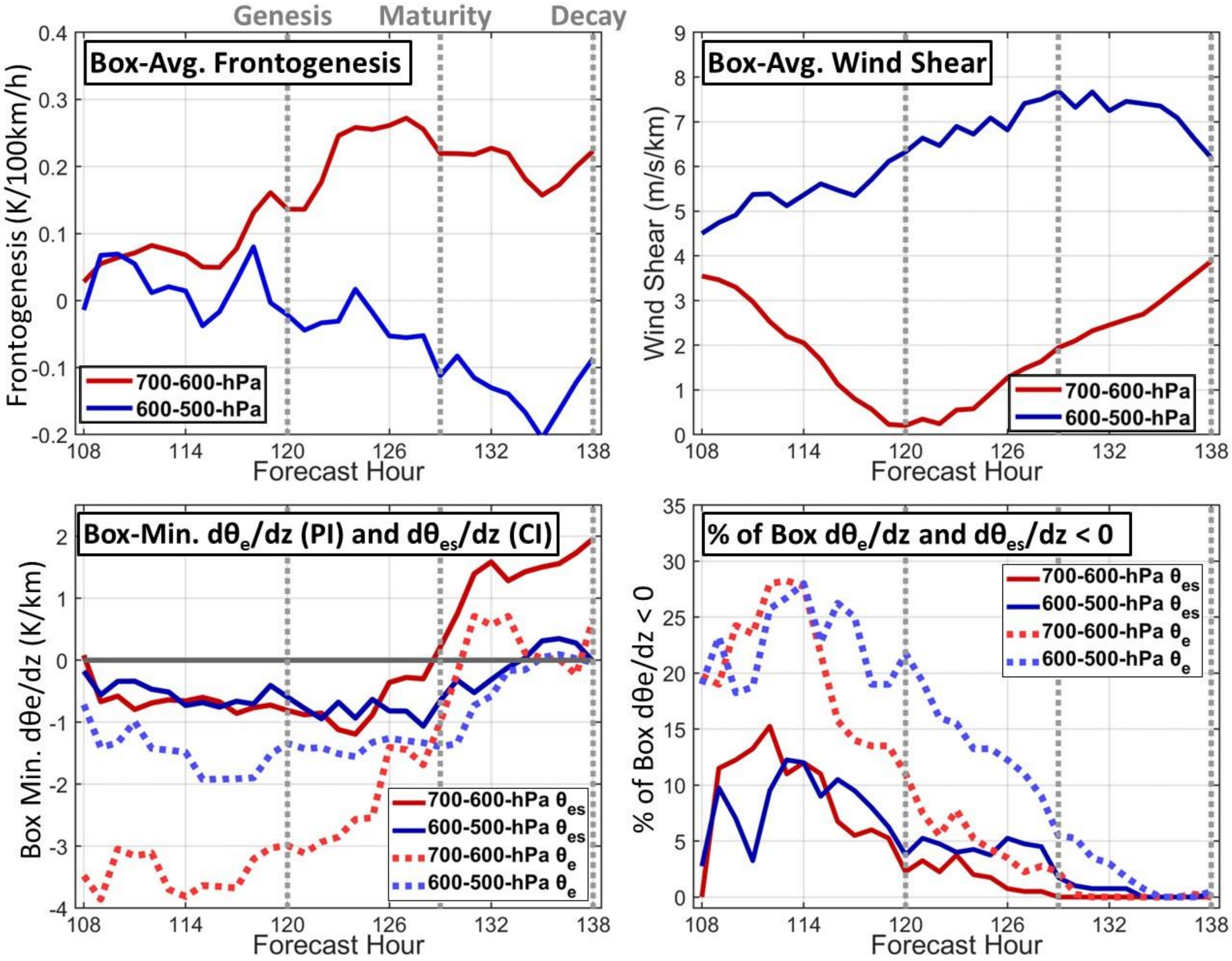

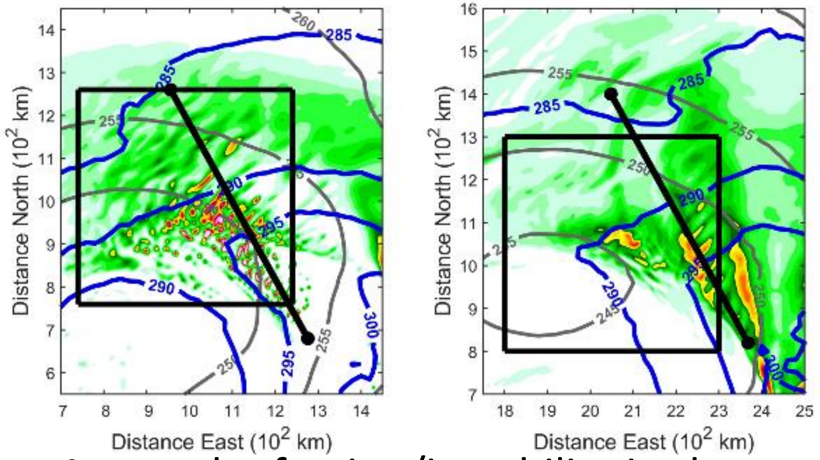

- Assess the forcing/instability in the 20-km grid. Took statistics within a box following the band activity.
- 700-600-mb fgen grows through genesis up to ~127 h.
- 600-500-mb SW (band-parallel) shear increases up to ~130 h.
- 600-500-hPa **potential instability (PI)** is largest 115-118 h, reaching 0 by 135-138 h during decay. Conditional instability (CI) is half of PI’s amplitude/extent.
- PI/CI grow due to differential advection, from drier air aloft wrapping in from behind the system.

Objectives

- Nested runs of an idealized baroclinic wave model are used to answer the following questions:
  1. How do the precipitation structures in the comma head evolve as the cyclone develops?
  2. How do changes in the ambient frontogenesis (forcing), vertical shear, and instability around the cyclone relate to changes in the precipitation structures.
  3. What mechanisms cause the bands to elongate and persist?
  4. How sensitive is the development of the multi-bands to small changes in the initial conditions?

Band Formation and Growth Via Generation of PV Dipoles and Resulting Circulation

Band Formation and Growth Via Generation of PV Dipoles and Resulting Circulation

- Tracked a cell that later grows into a SW-NE band as it moves around the NE flank of the low.
- An upper-level potential vorticity (PV) dipole extends NE of the cell, along which new convection develops afterwards.
- PV dipoles have been associated with the organization of warm convection (e.g., Chagnon and Gray 2009; Moon and Nolan 2015; Hitchman and Rowe 2019).

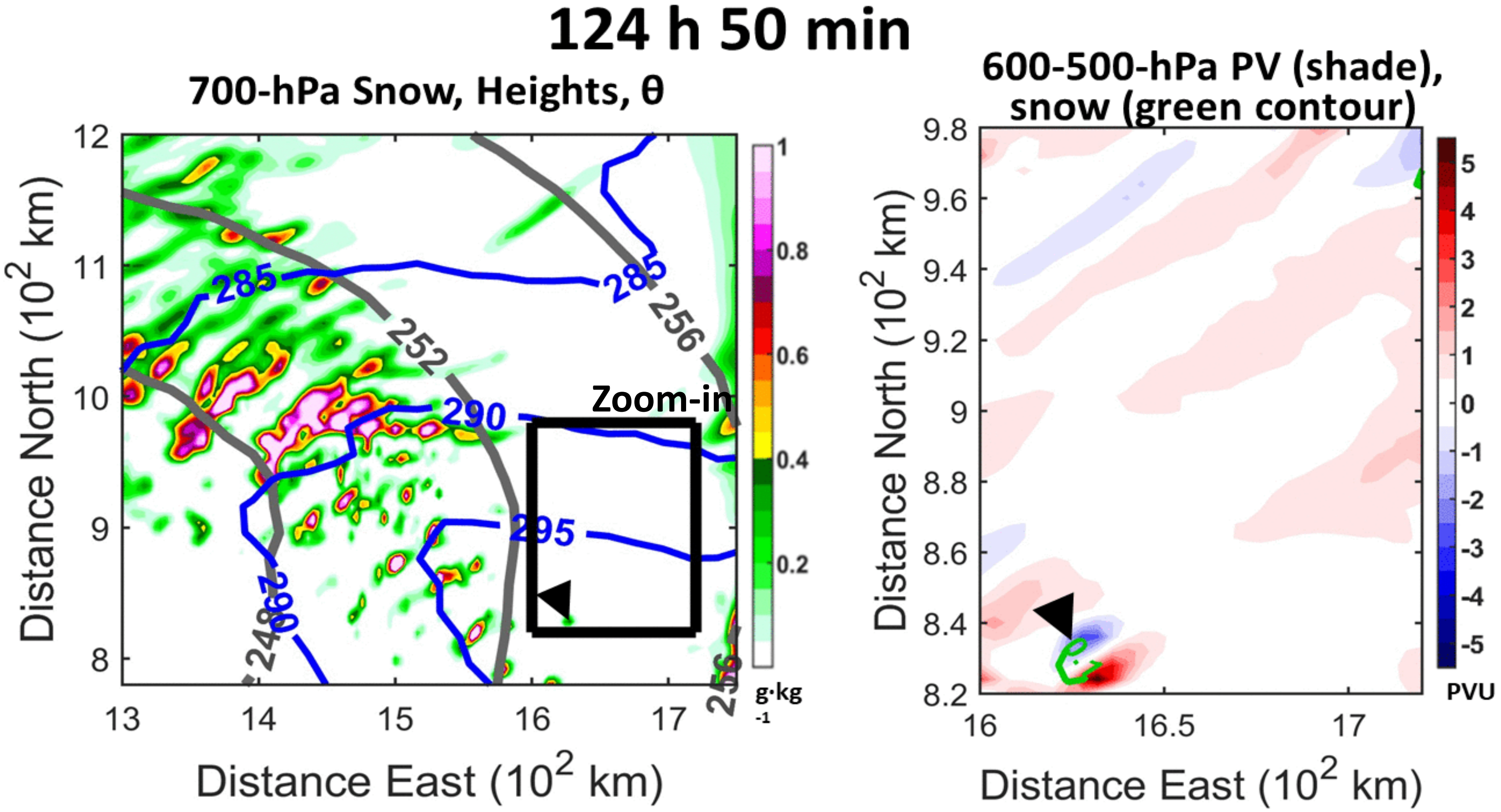

Band Formation and Growth Via Generation of PV Dipoles and Resulting Circulation

123 h 50 min

600-550-hPa PV (shade), Q_{SNOW} (green; g·kg^{-1})

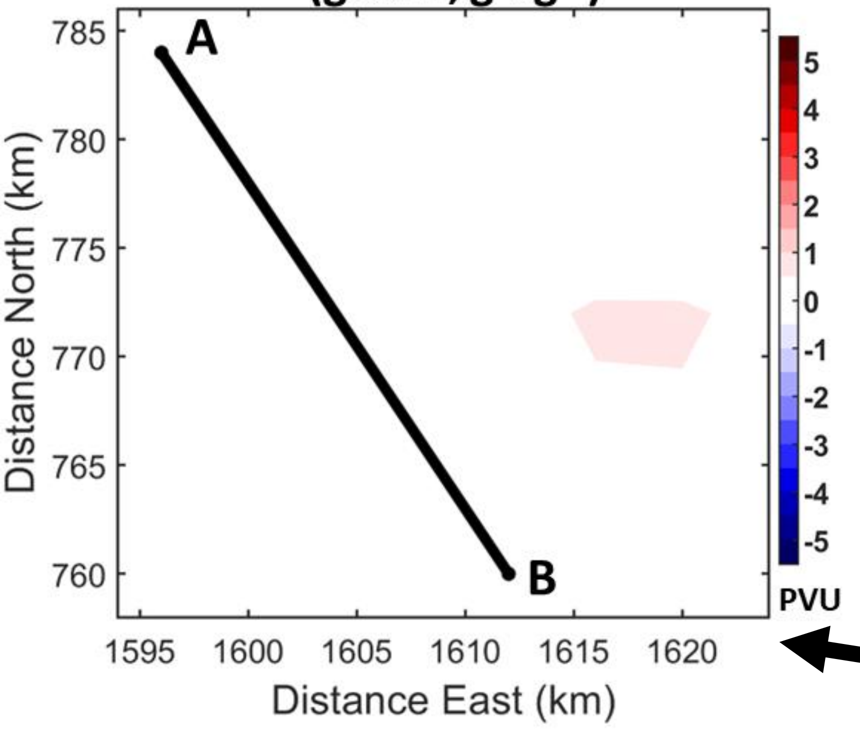

700-hPa Snow, Heights, θ

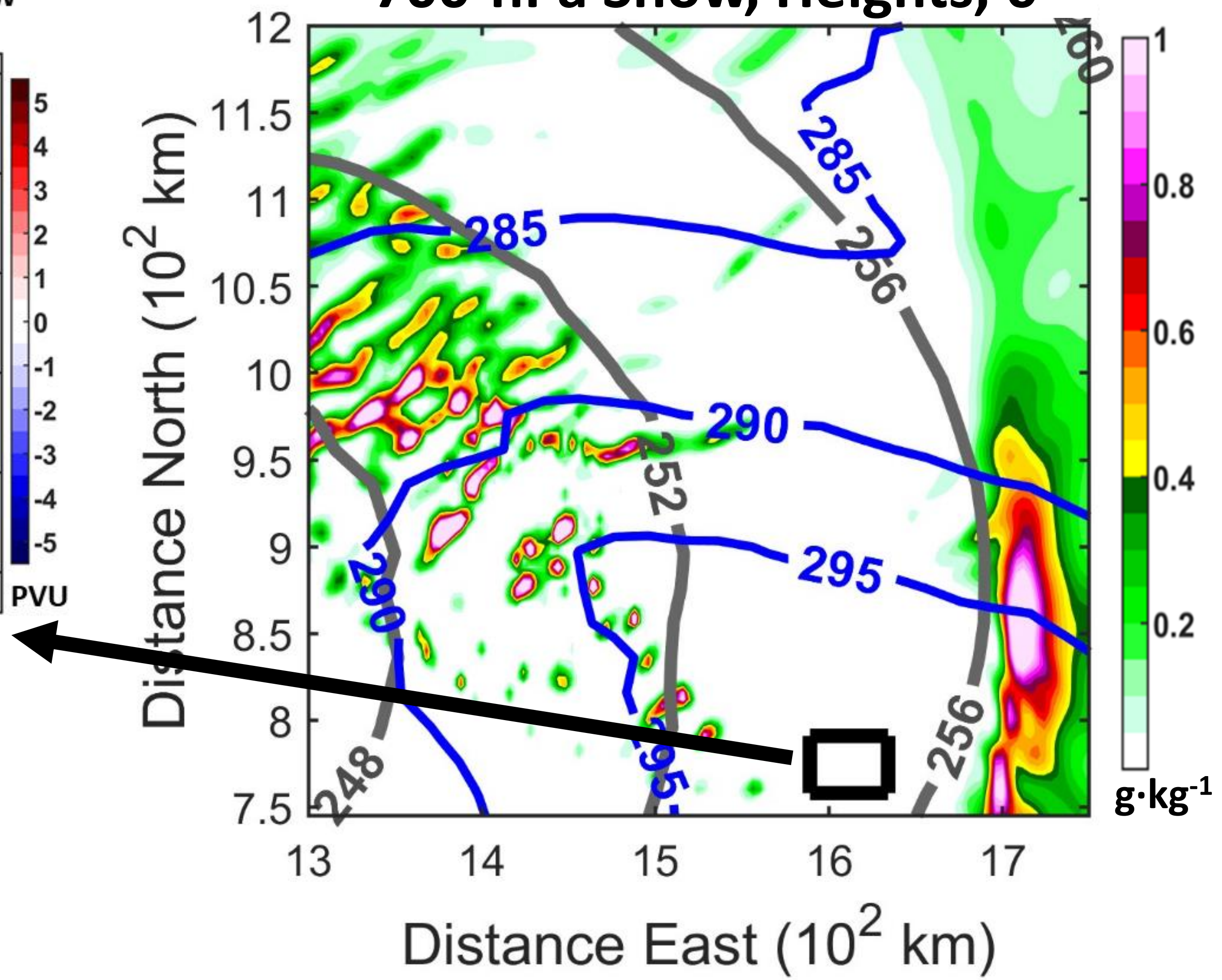

Band Formation and Growth Via Generation of PV Dipoles and Resulting Circulation

123 h 50 min

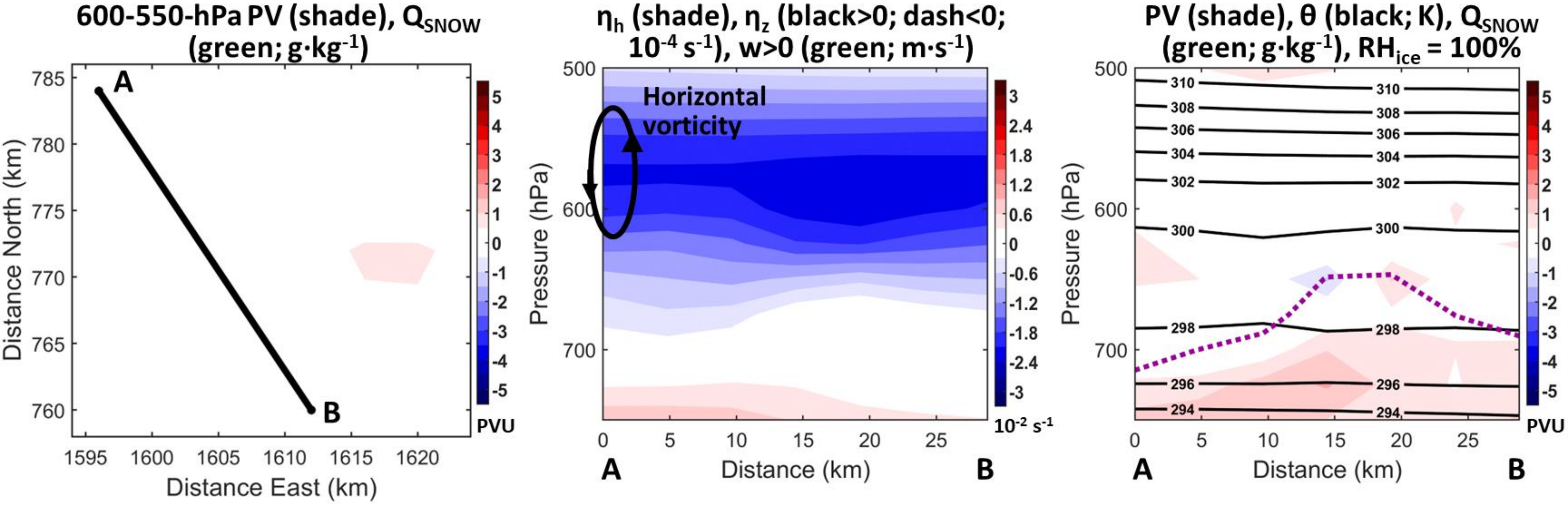

Band Formation and Growth Via Generation of PV Dipoles and Resulting Circulation

124 h 00 min

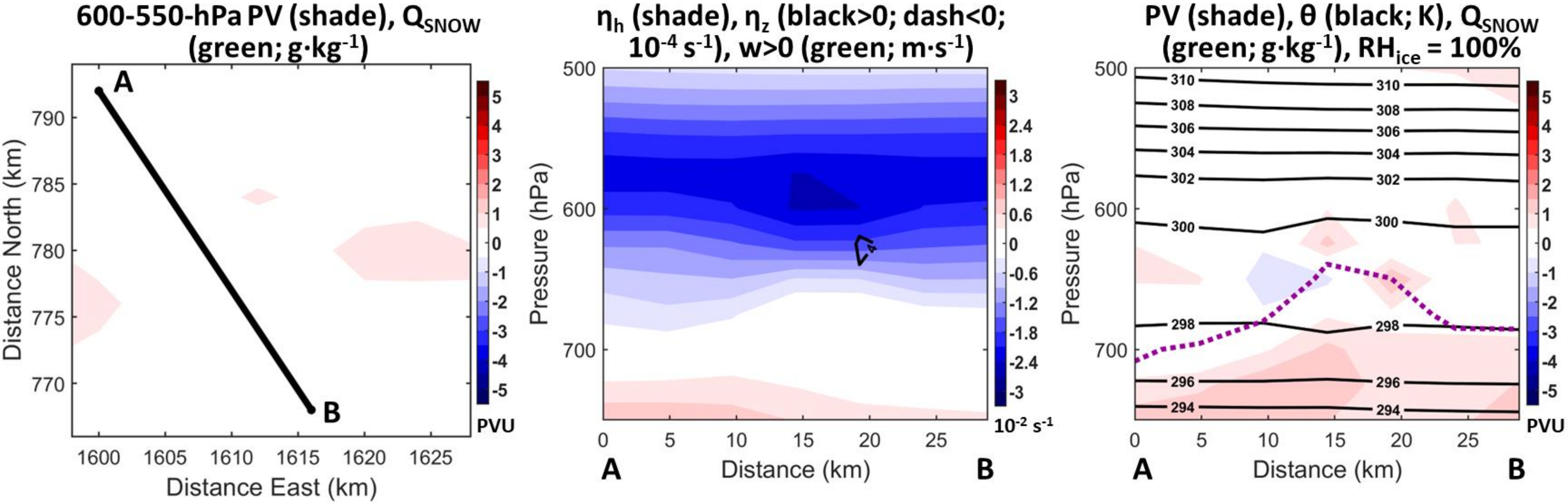

Band Formation and Growth Via Generation of PV Dipoles and Resulting Circulation

124 h 20 min

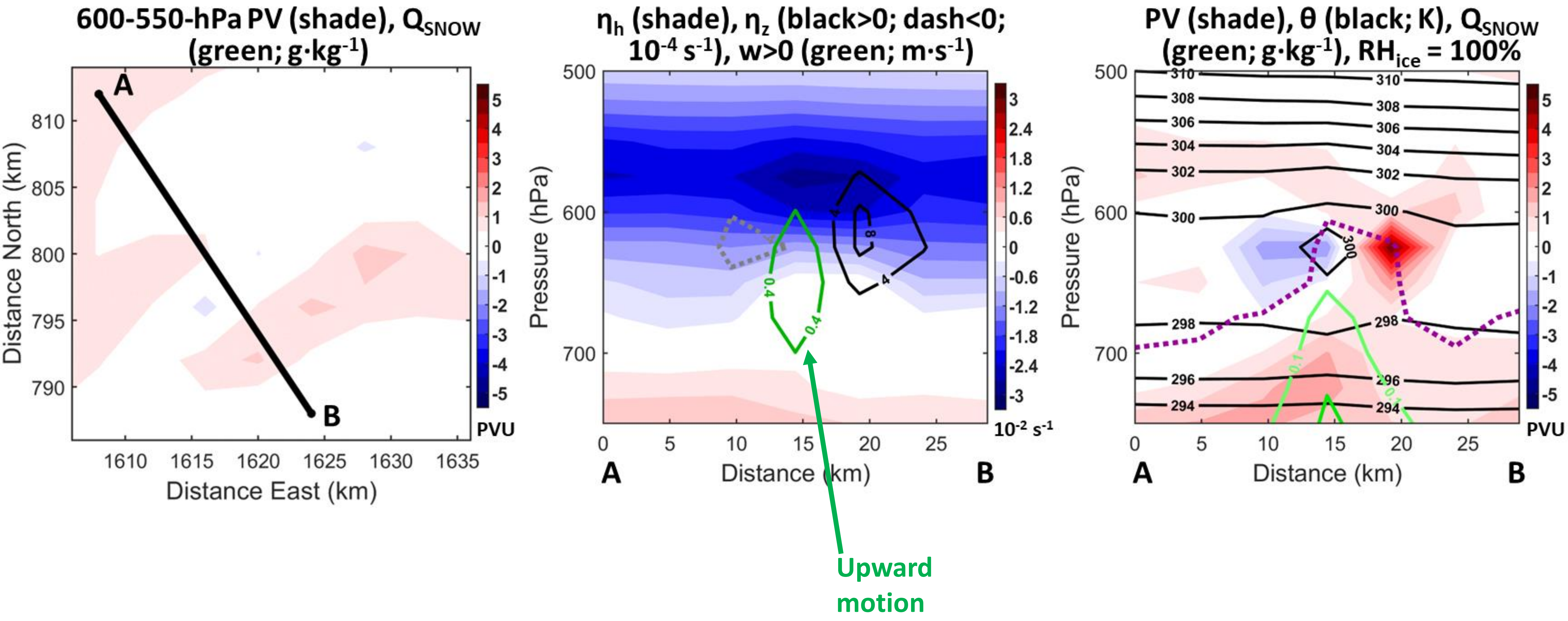

Band Formation and Growth Via Generation of PV Dipoles and Resulting Circulation

124 h 30 min

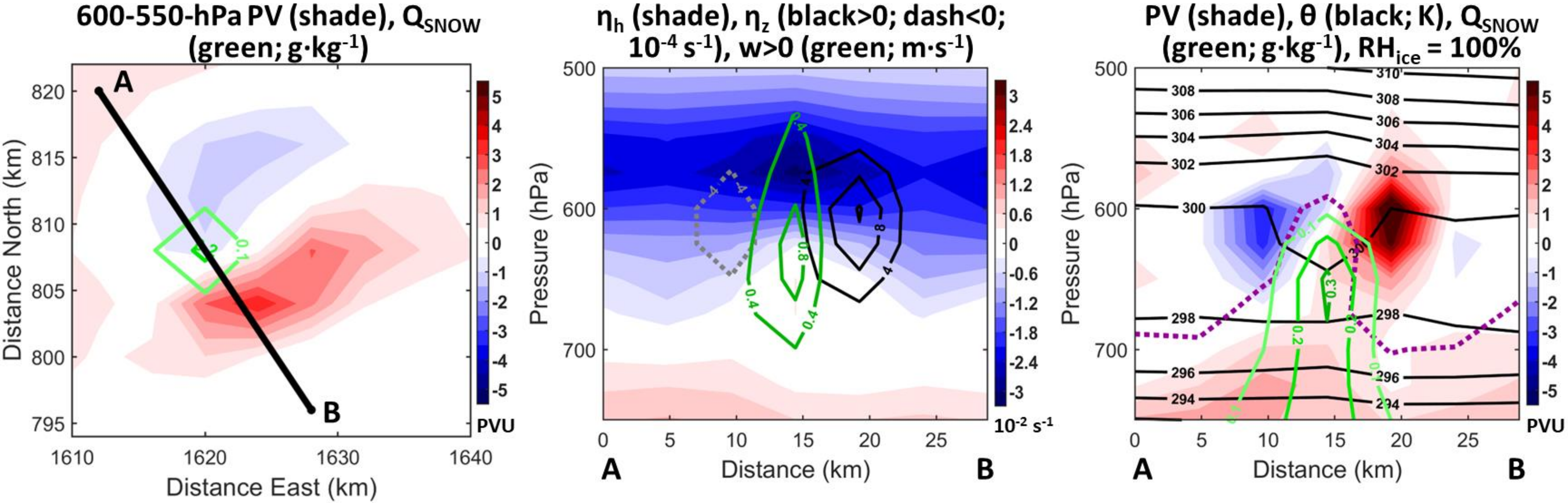

Band Formation and Growth Via Generation of PV Dipoles and Resulting Circulation

124 h 40 min

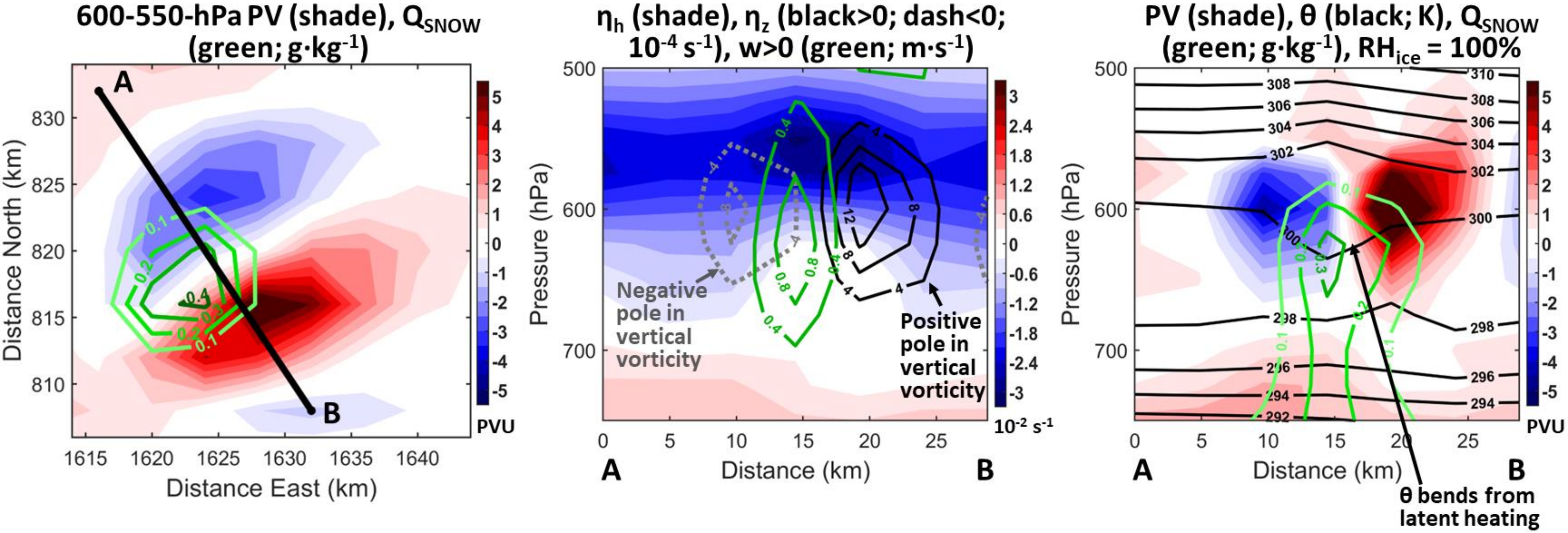

Band Formation and Growth Via Generation of PV Dipoles and Resulting Circulation

124 h 40 min: 600-550-hPa PV Tend. Terms (shade), PV (contour), Wind

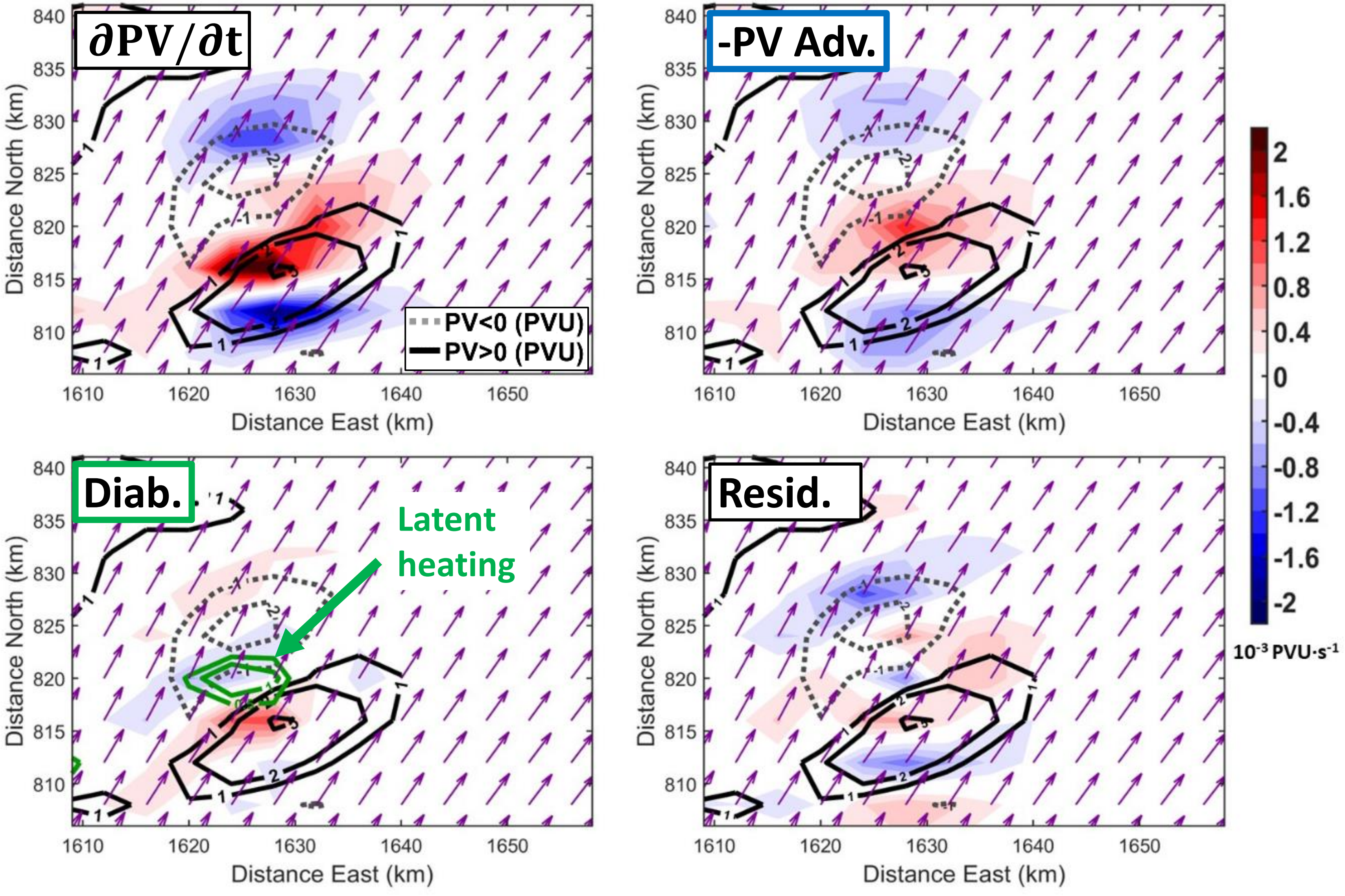

- Diagnosed the terms in the 600-550-hPa PV tendency equation as the PV dipole expanded.
  - Time derivatives are approximated with CFD of 2-minute output.
  - Diabatic heating rate ($\dot{\theta}$) is approximated by subtracting θ advection from the time-rate-of-change in θ.
- The diabatic term is contributing near the center of the dipole.

$$\frac{\partial PV}{\partial t} + \underbrace{\vec{V} \cdot \nabla PV}_{\text{Advection}} - \underbrace{\frac{1}{\rho} \vec{\eta} \cdot \nabla \dot{\theta}}_{\text{Diabatic}} = residual = 0$$

Band Formation and Growth Via Generation of PV Dipoles and Resulting Circulation

125 h 10 min: 600-550-hPa PV Tend. Terms (shade), PV (contour), Wind

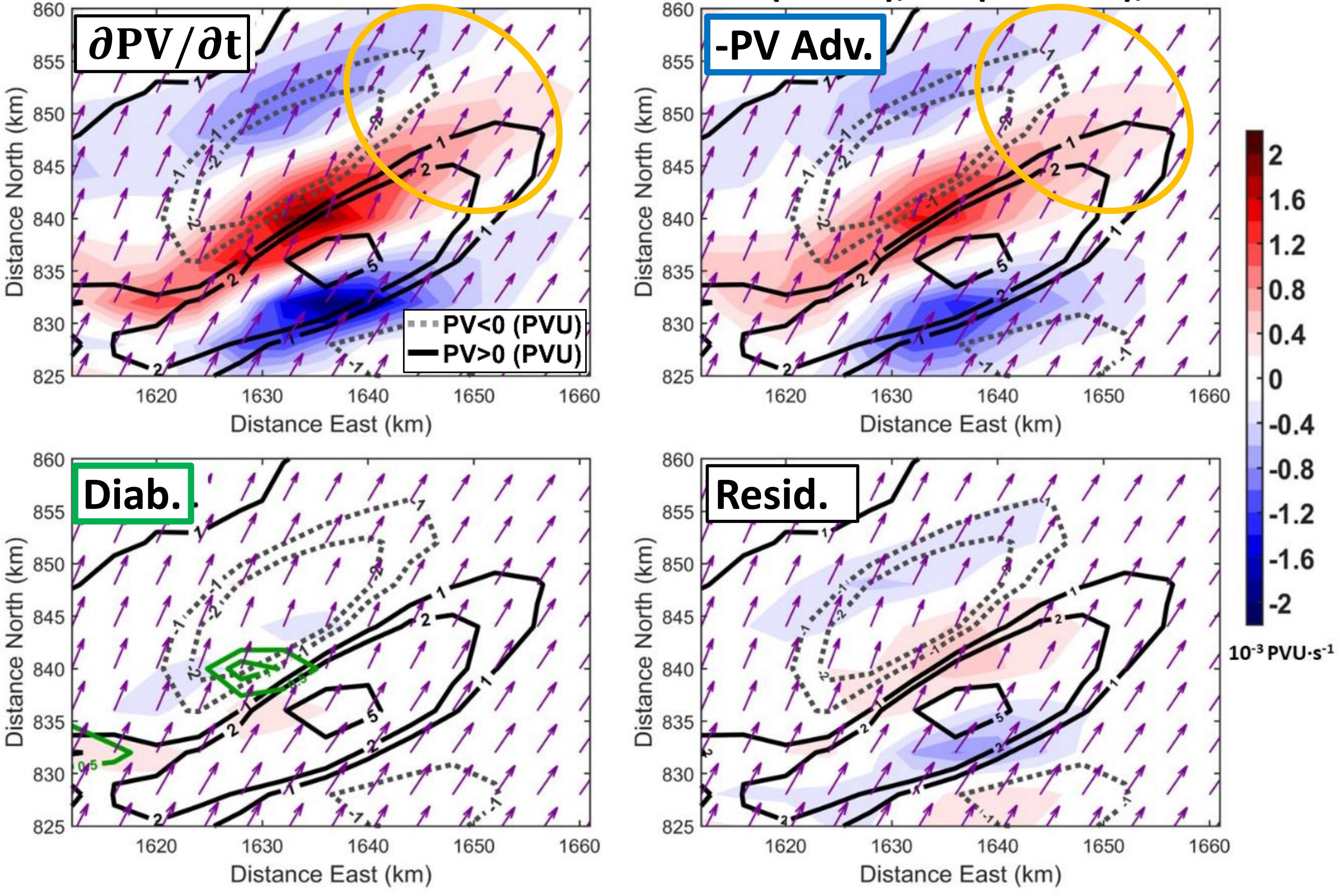

$$\frac{\partial PV}{\partial t} + \underbrace{\vec{V}\cdot\nabla PV}_{\text{Advection}} - \underbrace{\frac{1}{\rho}\vec{\eta}\cdot\nabla\dot{\theta}}_{\text{Diabatic}} = residual = 0$$

- Diagnosed the terms in the 600-550-hPa PV tendency equation as the PV dipole expanded.
  - Time derivatives are approximated with CFD of 2-minute output.
  - Diabatic heating rate ($\dot{\theta}$) is approximated by subtracting θ advection from the time-rate-of-change in θ.
- The diabatic term is contributing near the center of the dipole.
- Advection corresponds to >90% of NE expansion of PV after it's created from below (at the NE edge of PV dipoles).

Band Formation and Growth Via Generation of PV Dipoles and Resulting Circulation

125 h 00 min

600-550-hPa PV (shade) and Wind Anomaly, 650-hPa Q_{SNOW} (green)

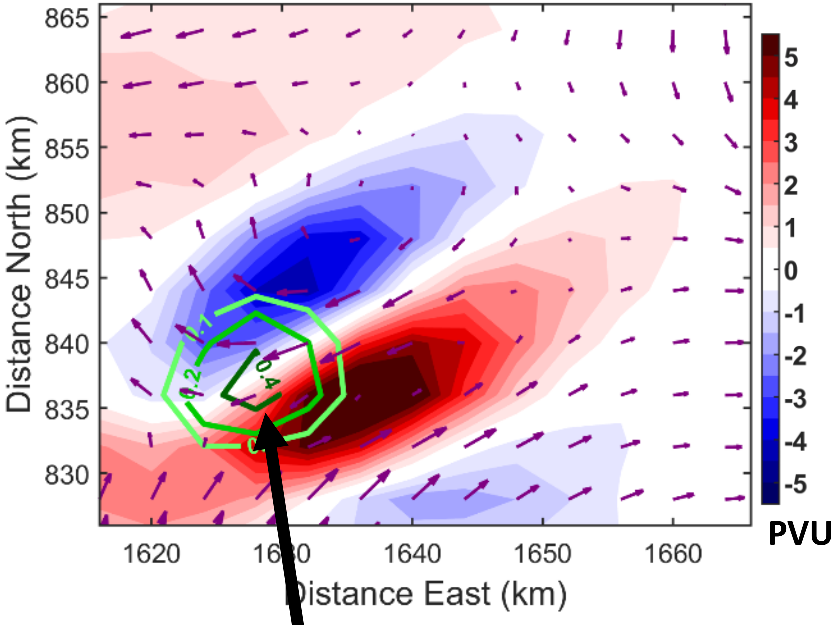

Original cell

600-550-hPa Wind Speed (shade) and Vectors

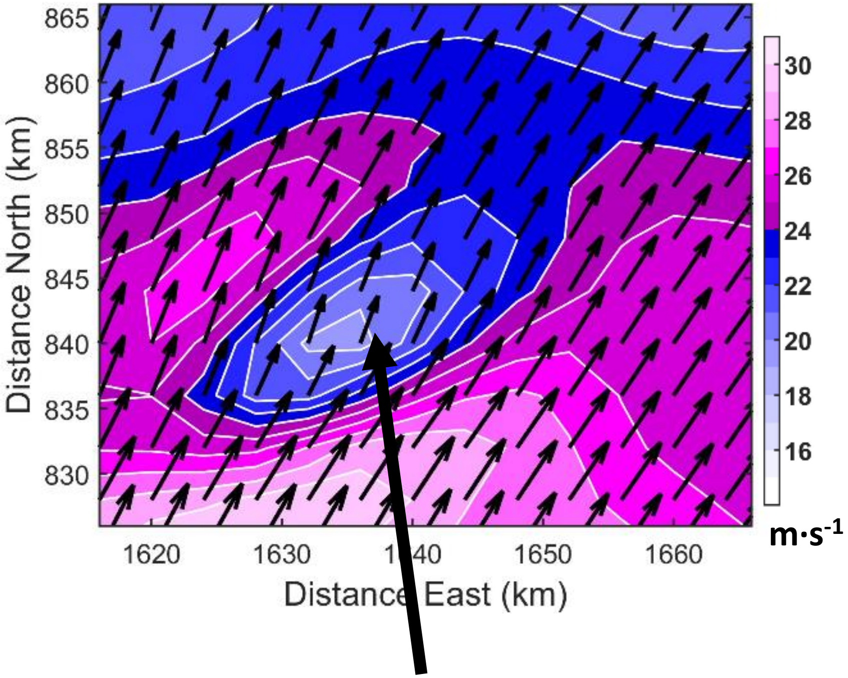

Winds slow down in between dipole…

600-550-hPa Divergence (shade), w (green)

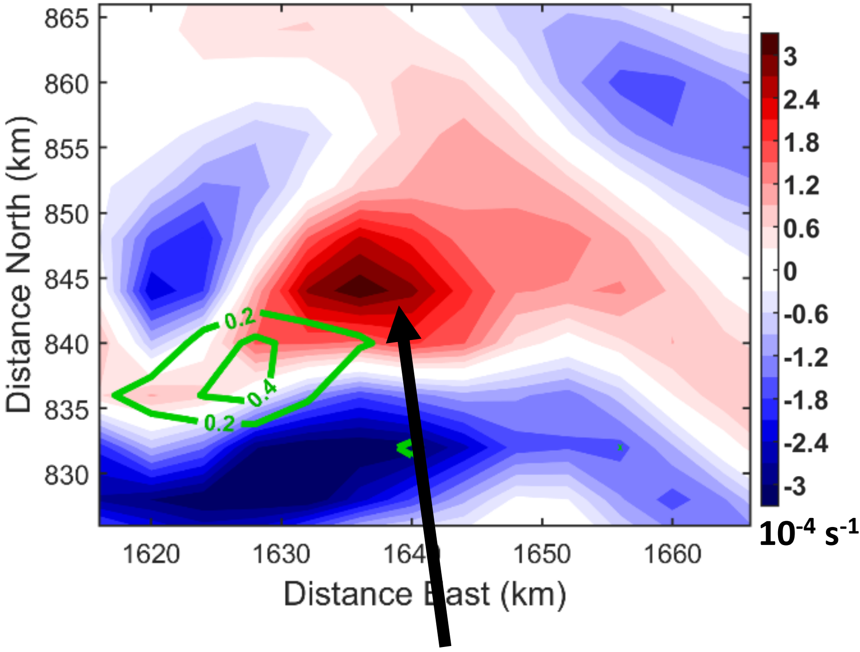

…Divergence where the winds speed back up exiting the dipole.

Band Formation and Growth Via Generation of PV Dipoles and Resulting Circulation

125 h 30 min

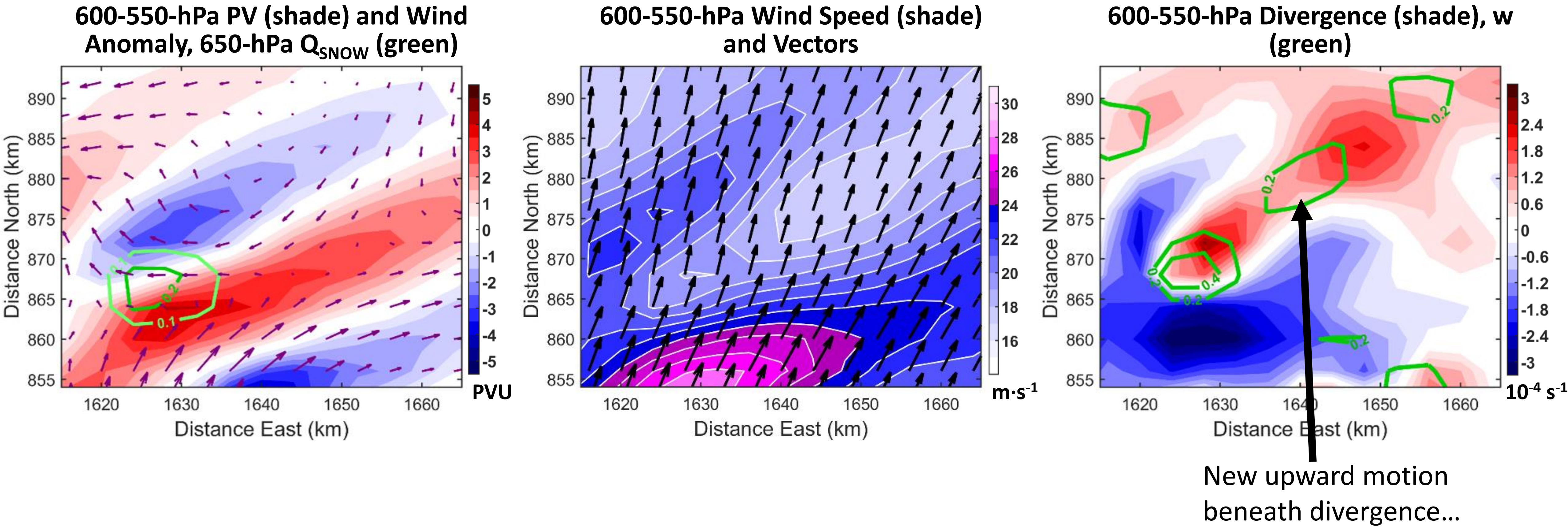

Band Formation and Growth Via Generation of PV Dipoles and Resulting Circulation

126 h 00 min

600-550-hPa PV (shade) and Wind Anomaly, 650-hPa Q_{SNOW} (green)

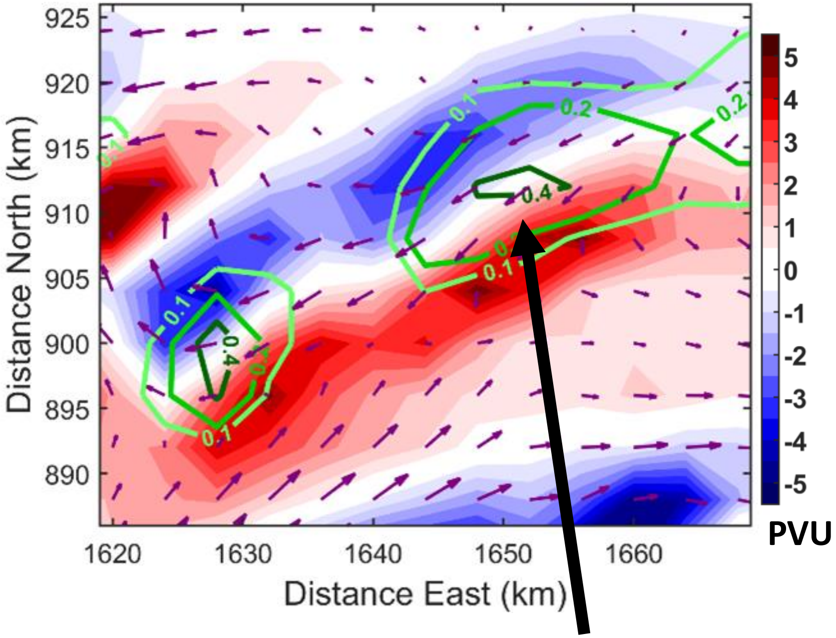

…New convection beneath divergence

600-550-hPa Wind Speed (shade) and Vectors

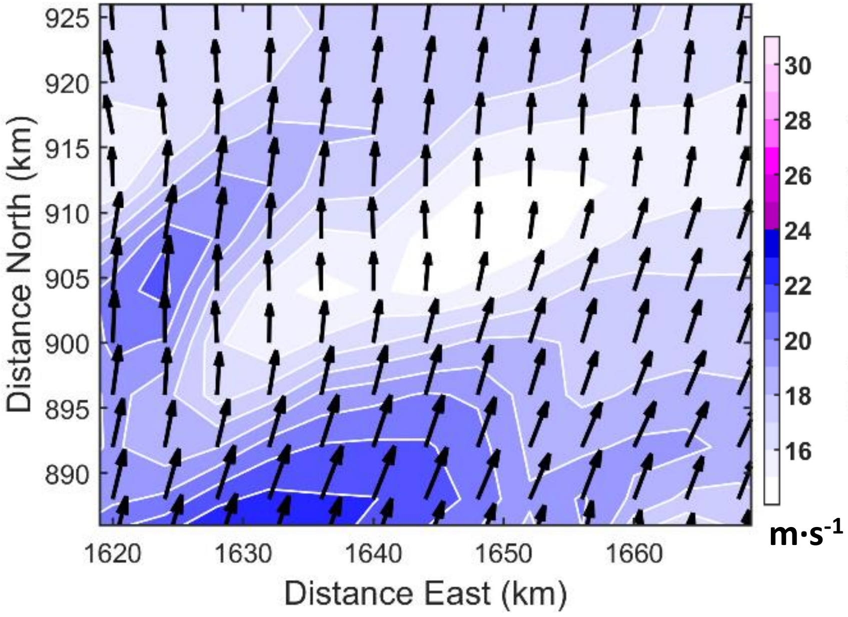

600-550-hPa Divergence (shade), w (green)

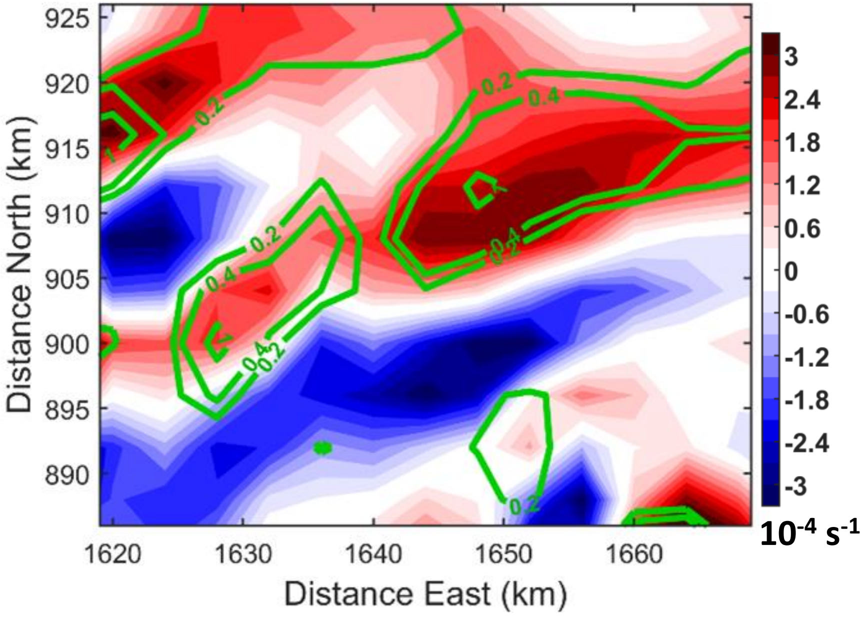

Band Formation and Growth Via Generation of PV Dipoles and Resulting Circulation

126 h 30 min

600-550-hPa PV (shade) and Wind Anomaly, 650-hPa Q_{SNOW} (green)

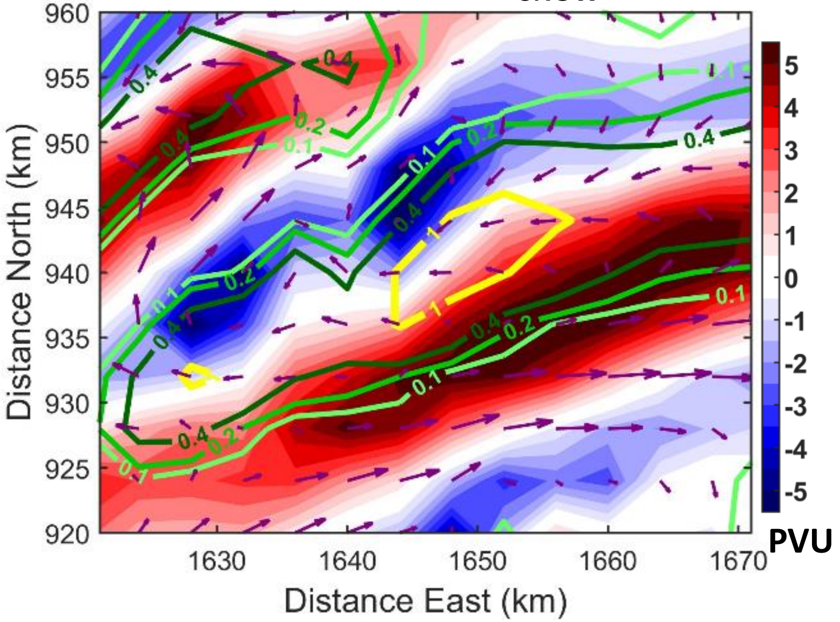

600-550-hPa Wind Speed (shade) and Vectors

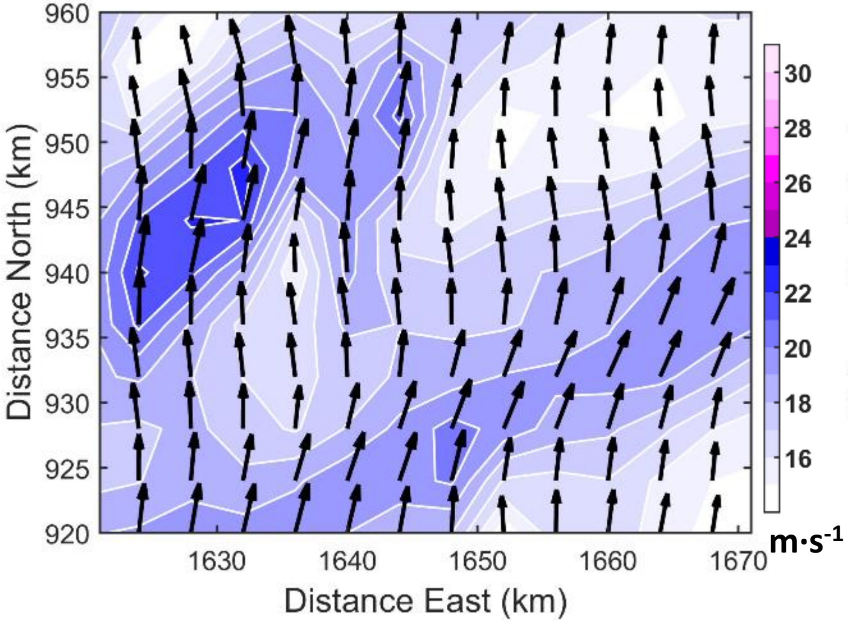

600-550-hPa Divergence (shade), w (green)

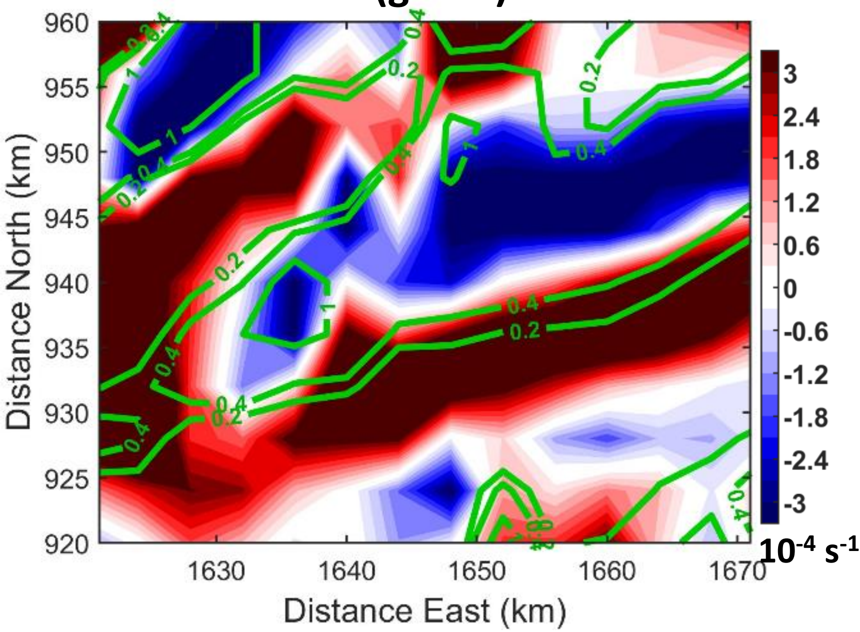

Objectives

- Nested runs of an idealized baroclinic wave model are used to answer the following questions:
    1. How do the precipitation structures in the comma head evolve as the cyclone develops?
    2. How do changes in the ambient frontogenesis (forcing), vertical shear, and instability around the cyclone relate to changes in the precipitation structures.
    3. What mechanisms cause the bands to elongate and persist?
    4. How sensitive is the development of the multi-bands to small changes in the initial conditions?

Forecast Challenges

Snowband Predictability Issues (2-km WRF runs of Dec 2010 Event)

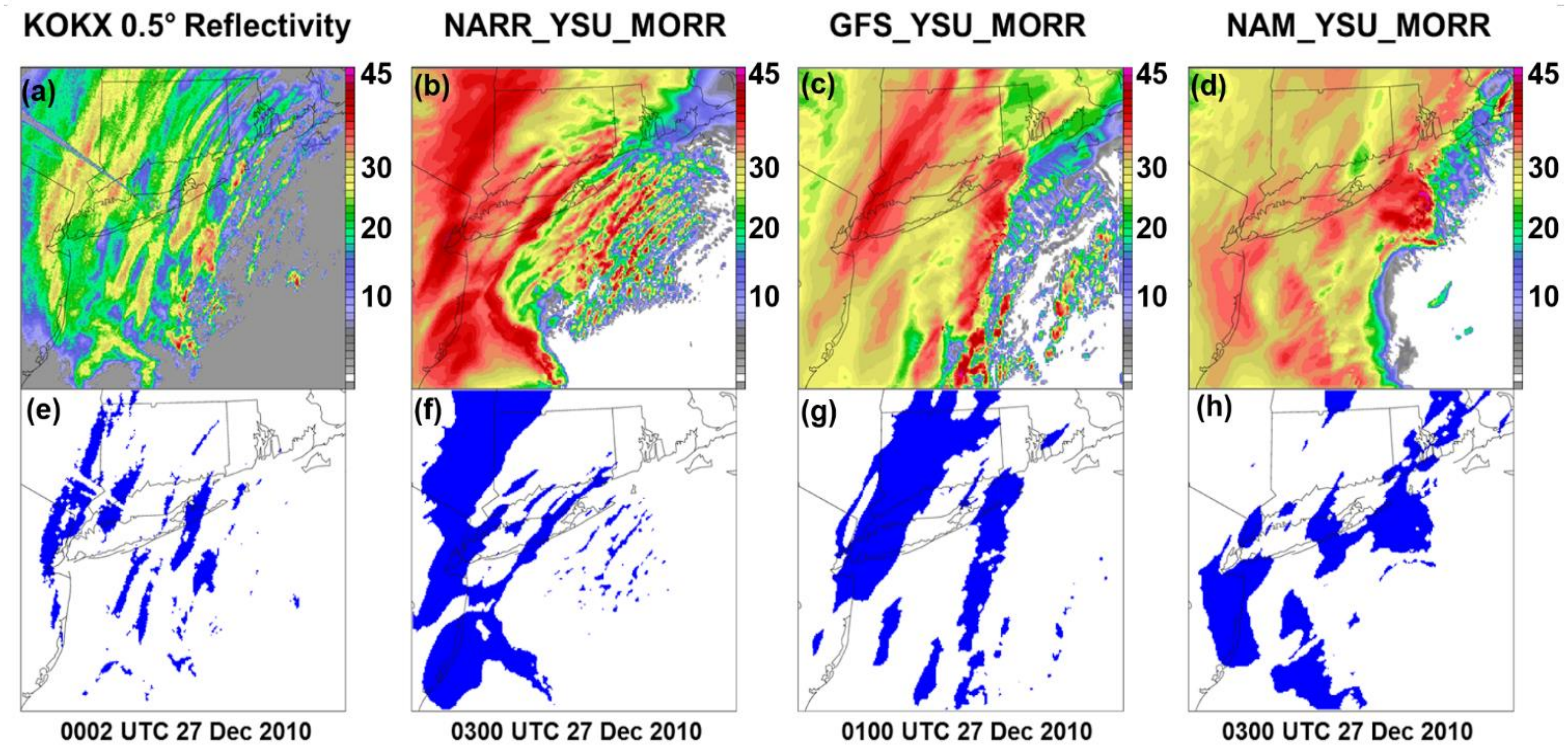

Snowband Predictability Issues (2-km WRF runs of Dec 2020 Event)

MRMS Reflectivity

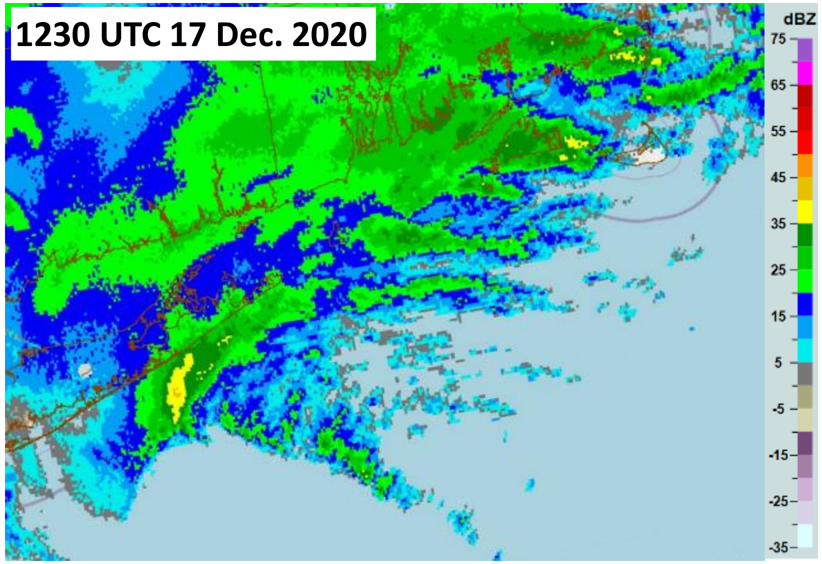

- WRF runs with same PBL and MP schemes, but different initial conditions.
- Each run generally produced multi-bands in this case.
- The extent of the banding and band orientation/morphology were sensitive to the initial conditions.

2-km WRF Simulated Reflectivity and SLP, valid 1230 UTC 17 Dec. 2020 (forecast hour 12)

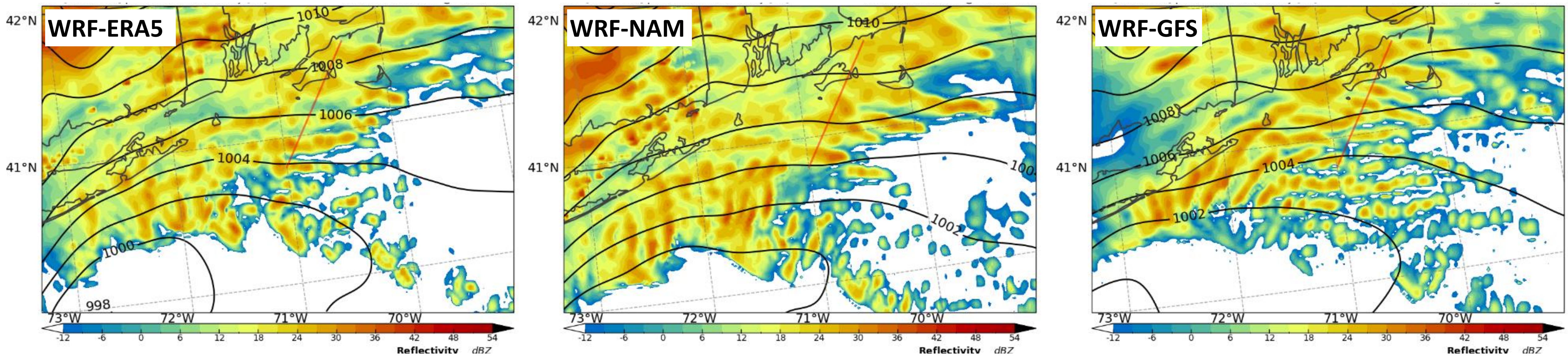

Sensitivity to Initial Conditions: +/- 10% change in Temperature Gradient

100-km Control Initial 500-hPa Heights (blue contour; dam)

Control Initial U-wind (shade) and θ (grey contour; K)

Control – TGRAD-10 Diff. in Initial θ (shade) and U-wind (green contour; m/s), TGRAD-10 θ (grey)

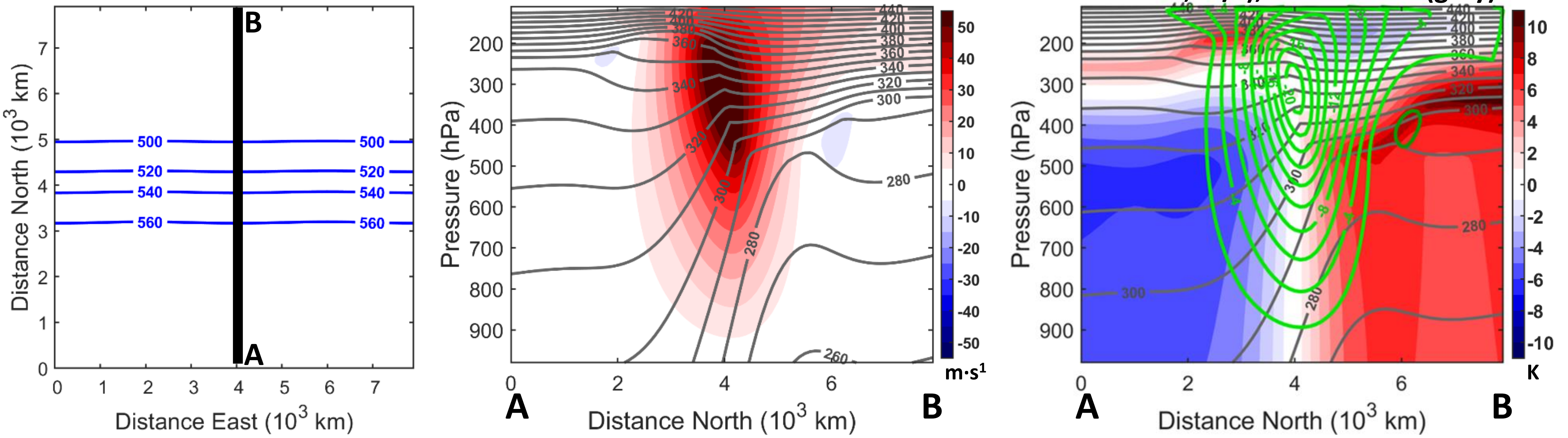

- Perturbed the initial conditions of the control run by decreasing or increasing the horizontal temperature gradient at each vertical level throughout the domain by 10% (“TGRAD-10” and “TGRAD+10”, respectively).

Sensitivity to Initial Conditions: +/- 10% change in Temperature Gradient

114 h: 700-hPa Snow (shade), Heights (black contour), and θ (blue contour)

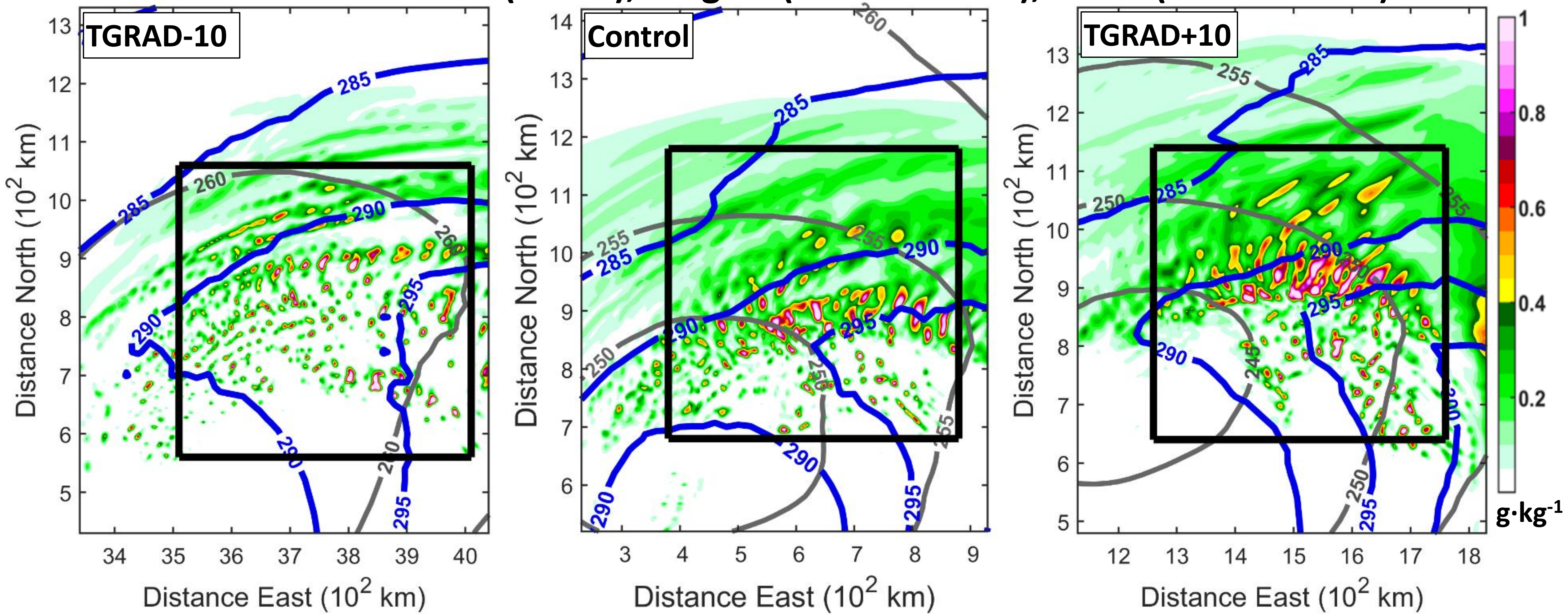

- Decreasing the initial horizontal temperature gradient by 10% delays multi-band until ~138 h.
- Increasing the gradient causes the multi-bands to develop/mature at ~120 h, at least 6 hours earlier than the Control. The activity then weakens after ~129 h.

Sensitivity to Initial Conditions: +/- 10% change in Temperature Gradient

120 h: 700-hPa Snow (shade), Heights (black contour), and θ (blue contour)

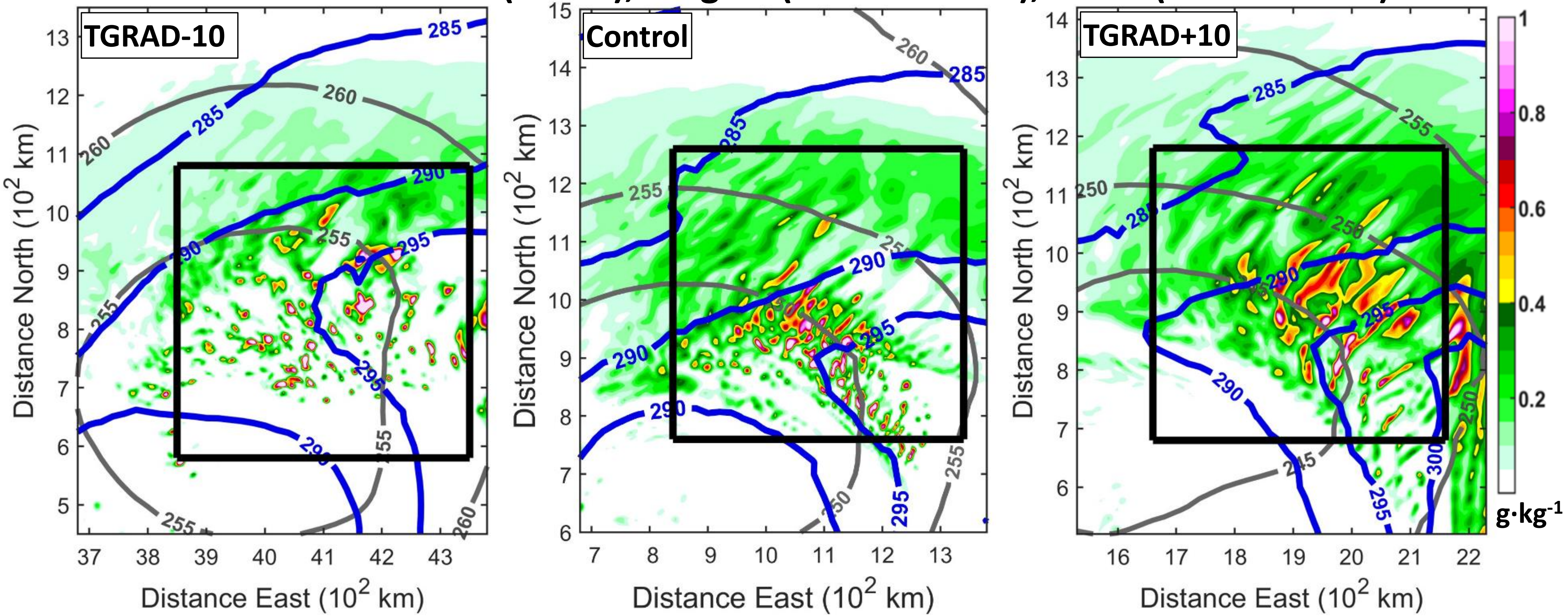

- Decreasing the initial horizontal temperature gradient by 10% delays multi-band until ~138 h.
- Increasing the gradient causes the multi-bands to develop/mature at ~120 h, at least 6 hours earlier than the Control. The activity then weakens after ~129 h.

Sensitivity to Initial Conditions: +/- 10% change in Temperature Gradient

129 h: 700-hPa Snow (shade), Heights (black contour), and θ (blue contour)

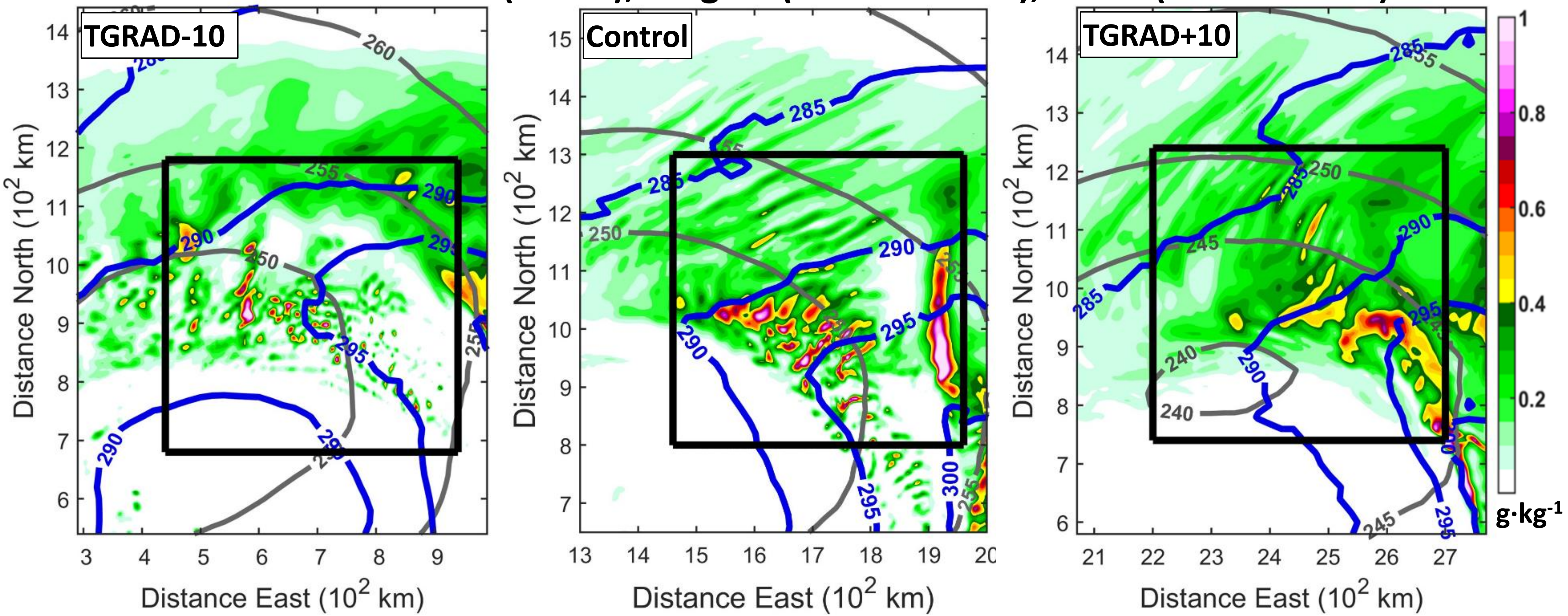

- Decreasing the initial horizontal temperature gradient by 10% delays multi-band until ~138 h.
- Increasing the gradient causes the multi-bands to develop/mature at ~120 h, at least 6 hours earlier than the Control. The activity then weakens after ~129 h.

Sensitivity to Initial Conditions: +/- 10% change in Temperature Gradient

138 h: 700-hPa Snow (shade), Heights (black contour), and θ (blue contour)

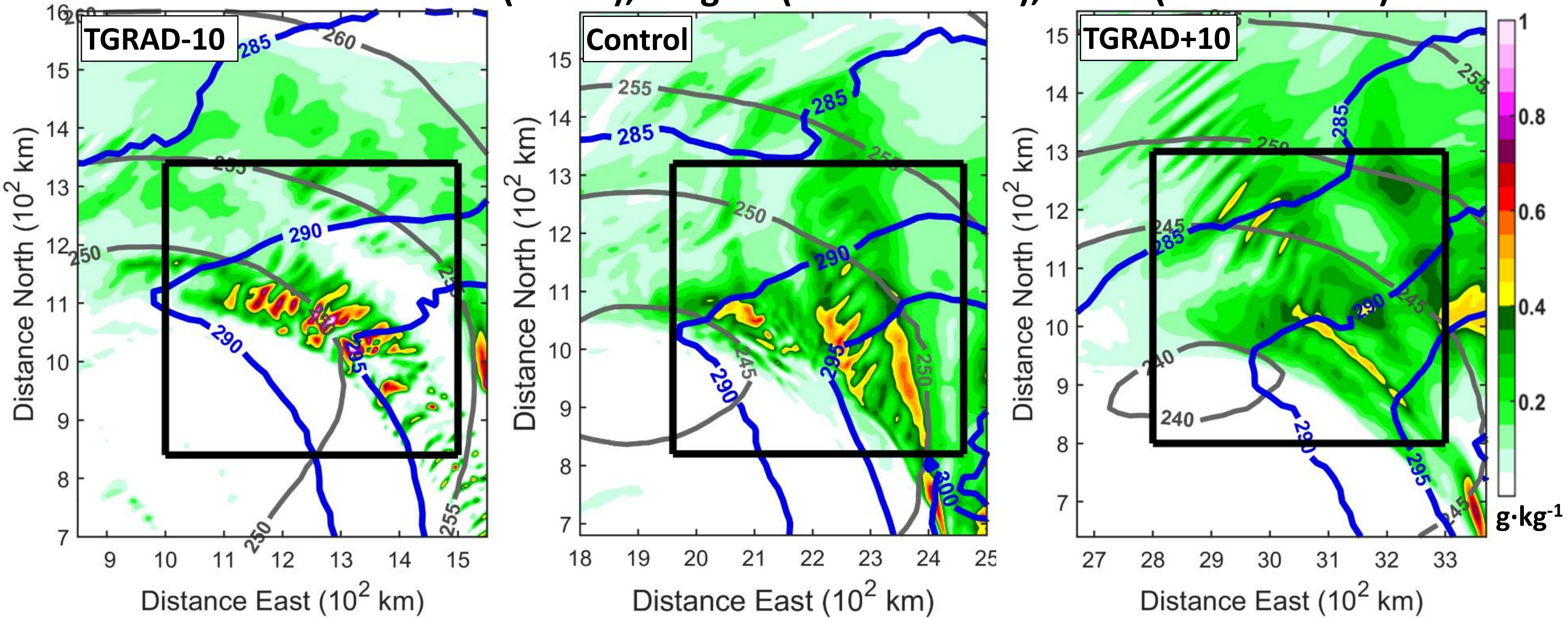

- Decreasing the initial horizontal temperature gradient by 10% delays multi-band until ~138 h.
- Increasing the gradient causes the multi-bands to develop/mature at ~120 h, at least 6 hours earlier than the Control. The activity then weakens after ~129 h.

Sensitivity to Initial Conditions: +/- 10% change in Temperature Gradient

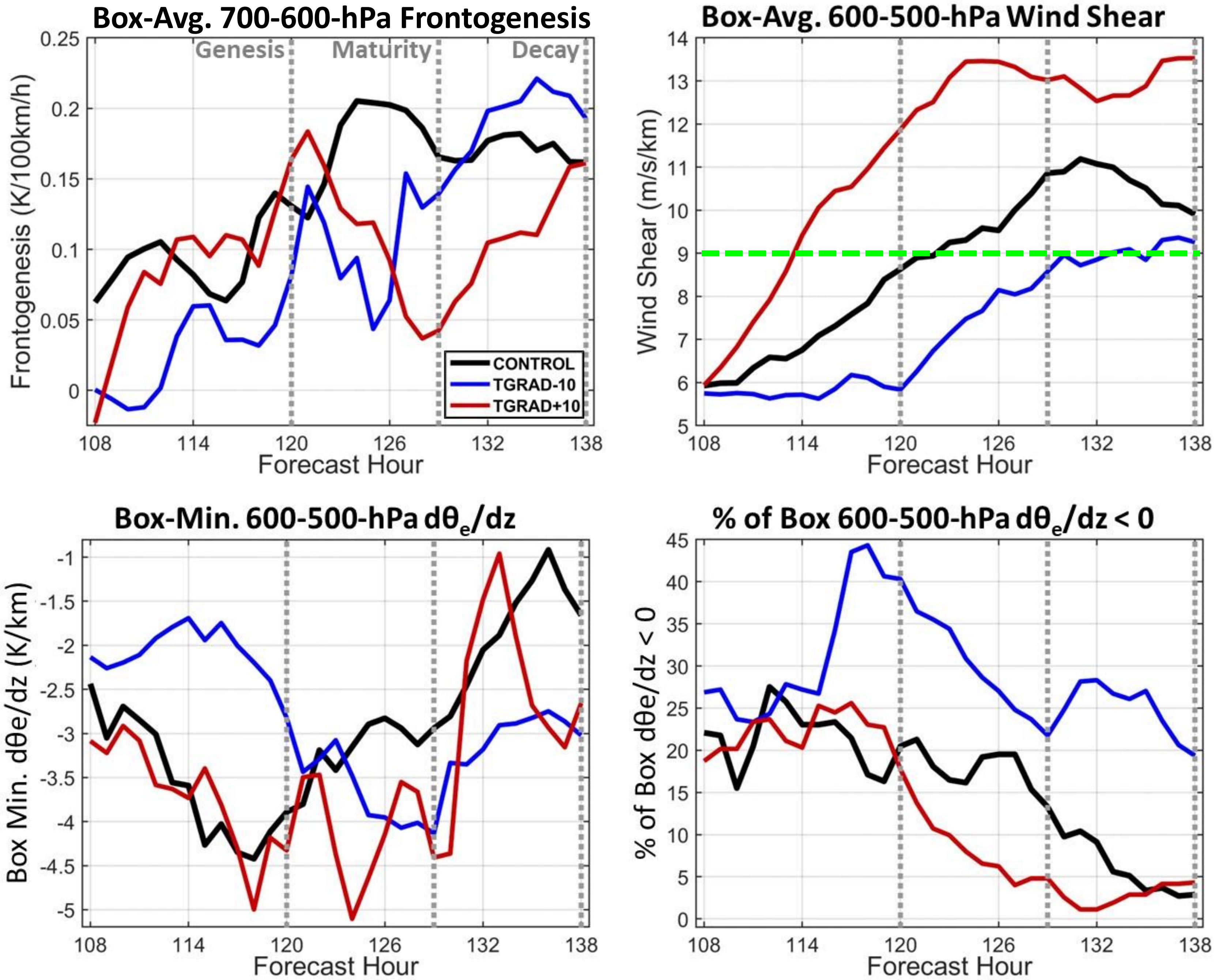

- TGRAD-10 and TGRAD+10 shear >9 m/s/km at ~136 h and 114 h, respectively.
- TGRAD-10 PI grows ~9 hours later, reaching -4 K/km by ~129 h.

Summary of Conceptual Model

- The 4-km baroclinic wave model develops multi-bands east of the surface low at 120-138 h. The bands start as cells that elongate and deepen as they move northward around the low.
- The activity coincides with a growth in 700-500-hPa PI east of the low and an increase in 600-500-hPa vertical shear. The activity dissipates after the instability is depleted.
- Bands expand northeastward due to a feedback between PV dipoles and ambient flow.
  - A cell updraft below 600-hPa tilts the 600-550-hPa horizontal absolute vorticity into the vertical. Latent heating in the updraft changes the local θ gradient, resulting in a PV dipole at 600-550-hPa.

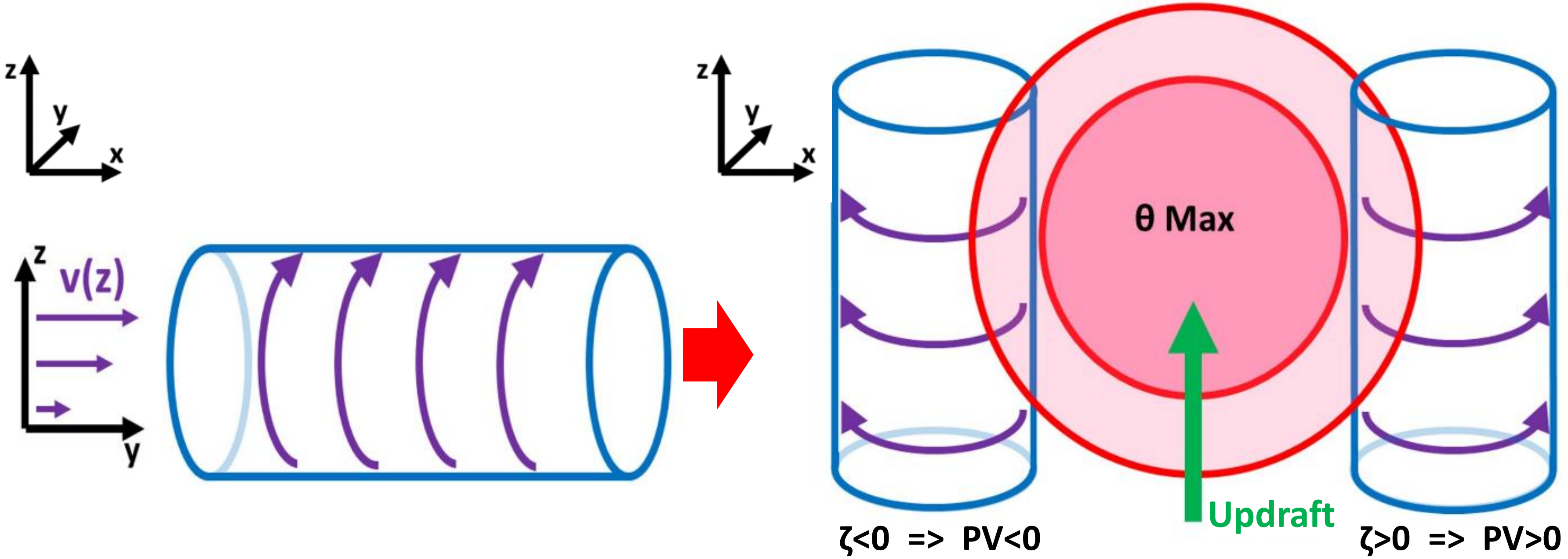

Summary of Conceptual Model

- The 4-km baroclinic wave model develops multi-bands east of the surface low at 120-138 h. The bands start as cells that elongate and deepen as they move northward around the low.
- The activity coincides with a growth in 700-500-hPa PI east of the low and an increase in 600-500-hPa vertical shear. The activity dissipates after the instability is depleted.
- Bands expand northeastward due to a feedback between PV dipoles and ambient flow.
  - A cell updraft below 600-hPa tilts the 600-550-hPa horizontal absolute vorticity into the vertical. Latent heating in the updraft changes the local θ gradient, resulting in a PV dipole at 600-550-hPa.
  - Southwest winds ~550-hPa advect the PV northeastward as it is continuously generated from below.

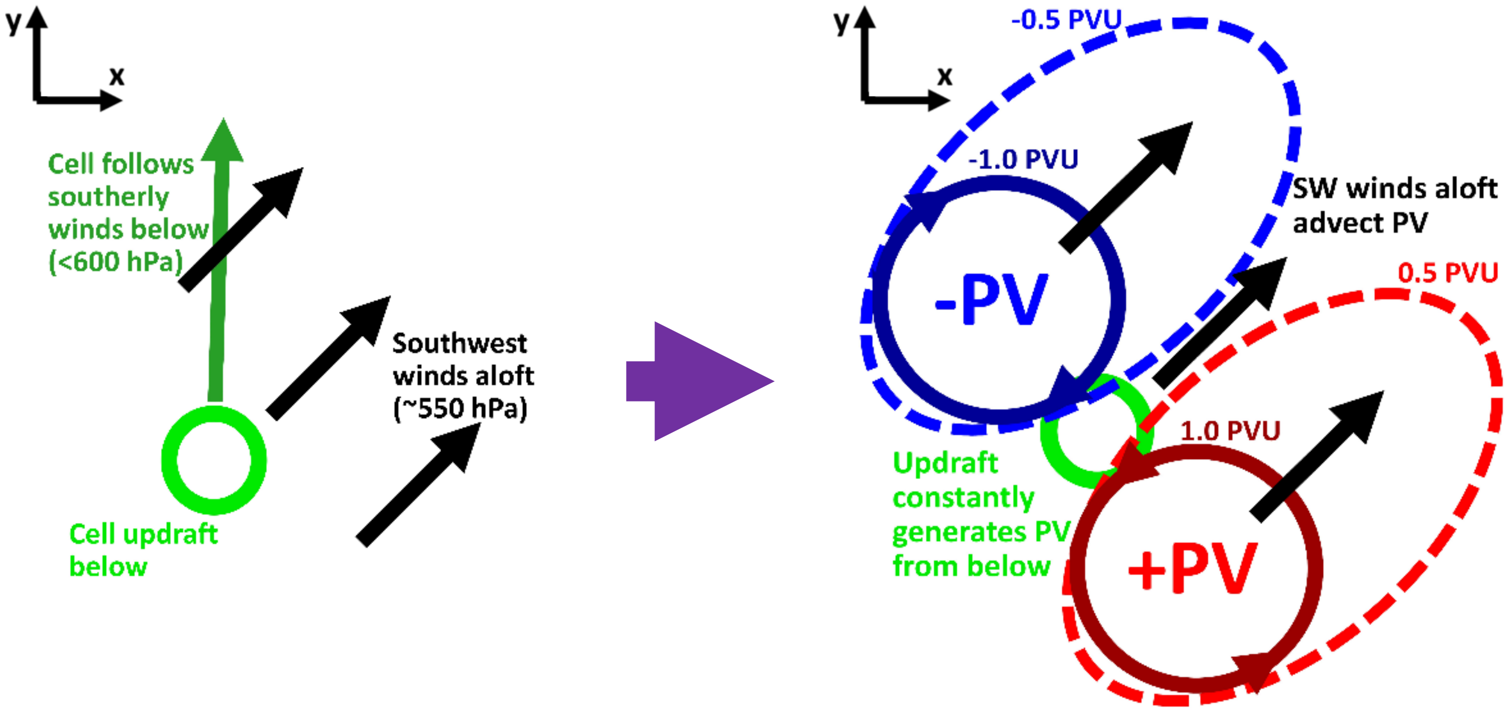

Summary of Conceptual Model (continued)

- The dipoles affect where the new convection develops- a line NE from the original cell.
- The circulations from the 2 PV poles cause a NE flow anomaly in between them, opposing the large-scale 600-550-hPa SW flow. Thus, the total wind slows down entering the dipole and speeds up exiting it. The latter corresponds to divergence (closer to 550-hPa) extending NE from the dipole. New upward motion and snow develop from beneath this divergence.
- The band dissipates over ~2-3 h after it moves away from the PI and shear. Gradual PV destruction from evaporative cooling north and south of the band.

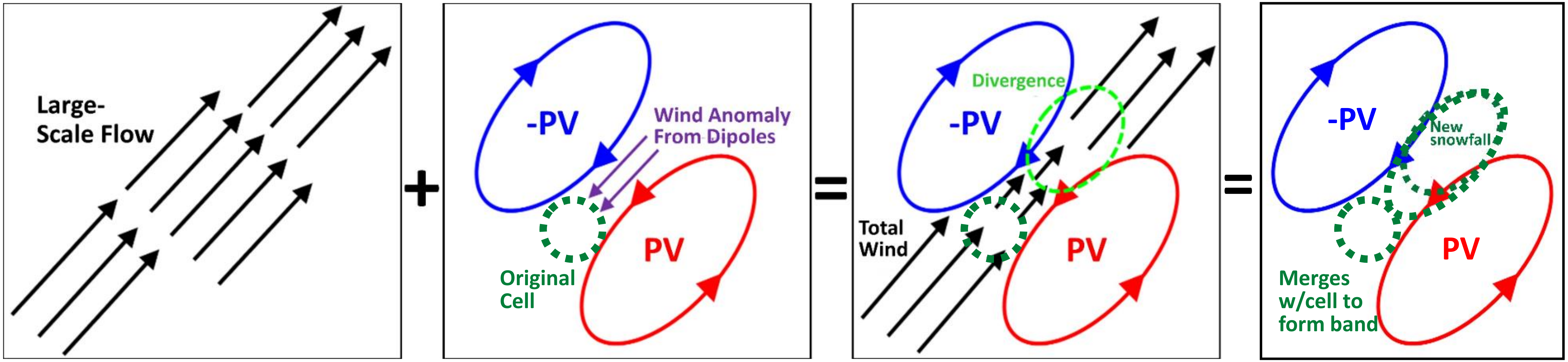

Conclusions and Takeaways for Forecasters

MRMS Reflectivity (shade), HRRR ANL 700-hPa height (black contour) and θ (blue), valid 1500 UTC 16 Jan 2022

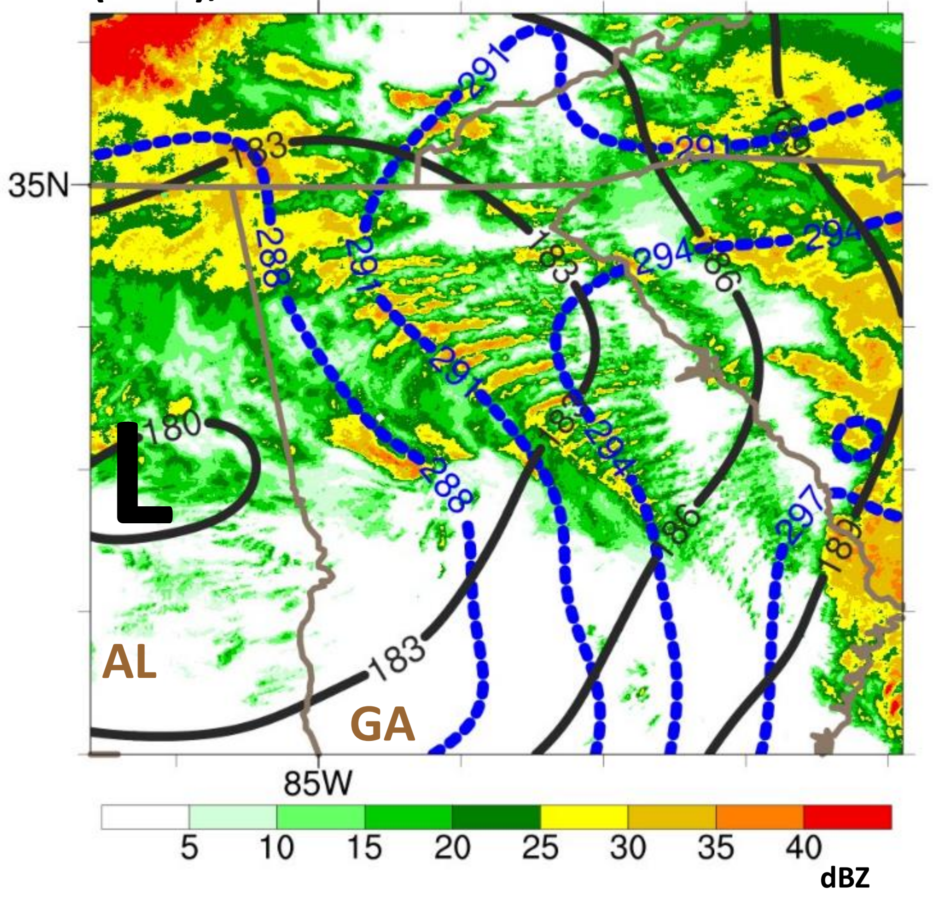

HRRR ANL 750-550-hPa $d\theta_e/dz$ (shade) and Wind Shear Vectors, valid 1500 UTC 16 Jan 2022

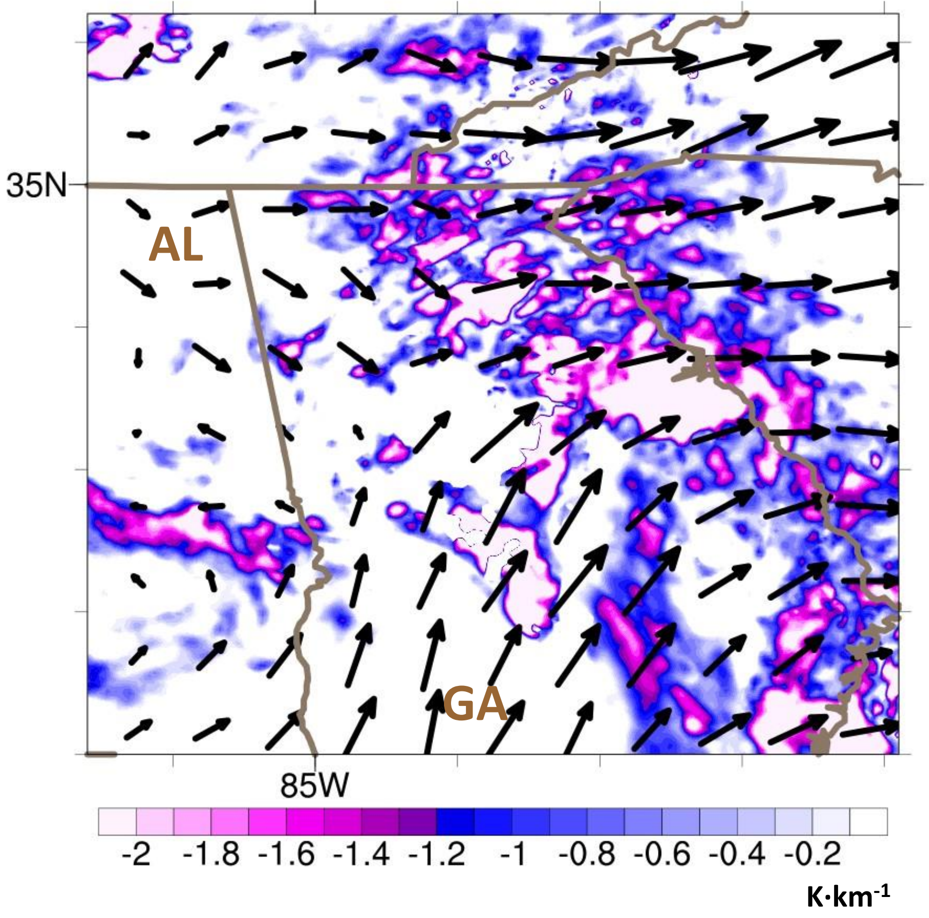

- PI east of the surface low is the dominant instability in the development of multi-band convection.
- Mid-level vertical shear is crucial in the organization/growth of the multi-bands.
- The development of both parameters in forecasts can be highly sensitive to the initial conditions.

References

- Chagnon, J. M., and S. L. Gray, 2009: Horizontal Potential Vorticity Dipoles on the Convective Storm Scale. *Q. J. R. Meteorol. Soc.*, **135**, 1392–1408. https://doi.org/10.1002/qj.468.
- Ganetis, S. A., B. A. Colle, S. E. Yuter, and N. P. Hoban, 2018: Environmental Conditions Associated with Observed Snowband Structures Within Northeast U.S. Winter Storms. *Mon. Wea. Rev.*, **146**, 3675–3690. DOI:10.1175/MWR-D-18-0054.1.
- Hitchman, M. H., and S. M. Rowe, 2019: On the Structure and Formation of UTLS PV Dipole/Jetlets in Tropical Cyclones by Convective Momentum Surges. *Mon. Wea. Rev.*, **147**, 4107-4125, doi: 10.1175/MWR-D-18-0232.1
- Keeler, K. M., B. F. Jewett, R. M. Rauber, G. M. McFarquhar, R. M. Rasmussen, L. Xue, C. Liu, and G. Thompson, 2016: Dynamics of Cloud-Top Generating Cells in Winter Cyclones. Part I: Idealized Simulations in the Context of Field Observations. *J. Atmos. Sci.*, **73**, 1507-1527. DOI:10.1175/JAS-D-15-0126.1.
- Leonardo, N., and B. Colle, 2024 (in press): Analysis of Snow Multi-Bands and Their Environments with High-Resolution Idealized Simulations. *Mon. Wea. Rev.*, doi: 10.1175/MWR-D-23-0211.1
- Moon, Y. and D. S. Nolan, 2015: Spiral Rainbands in a Numerical Simulation of Hurricane Bill (2009). Part I: Structures and Comparisons to Observations. *J. Atmos. Sci.*, **72**, 164-190, doi: https://doi.org/10.1175/JAS-D-14-0058.1

References

- Norris, J., G. Vaughan, and D. M. Schultz, 2014: Precipitation Banding in Idealized Baroclinic Waves. *Mon. Wea. Rev*., **142**, 3081–3099, doi: 10.1175/MWR-D-13-00343.1
- Norris, J., G. Vaughan, and D. M. Schultz, 2017: Variability of Precipitation Along Cold Fronts in Idealized Baroclinic Waves. *Mon. Wea. Rev*., **145**, 2971–2992, doi: 10.1175/MWR-D-16-0409.1
- Novak, D. R., J. S. Waldstreicher, D. Keyser, and L. F. Bosart, 2006: A Forecast Strategy for Anticipating Cold Season Mesoscale Band Formation within Eastern U.S. Cyclones. *Wea. Forecasting*, **21**, 3–23, https://doi.org/10.1175/WAF907.1.
- Rosenow, A. A., D. M. Plummer, R. M. Rauber, G. M. McFarquhar, B. F. Jewett, and D. Leon, 2014: Vertical Velocity and Physical Structure of Generating Cells and Convection in the Comma Head Region of Continental Winter Cyclones. *J. Atmos. Sci*., **71**, 1538–1558. DOI:10.1175/JAS-D-13-0249.1
- Sanders, F., and L. F. Bosart, 1985: Mesoscale structure in the Megalopolitan Snowstorm of 11–12 February 1983. Part I: Frontogenetical Forcing and Symmetric Instability. *J. Atmos. Sci*., **42**, 1050–1061, https://doi.org/10.1175/1520-0469(1985)042,1050:MSITMS.2.0.CO;2.
- Skamarock, W., J. B. Klemp, J. Dudhia, D. O. Gill, D. Barker, M. G. Duda, X. -Y. Huang, and W. Wang, 2008: A Description of the Advanced Research WRF Version 3. NCAR Technical Note NCAR/TN-475+STR. DOI:10.5065/D68S4MVH.
- Xu, Q., 1992: Formation and Evolution of Frontal Rainbands and Geostrophic Potential Vorticity Anomalies. *J. Atmos. Sci*., 49, 629–648, DOI:10.1175/1520-0469(1992)049,0629:FAEOFR.2.0.CO;2.

Thank you!

Extra Slides

126 h 20 min

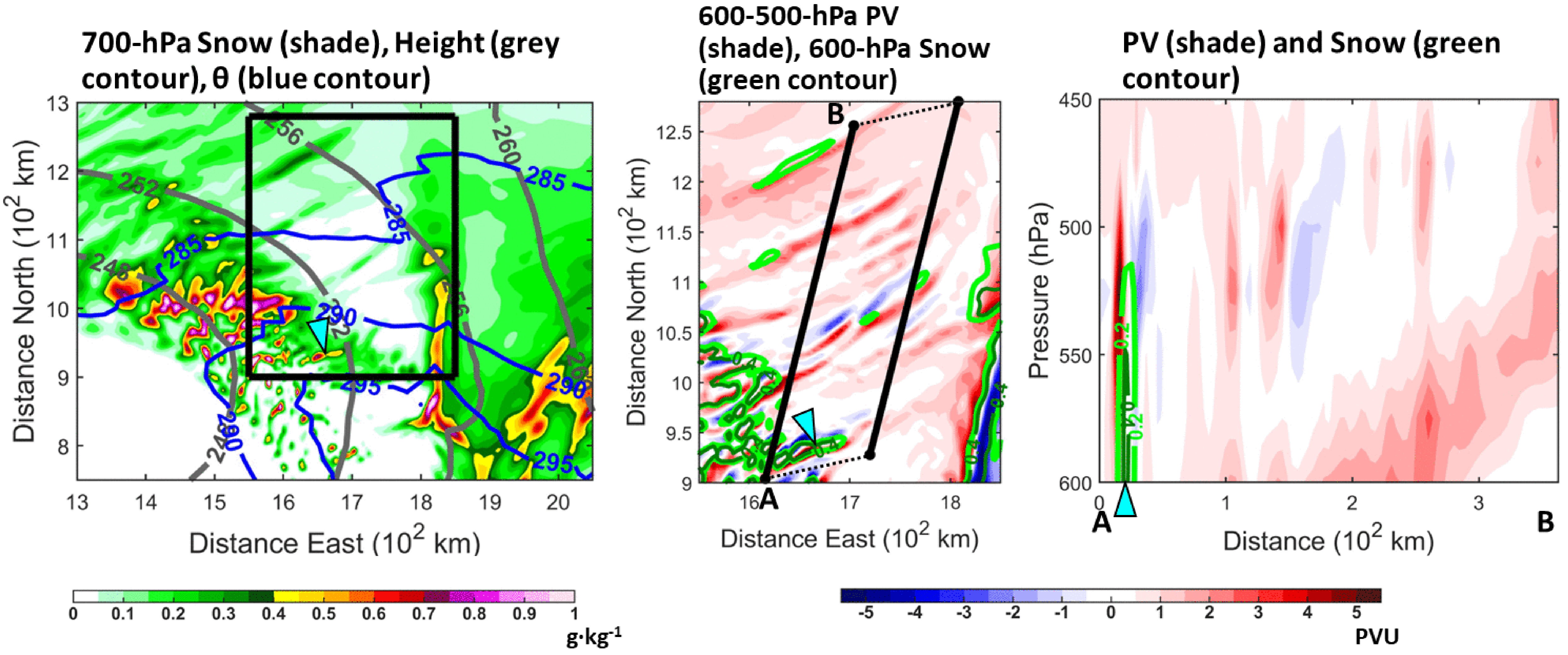

700-hPa Snow (shade), Height (grey contour), θ (blue contour)
600-500-hPa PV (shade), 600-hPa Snow (green contour)
PV (shade) and Snow (green contour)
Distance North (10^2 km)
Distance East (10^2 km)
Pressure (hPa)
Distance (10^2 km)
A
B
g·kg^{-1}
PVU

126 h 20 min

600-500-hPa Vertical Shear (shade and vectors), 600-hPa Snow (grey contour)

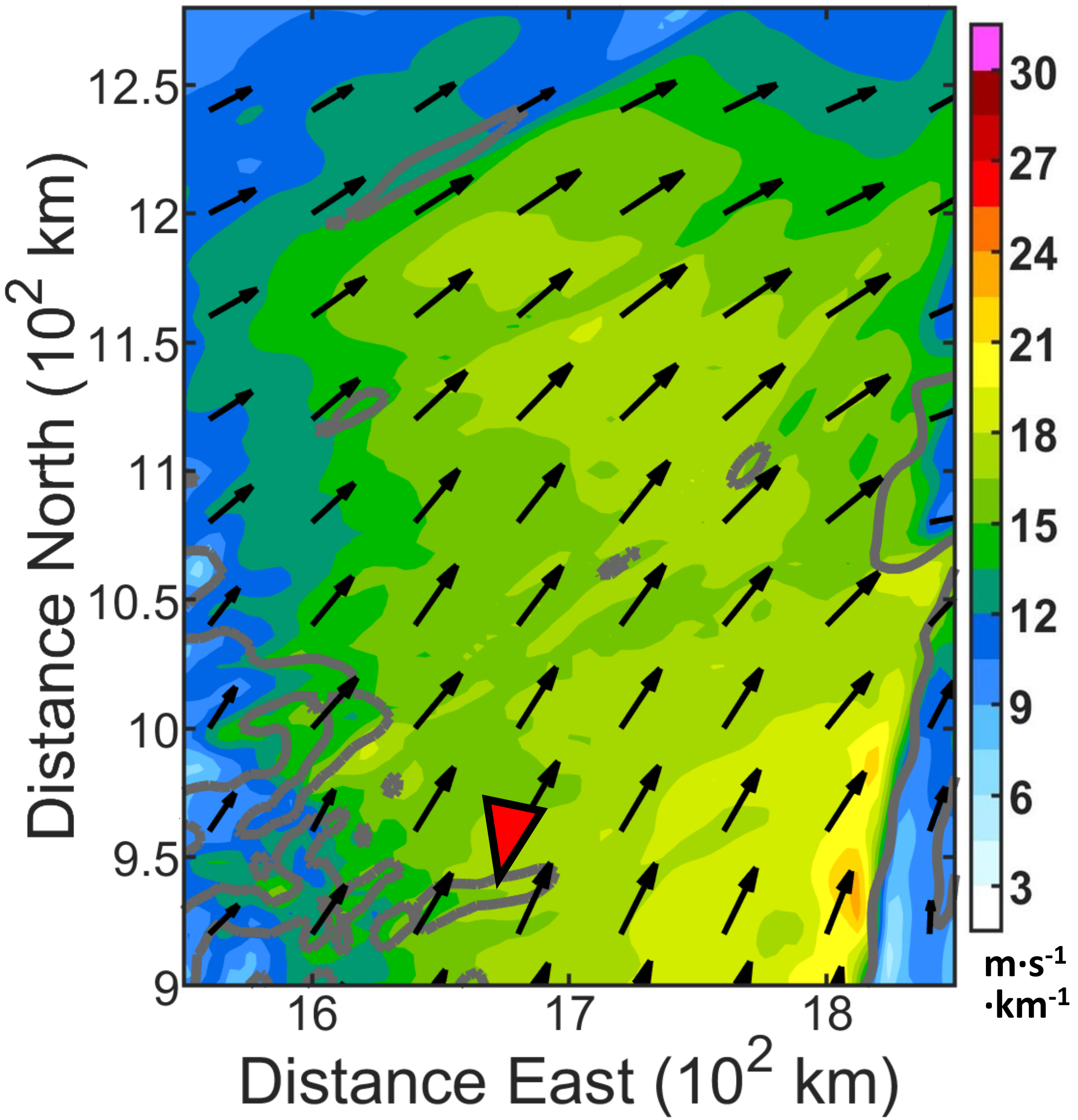

600-500-hPa $d\theta_e/dz$ (shade), 700-600-hPa θ (black contour) and Fgen. (red contour), 600-hPa Snow (green contour)

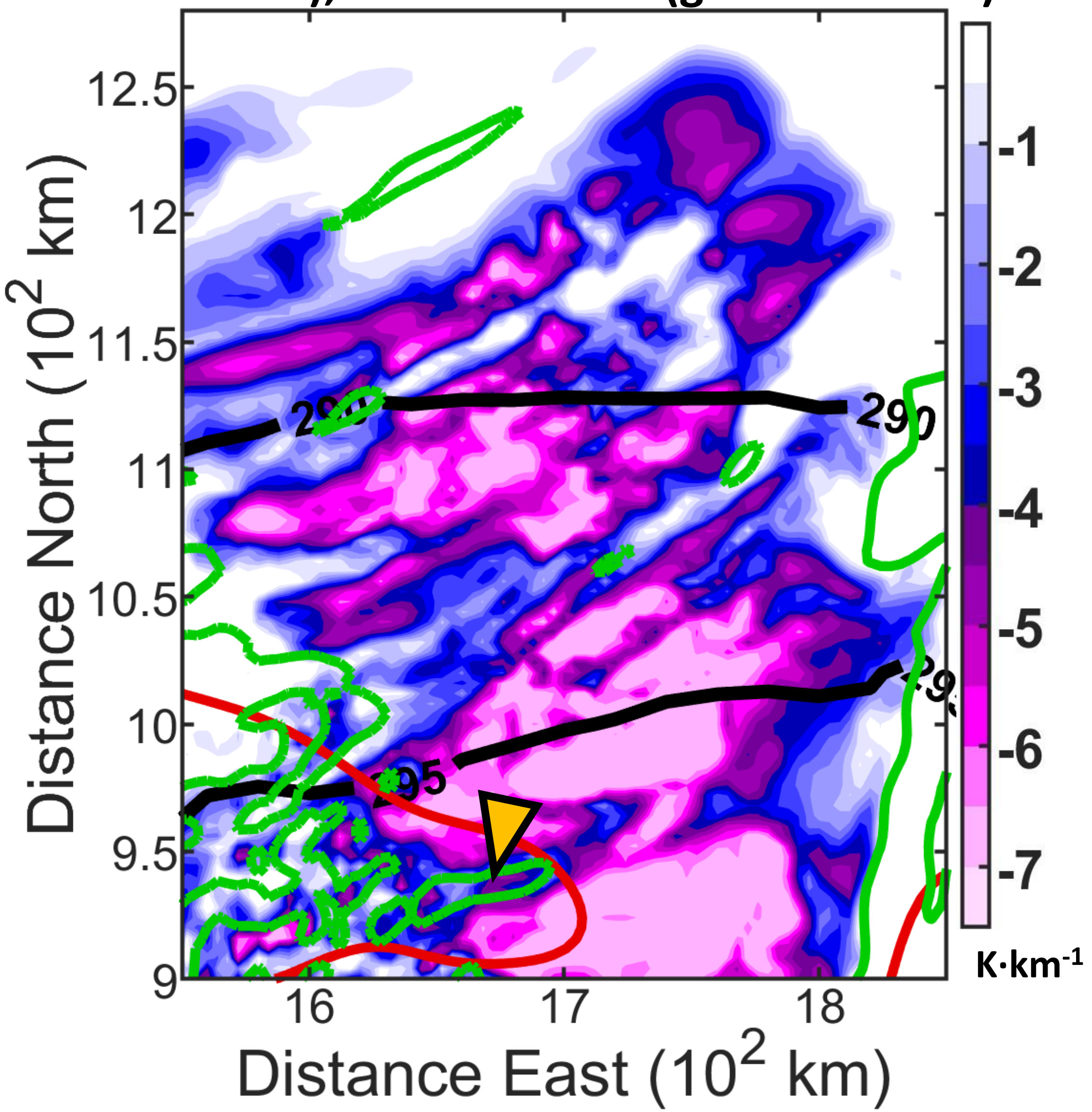

128 h 00 min

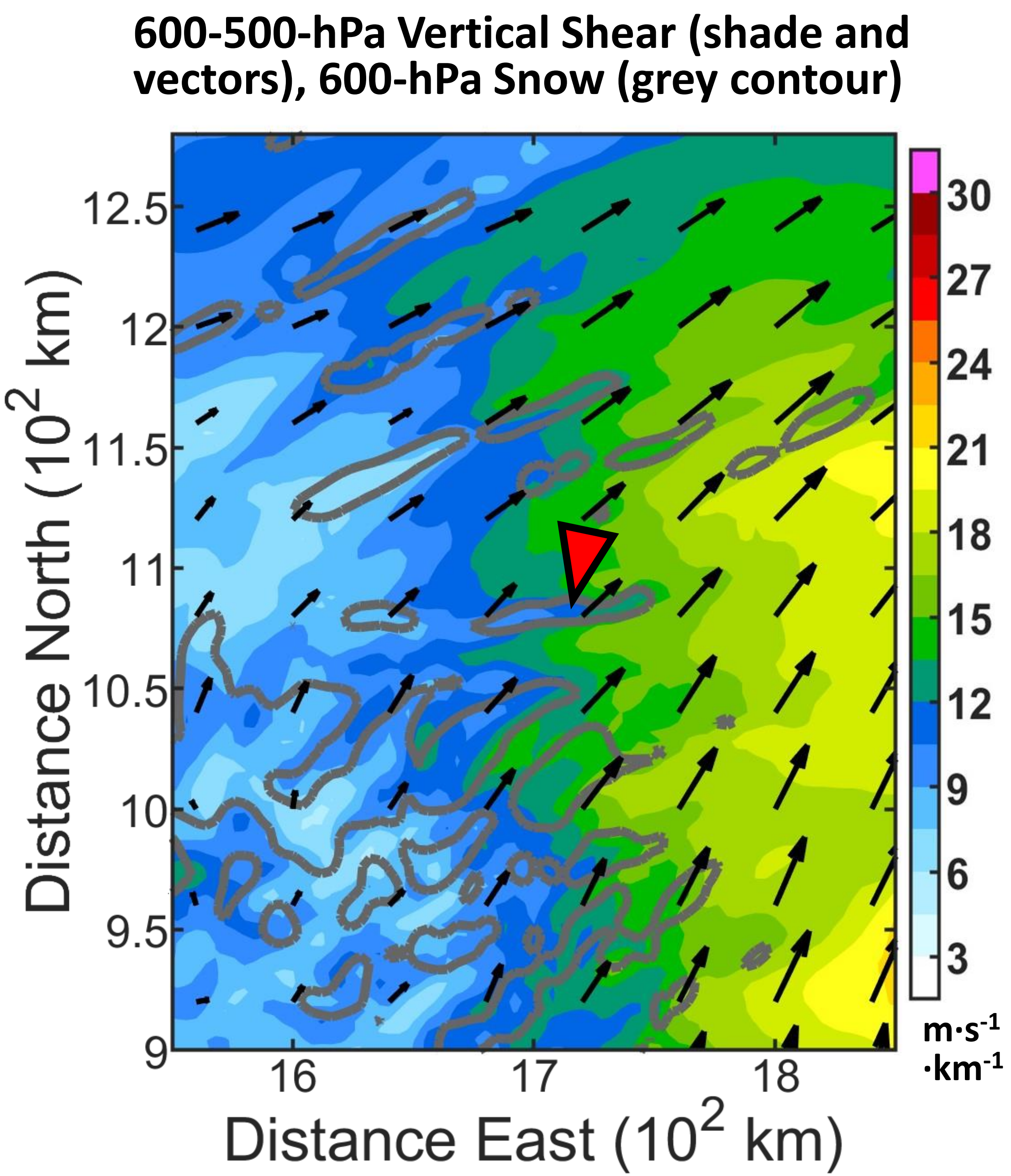

600-500-hPa Vertical Shear (shade and vectors), 600-hPa Snow (grey contour)
Distance North (10^2 km)
Distance East (10^2 km)
12.5
12
11.5
11
10.5
10
9.5
9
16
17
18
30
27
24
21
18
15
12
9
6
3
m·s^{-1} ·km^{-1}

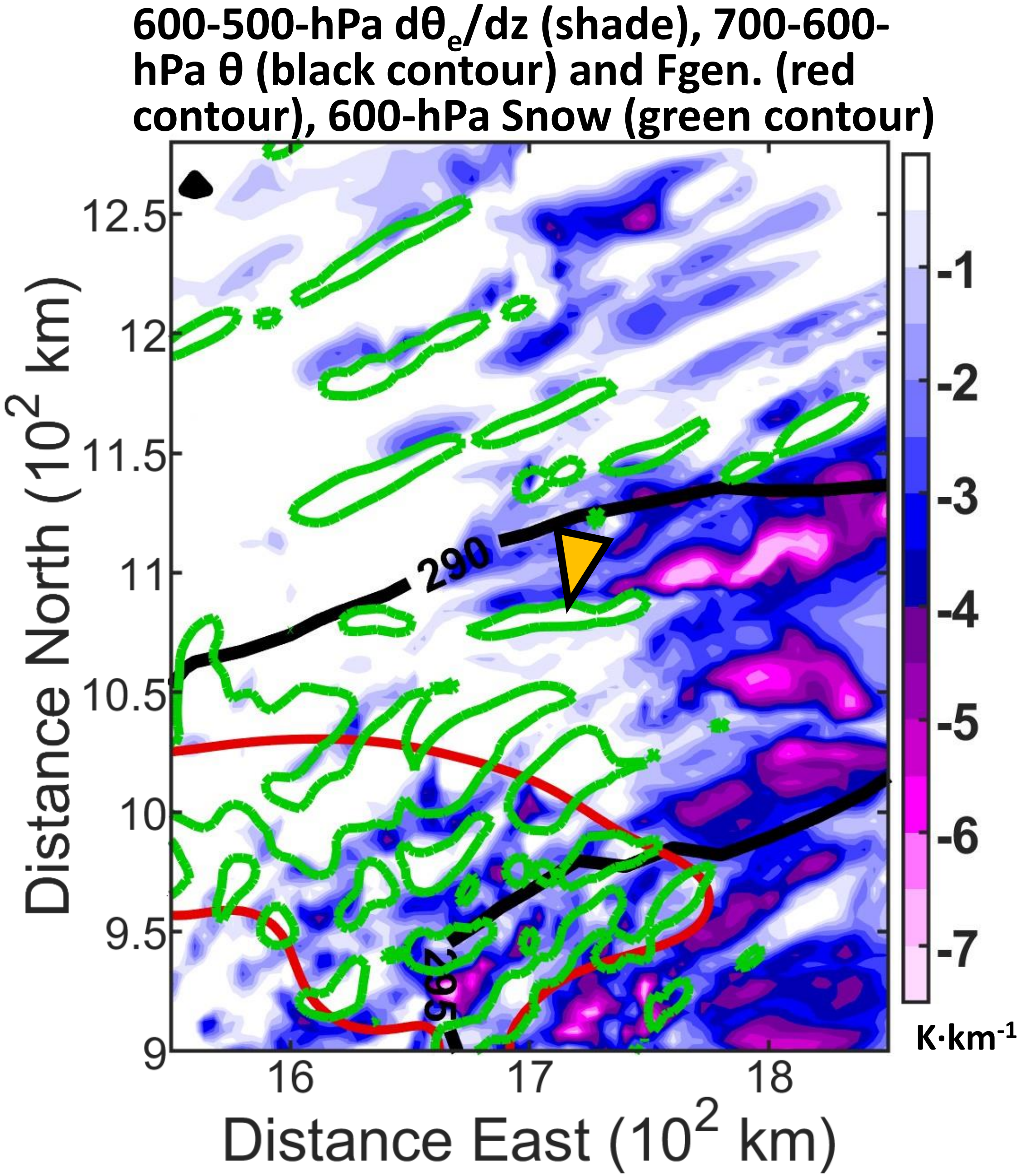

600-500-hPa dθ$_e$/dz (shade), 700-600-hPa θ (black contour) and Fgen. (red contour), 600-hPa Snow (green contour)
Distance North (10^2 km)
Distance East (10^2 km)
12.5
12
11.5
11
10.5
10
9.5
9
16
17
18
290
295
-1
-2
-3
-4
-5
-6
-7
K·km^{-1}

129 h 30 min

600-500-hPa Vertical Shear (shade and vectors), 600-hPa Snow (grey contour)

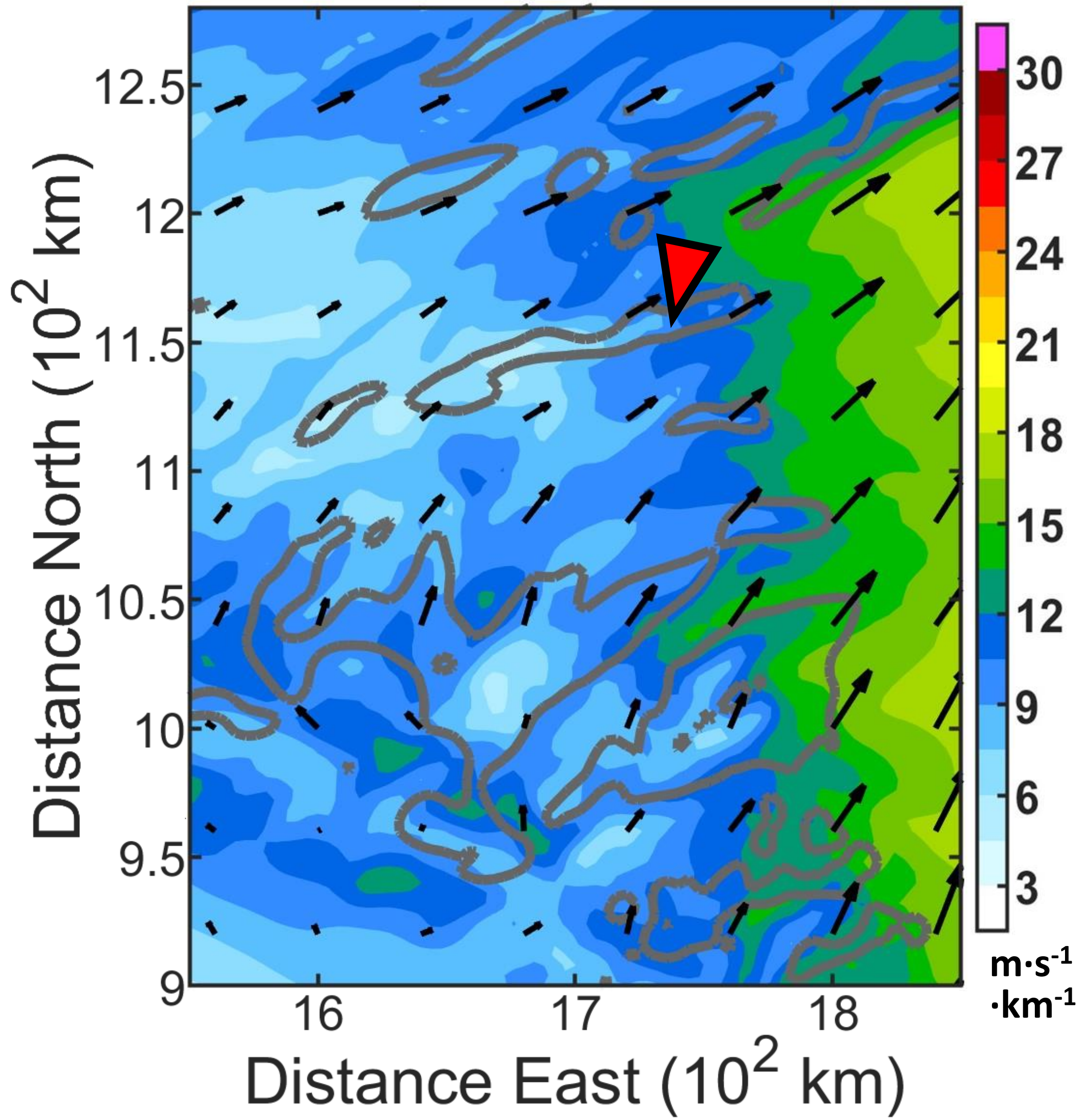

600-500-hPa dθ_e/dz (shade), 700-600-hPa θ (black contour) and Fgen. (red contour), 600-hPa Snow (green contour)

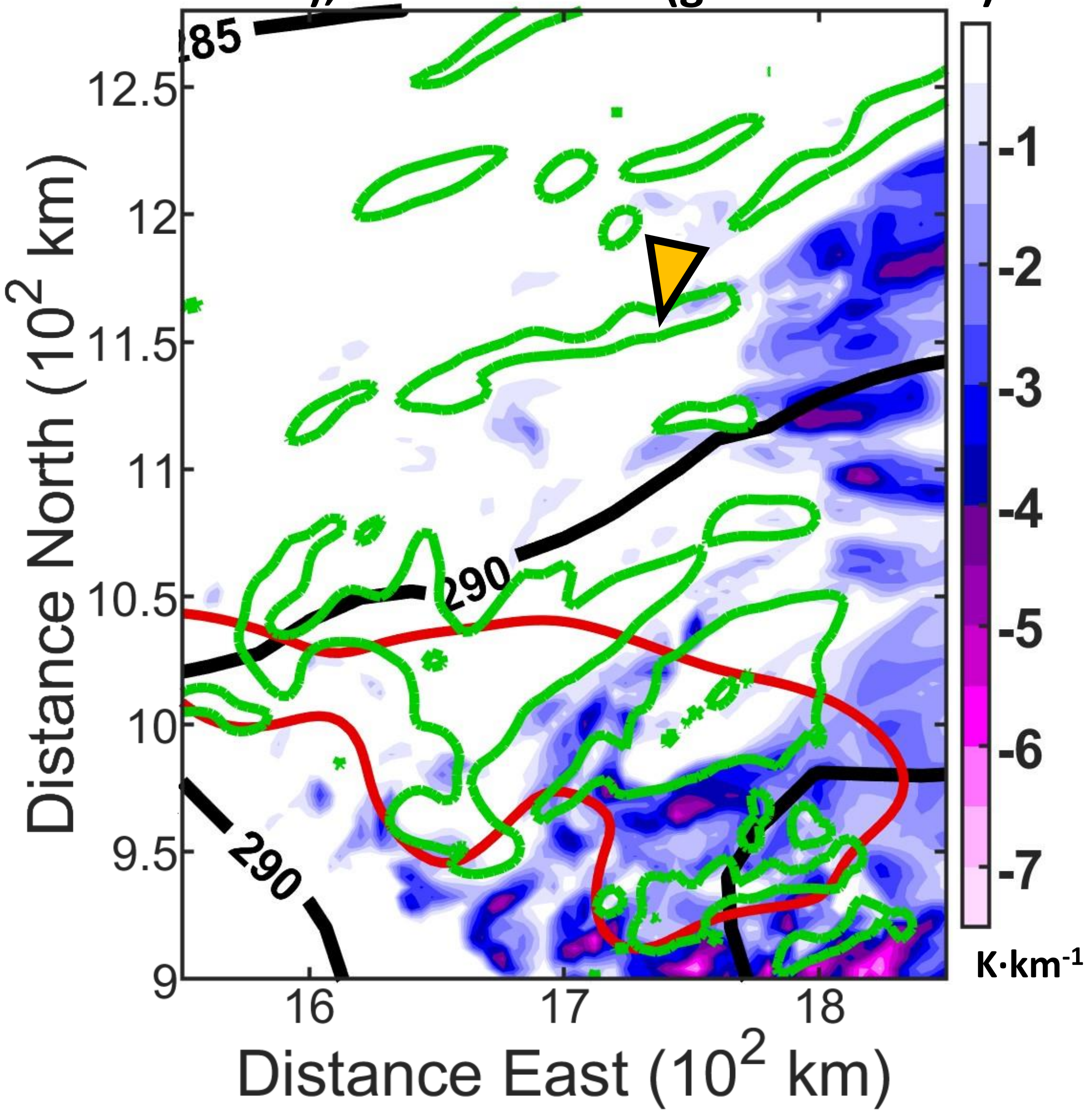

131 h 00 min

600-500-hPa Vertical Shear (shade and vectors), 600-hPa Snow (grey contour)

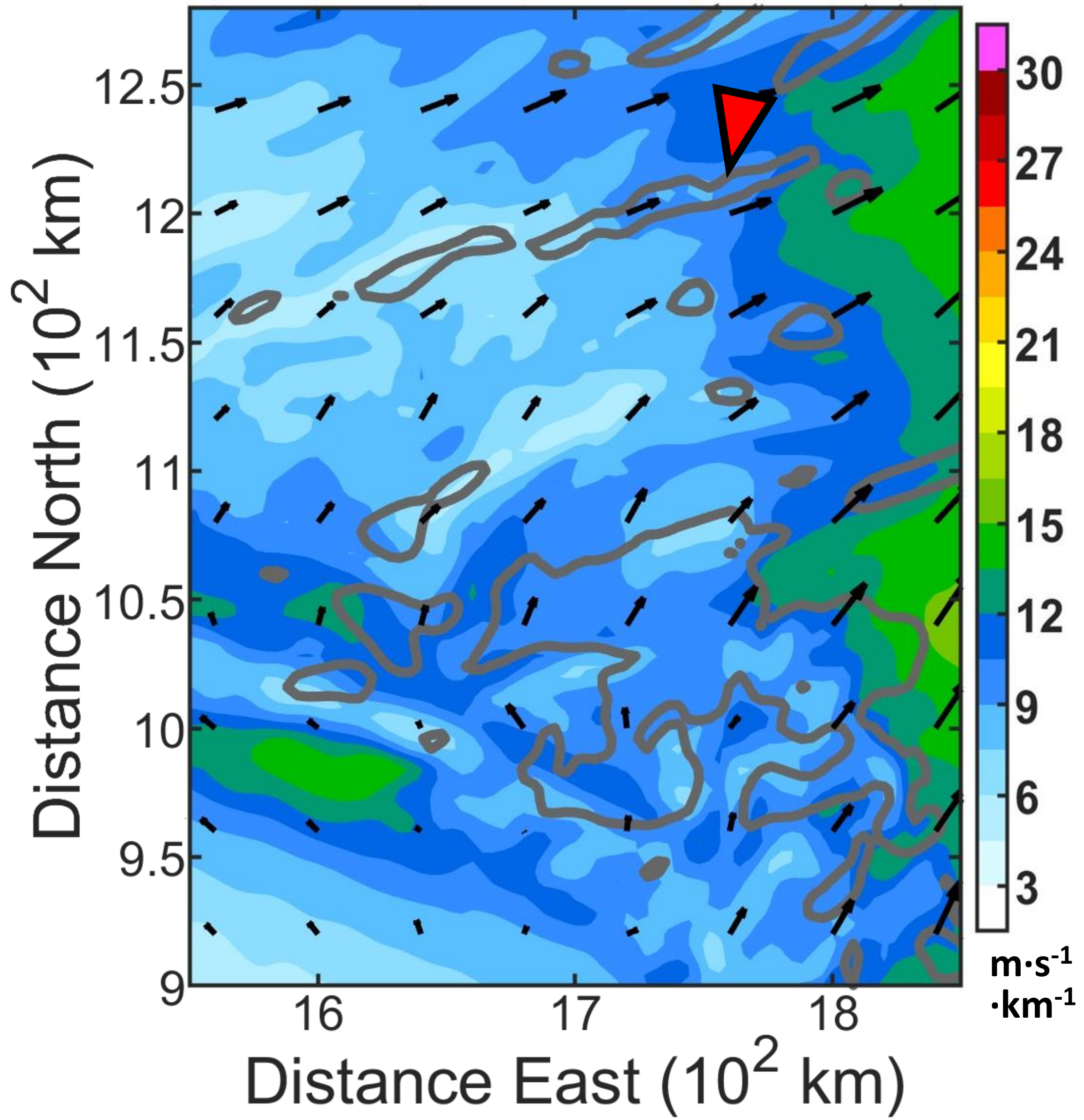

600-500-hPa $d\theta_e/dz$ (shade), 700-600-hPa θ (black contour) and Fgen. (red contour), 600-hPa Snow (green contour)

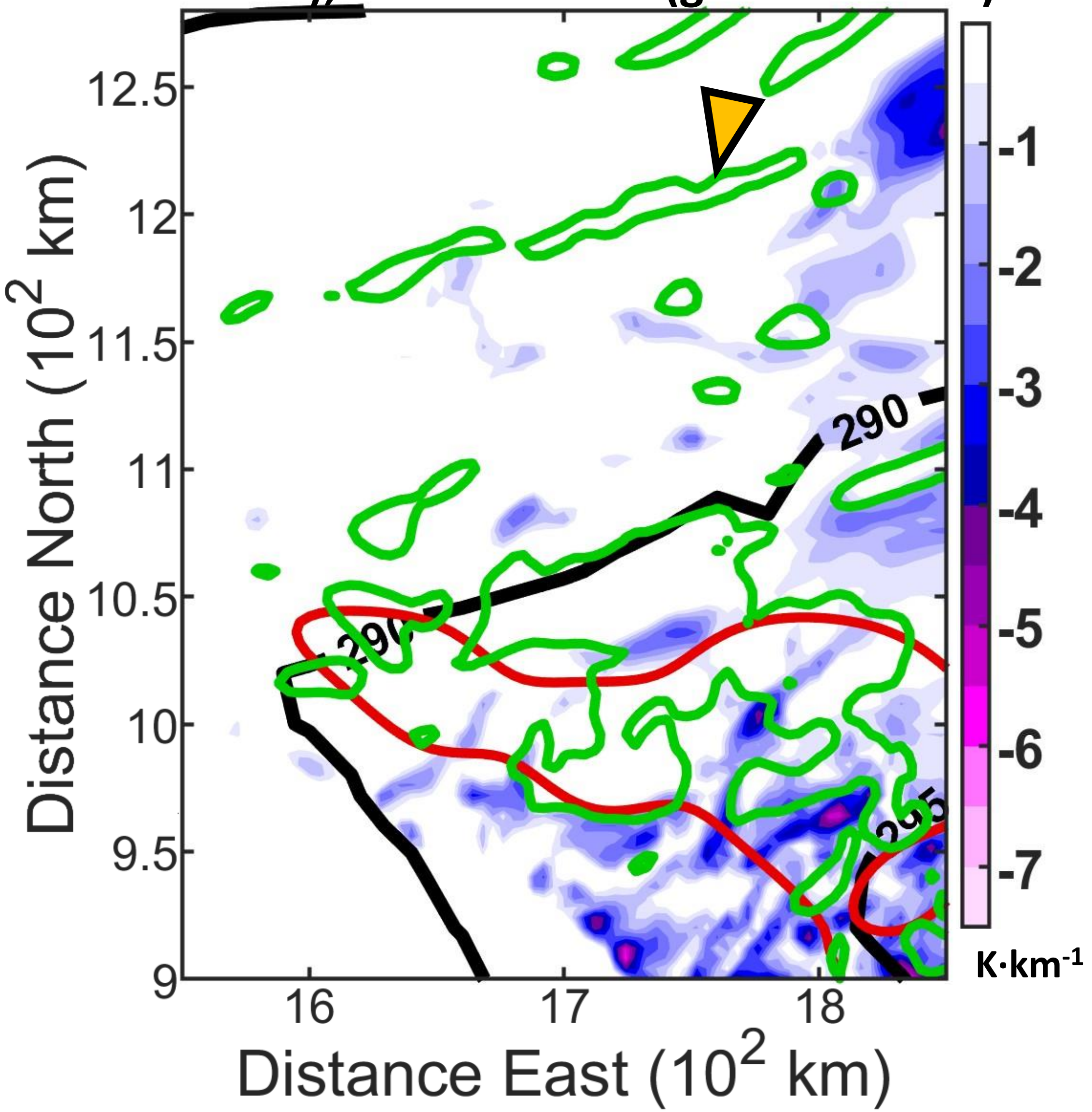

131 h 00 min

600-500-hPa Vertical Shear (shade and vectors), 600-hPa Snow (grey contour)

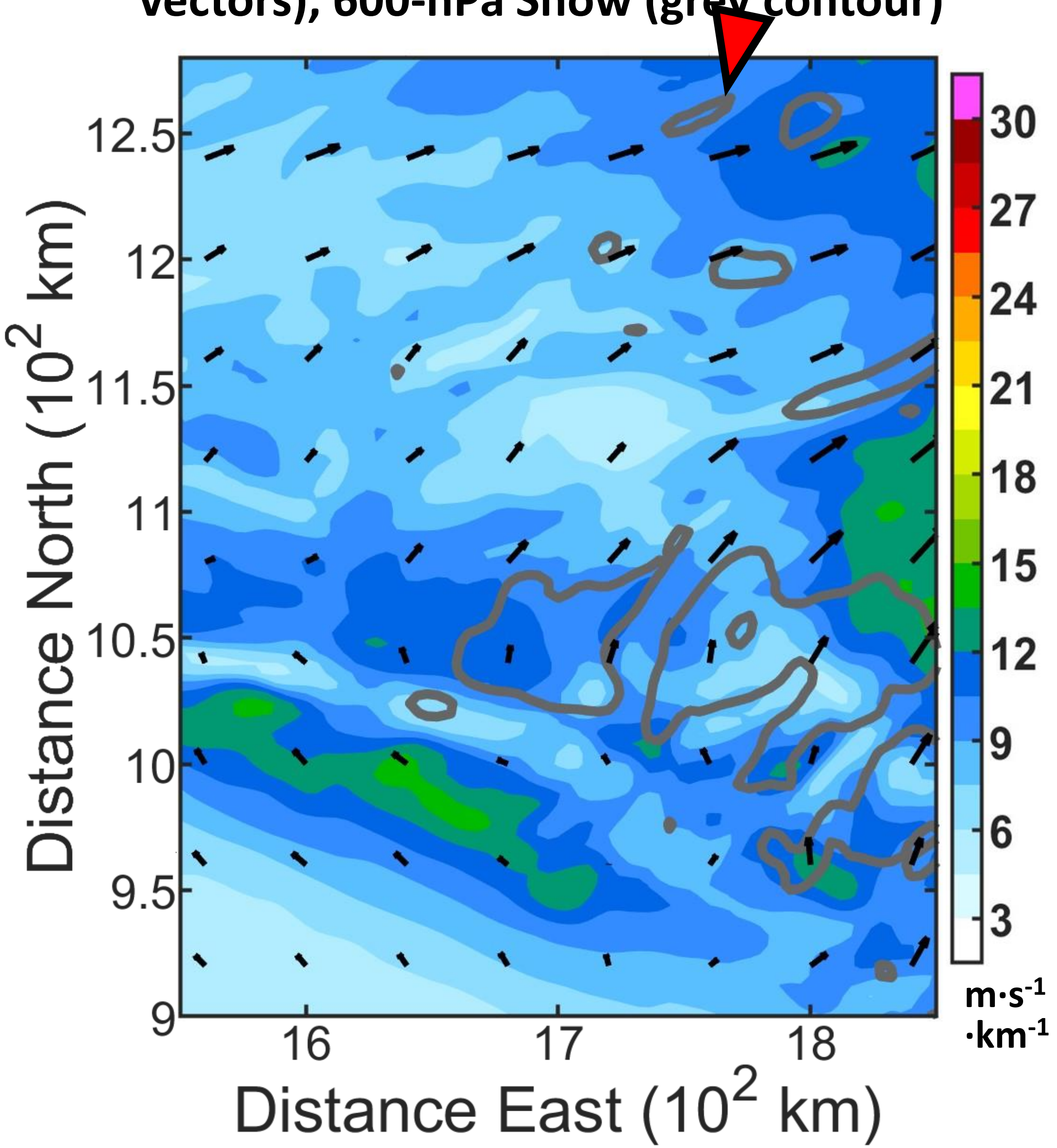

600-500-hPa dθe/dz (shade), 700-600-hPa θ (black contour) and Fgen. (red contour), 600-hPa Snow (green contour)

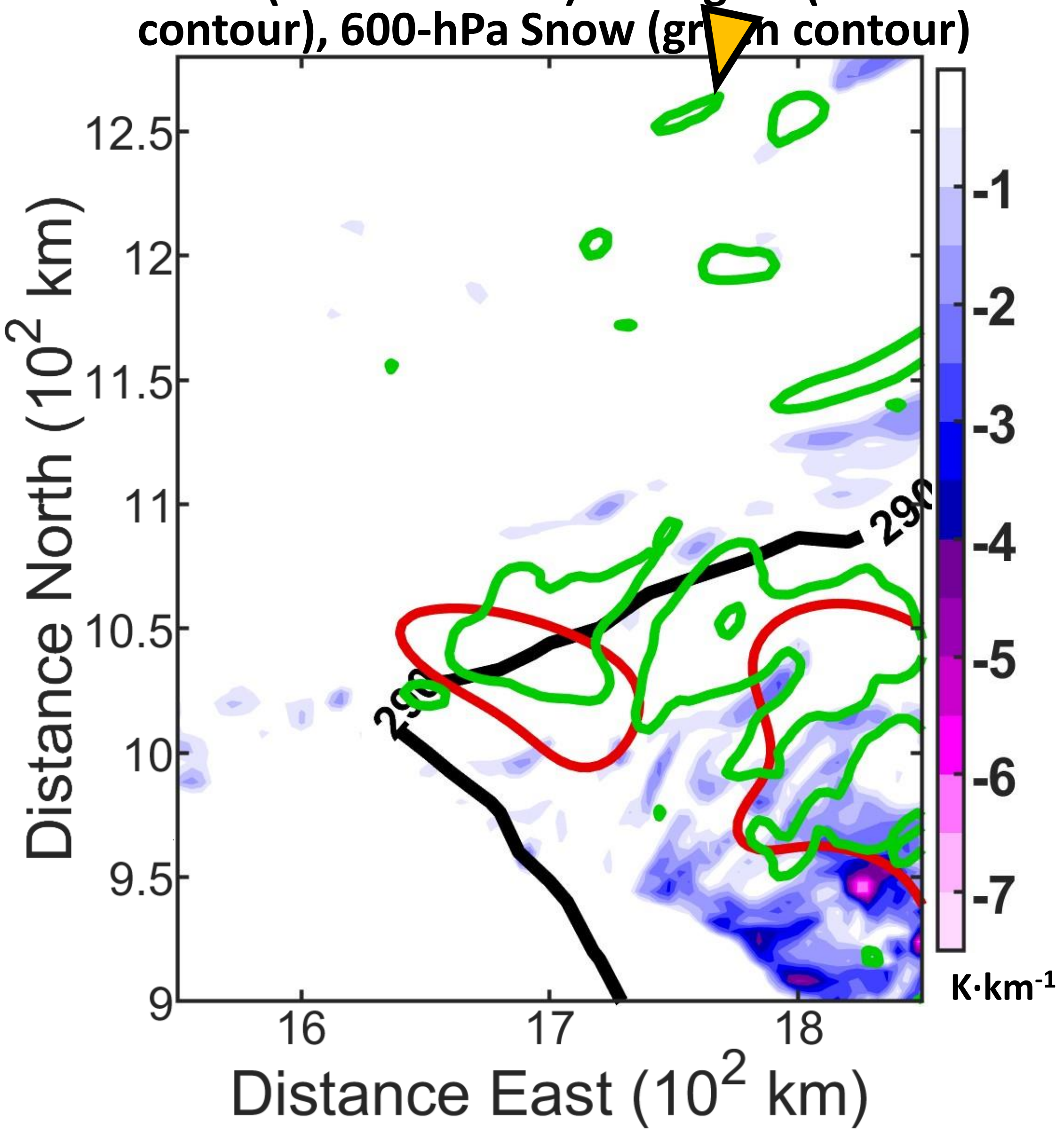

- **PV equation**: $PV = \frac{1}{\rho}\overrightarrow{\boldsymbol{\omega_a}} \cdot \nabla\theta = \frac{1}{\rho}\left(\left(\frac{\partial w}{\partial y} - \frac{\partial v}{\partial z}\right)\frac{\partial \theta}{\partial x} + \left(\frac{\partial u}{\partial z} - \frac{\partial w}{\partial x}\right)\frac{\partial \theta}{\partial y} + \left(\frac{\partial v}{\partial x} - \frac{\partial u}{\partial y} + f\right)\frac{\partial \theta}{\partial z}\right)$
- **PV tendency**: $\frac{\partial PV}{\partial t} + \vec{\boldsymbol{V}} \cdot \nabla PV - \frac{1}{\rho}\overrightarrow{\boldsymbol{\omega_a}} \cdot \nabla\dot{\theta} = resid.$
- **Diabatic Term**: $\frac{1}{\rho}\overrightarrow{\boldsymbol{\omega_a}} \cdot \nabla\dot{\boldsymbol{\theta}} = \frac{1}{\rho}\left(\left(\frac{\partial w}{\partial y} - \frac{\partial v}{\partial z}\right)\frac{\partial \dot{\boldsymbol{\theta}}}{\partial \boldsymbol{x}} + \left(\frac{\partial u}{\partial z} - \frac{\partial w}{\partial x}\right)\frac{\partial \dot{\boldsymbol{\theta}}}{\partial \boldsymbol{y}} + \left(\frac{\partial v}{\partial x} - \frac{\partial u}{\partial y} + f\right)\frac{\partial \dot{\boldsymbol{\theta}}}{\partial \boldsymbol{z}}\right)$

  where $\vec{\boldsymbol{V}}$ is the 3D wind, $\overrightarrow{\boldsymbol{\omega_a}}$ is the 3D absolute vorticity, and $\dot{\boldsymbol{\theta}}$ is the diabatic heating rate.
- Derivatives are approximated with CFD, using 2-minute output.
- **Next 4 slides**:
  - Left: 600-500-hPa $\partial PV/\partial t$ (shade) and PV (black contour > 0 PVU, grey dash < 0 PVU), and 600-hPa snow mixing ratio (green contour; $g{\cdot}kg^{-1}$).
  - Middle: 600-500-hPa PV advection (shade), PV, and wind vectors.
  - Right: 600-500-hPa diabatic term (shade), PV, and diabatic heating rate (dark green contour>0, light green dash<0; 10^{-3} $K{\cdot}s^{-1}$).

127 h 00 min

600-500-hPa ∂PV/∂t (shade), PV (black contour>0; grey dash<0), 600-hPa Snow (green contour)

600-500-hPa PV Adv. (shade), PV (black contour>0; grey dash<0), Wind Vectors

600-500-hPa Diab. Term. (shade), PV (black contour>0; grey dash<0), Diab. Heat Rate (green contour>0; green dash<0)

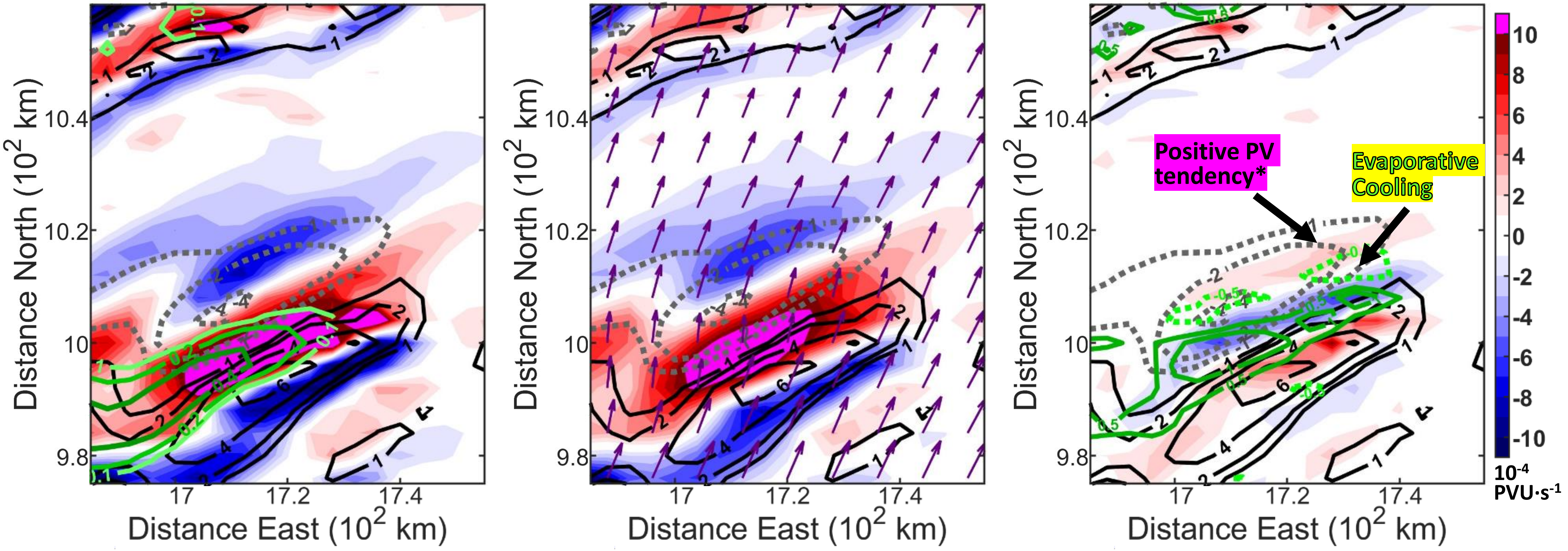

PV<0 (PVU)
PV>0 (PVU)

$$* \frac{\partial \dot{\theta}}{\partial y} > 0; \ \frac{\partial u}{\partial z} > 0 \Rightarrow \frac{1}{\rho}\overrightarrow{\boldsymbol{\omega_a}} \cdot \nabla\dot{\theta} = \frac{1}{\rho}\left(\left(\frac{\partial w}{\partial y} - \frac{\partial v}{\partial z}\right)\frac{\partial \dot{\theta}}{\partial x} + \left(\frac{\partial u}{\partial z} - \frac{\partial w}{\partial x}\right)\frac{\partial \dot{\theta}}{\partial y} + \left(\frac{\partial v}{\partial x} - \frac{\partial u}{\partial y} + f\right)\frac{\partial \dot{\theta}}{\partial z}\right) > 0$$

127 h 10 min

600-500-hPa ∂PV/∂t (shade), PV (black contour>0; grey dash<0), 600-hPa Snow (green contour)

600-500-hPa PV Adv. (shade), PV (black contour>0; grey dash<0), Wind Vectors

600-500-hPa Diab. Term. (shade), PV (black contour>0; grey dash<0), Diab. Heat Rate (green contour>0; green dash<0)

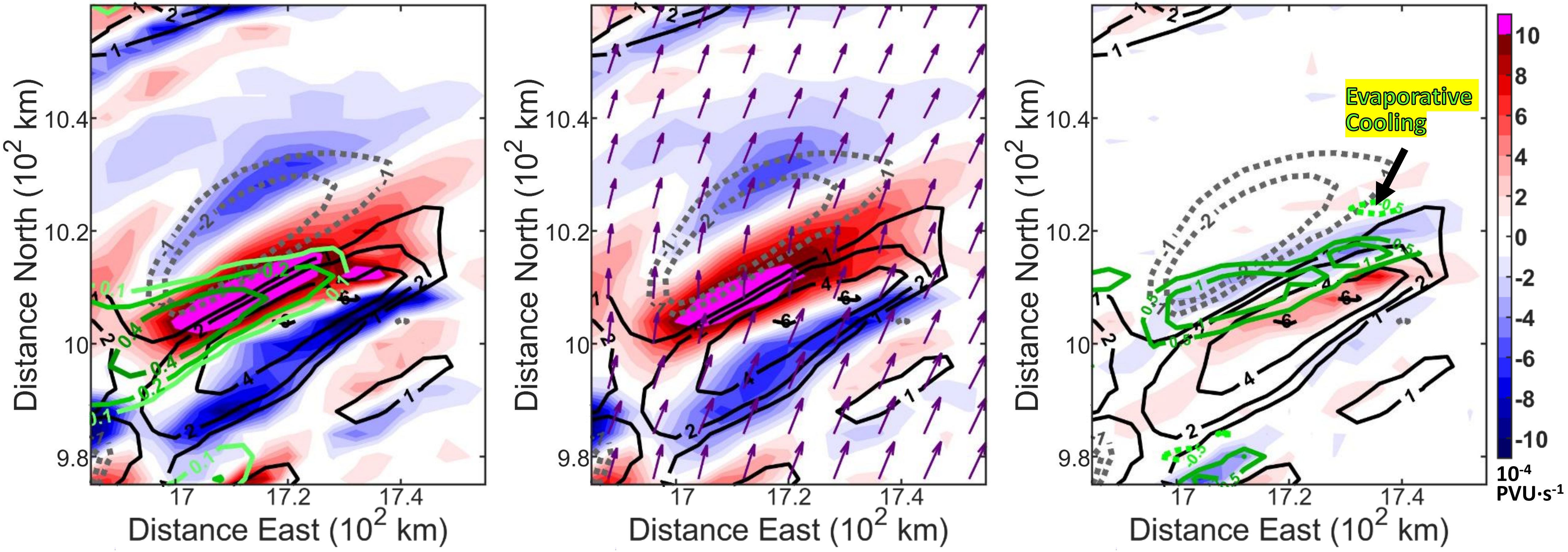

PV<0 (PVU)
PV>0 (PVU)

- While the diabatic cooling weakens, it has a cumulative impact on the temperature field, increasing the cold anomaly and thus the northward temperature gradient (and PV).

127 h 20 min

600-500-hPa ∂PV/∂t (shade), PV (black contour>0; grey dash<0), 600-hPa Snow (green contour)

600-500-hPa PV Adv. (shade), PV (black contour>0; grey dash<0), Wind Vectors

600-500-hPa Diab. Term. (shade), PV (black contour>0; grey dash<0), Diab. Heat Rate (green contour>0; green dash<0)

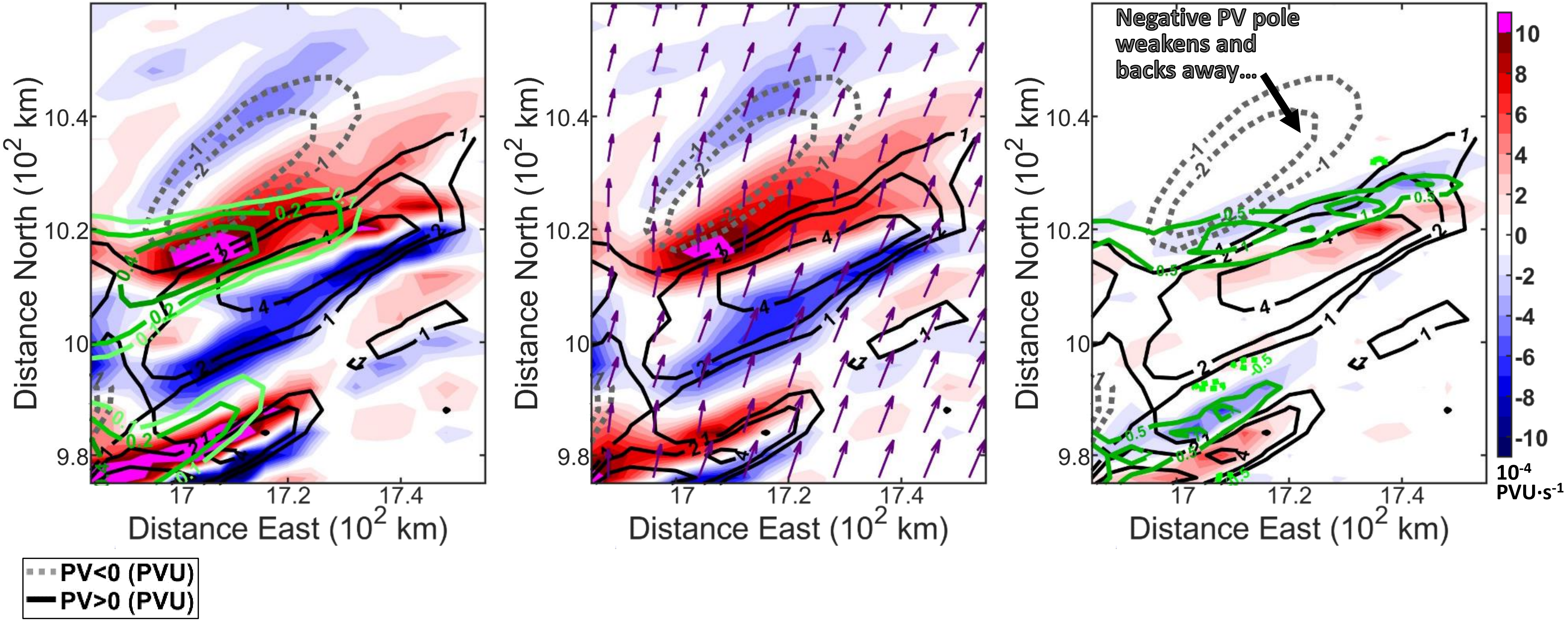

127 h 30 min

600-500-hPa ∂PV/∂t (shade), PV (black contour>0; grey dash<0), 600-hPa Snow (green contour)

600-500-hPa PV Adv. (shade), PV (black contour>0; grey dash<0), Wind Vectors

600-500-hPa Diab. Term. (shade), PV (black contour>0; grey dash<0), Diab. Heat Rate (green contour>0; green dash<0)

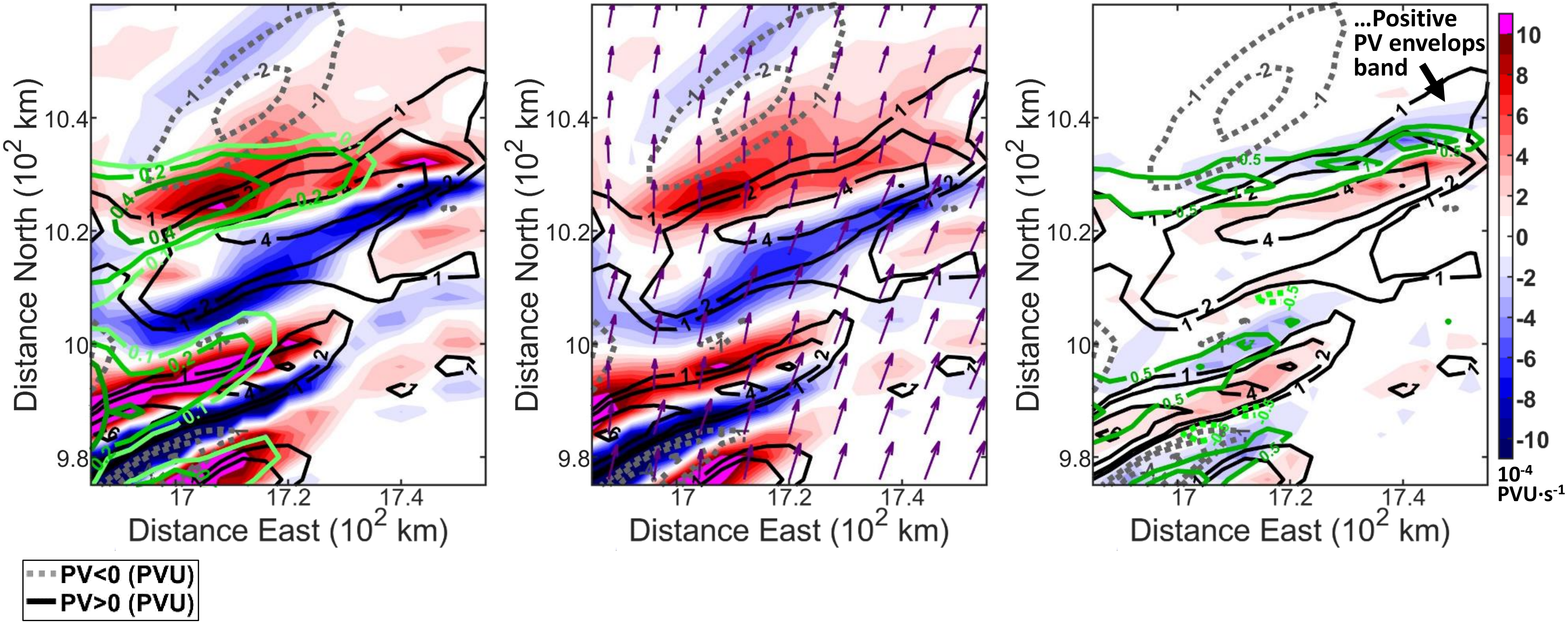

127 h 00 min

600-500-hPa Ice Mixing Ratio (shade), Diab. Heat Rate (blue contour>0; blue dash<0)

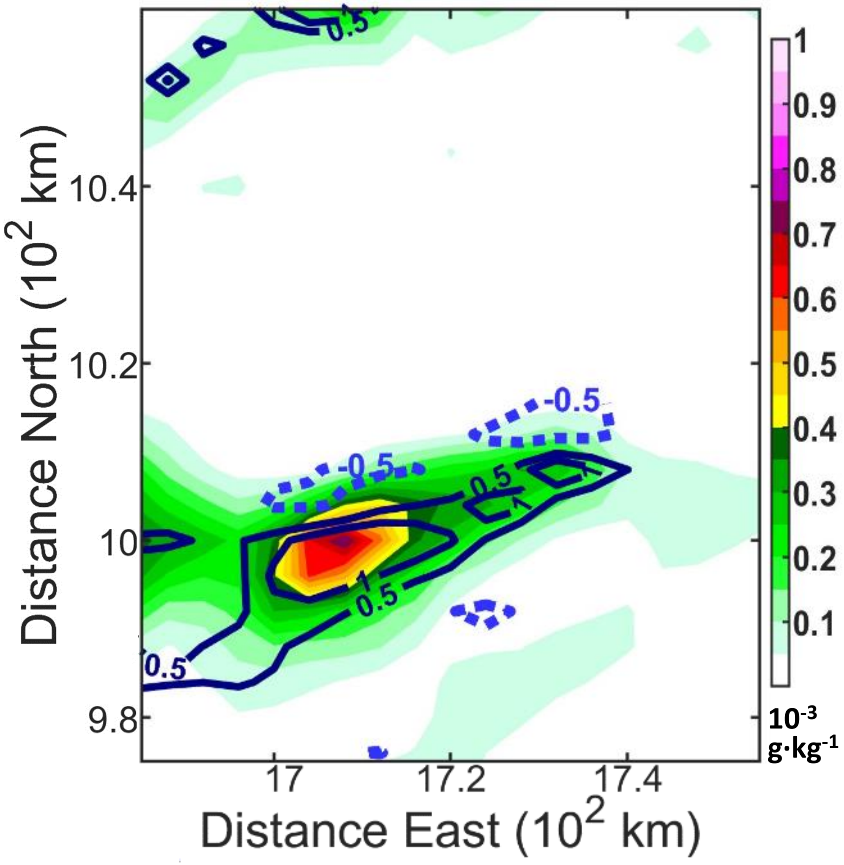

600-500-hPa Cloud Mixing Ratio (shade), Diab. Heat Rate (blue contour>0; blue dash<0)

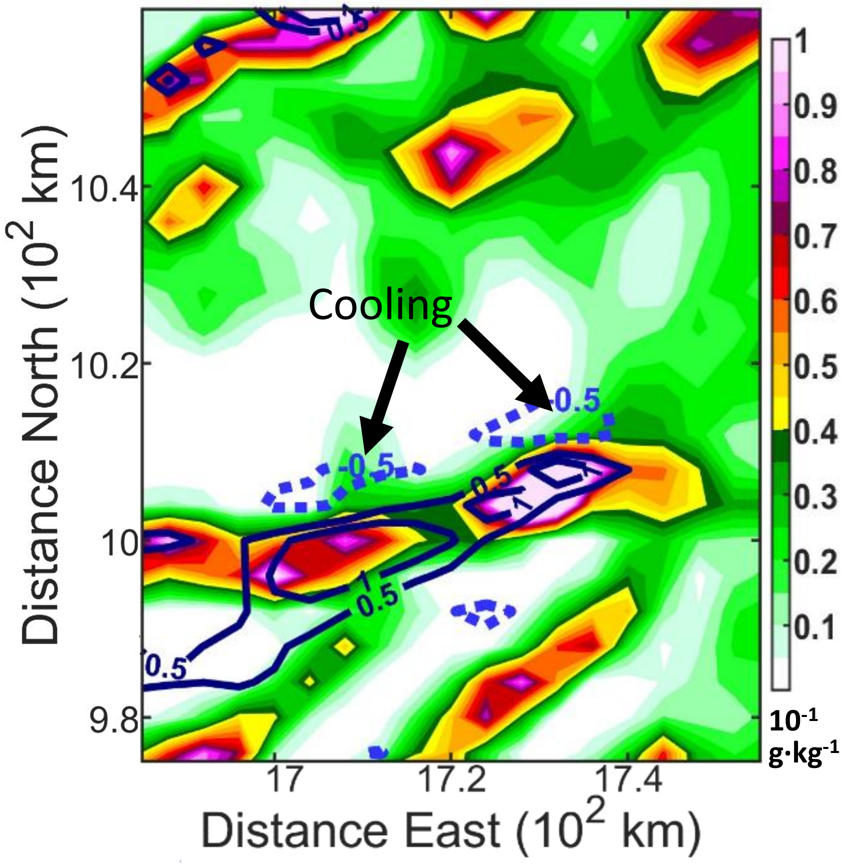

600-500-hPa RH W.R.T. Ice (shade), Diab. Heat Rate (blue contour>0; blue dash<0)

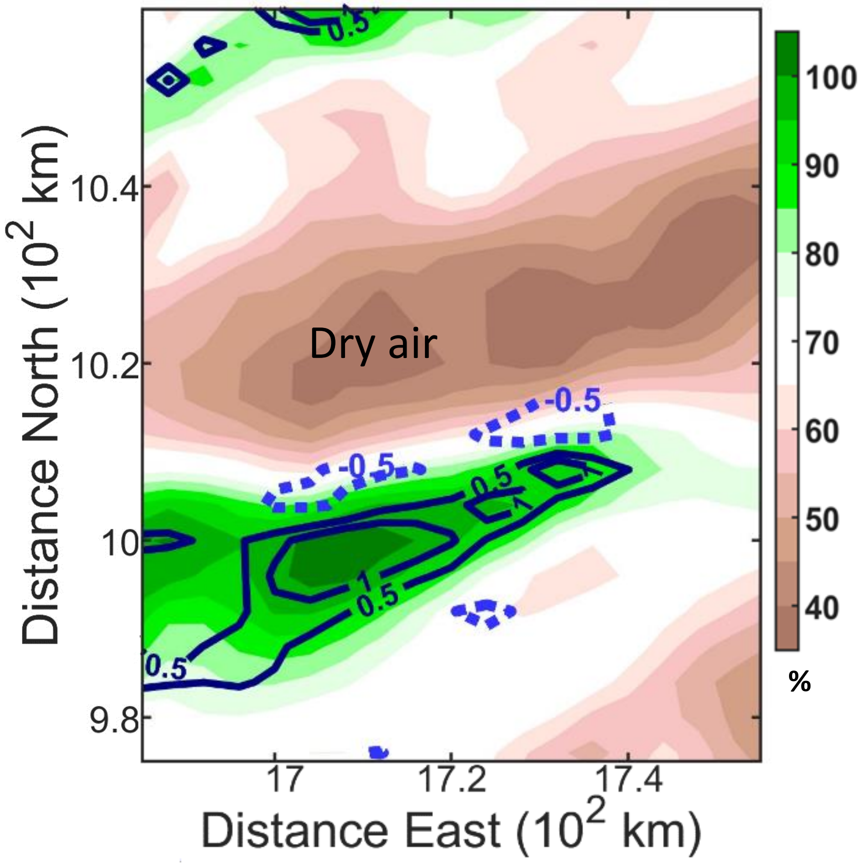

- Region of cooling on outer fringes of band, within QCLOUD and QICE extending into the subsaturated air.

127 h 00 min

600-500-hPa Vert. Abs. Vort. (ζ_z; shade), PV (black contour>0; grey dash<0)

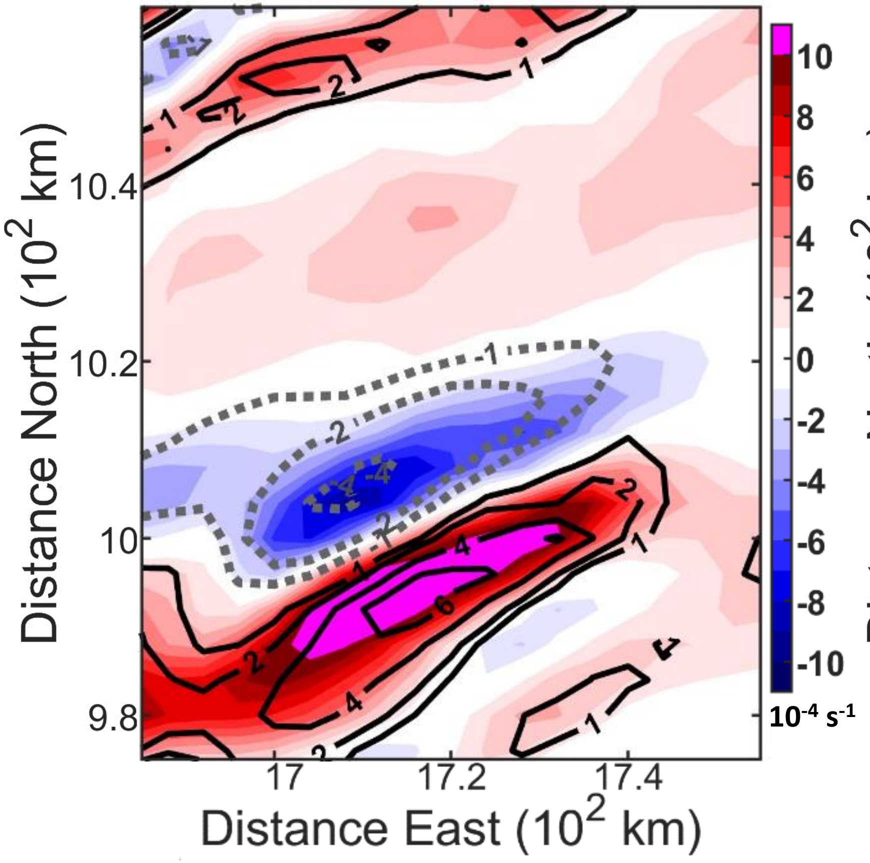

600-500-hPa W-wind (shade), PV (black contour>0; grey dash<0)

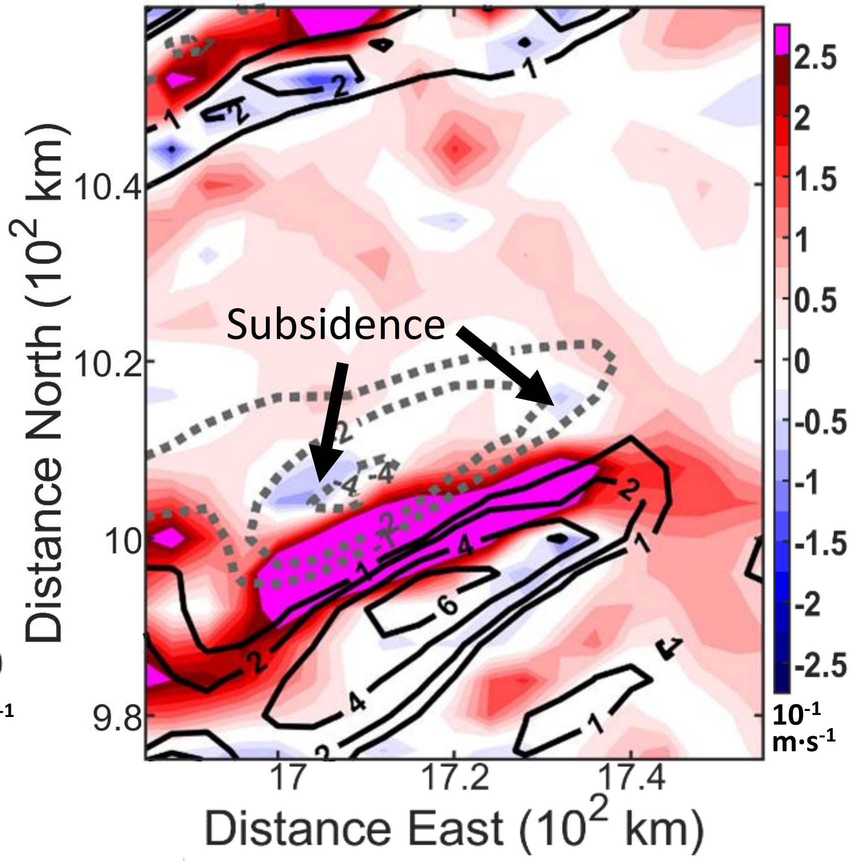

600-500-hPa θ Anom. (shade), PV (black contour>0; grey dash<0), θ (green contour), Shear Vectors

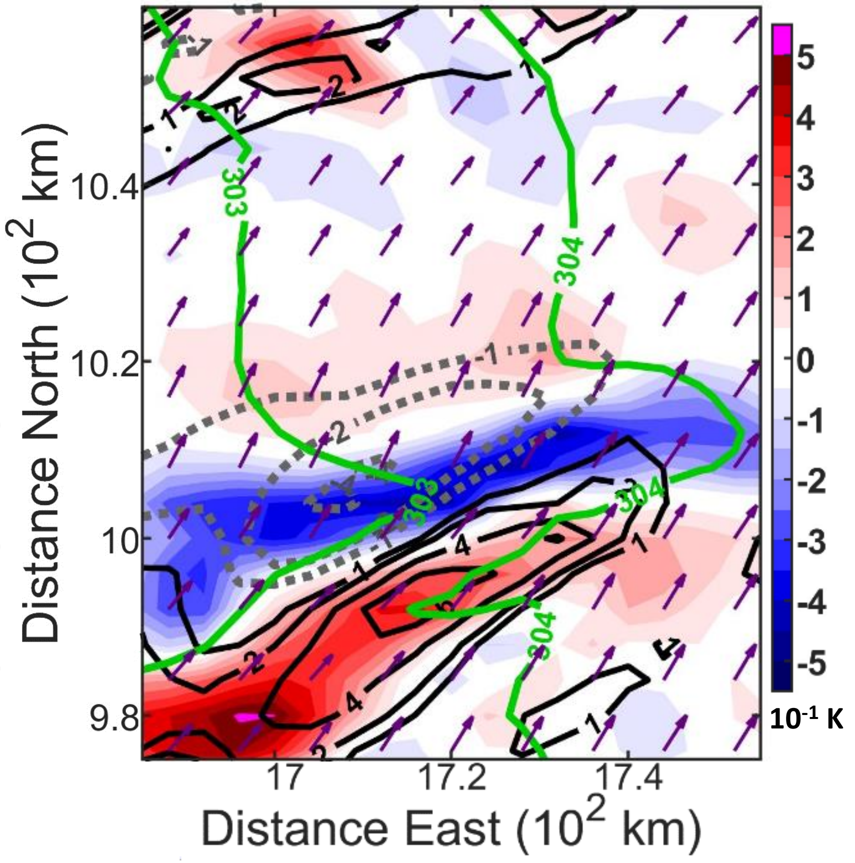

PV<0 (PVU)
PV>0 (PVU)

- Subsidence within cold air anomaly.

127 h 30 min

600-500-hPa Vert. Abs. Vort. (ζ_z; shade), PV (black contour>0; grey dash<0)

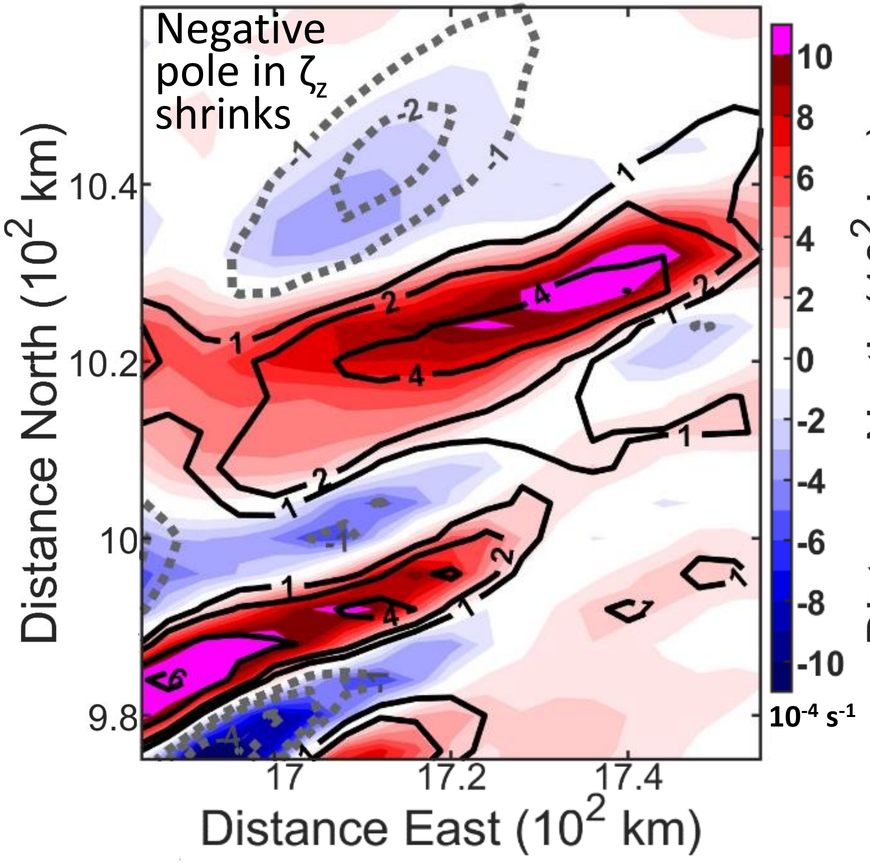

600-500-hPa W-wind (shade), PV (black contour>0; grey dash<0)

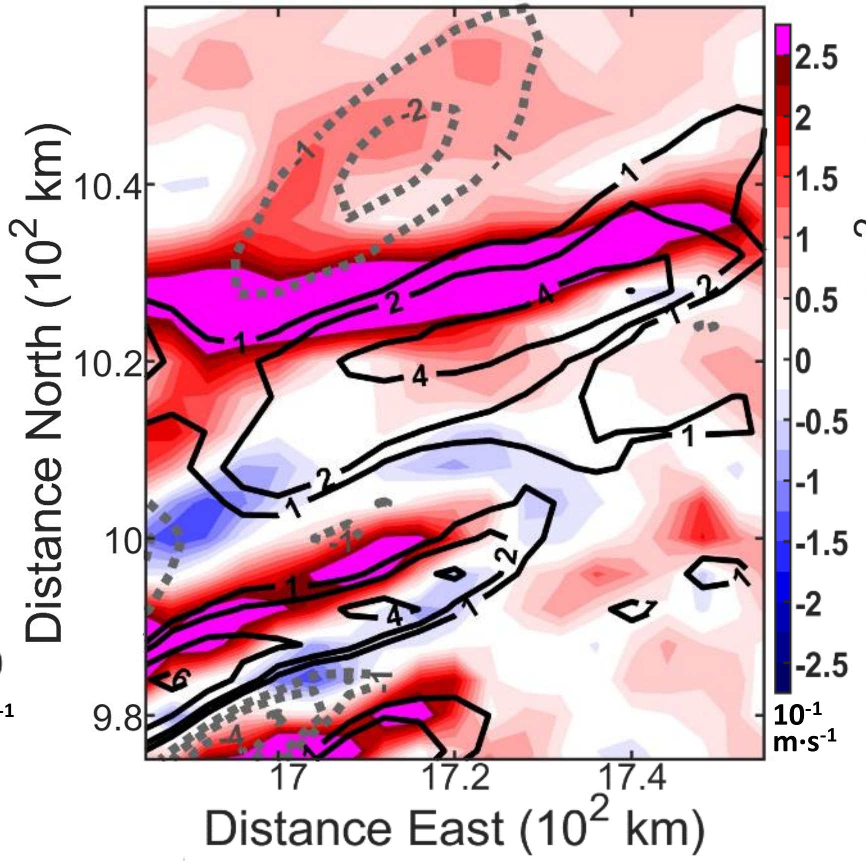

600-500-hPa θ Anom. (shade), PV (black contour>0; grey dash<0), θ (green contour), Shear Vectors

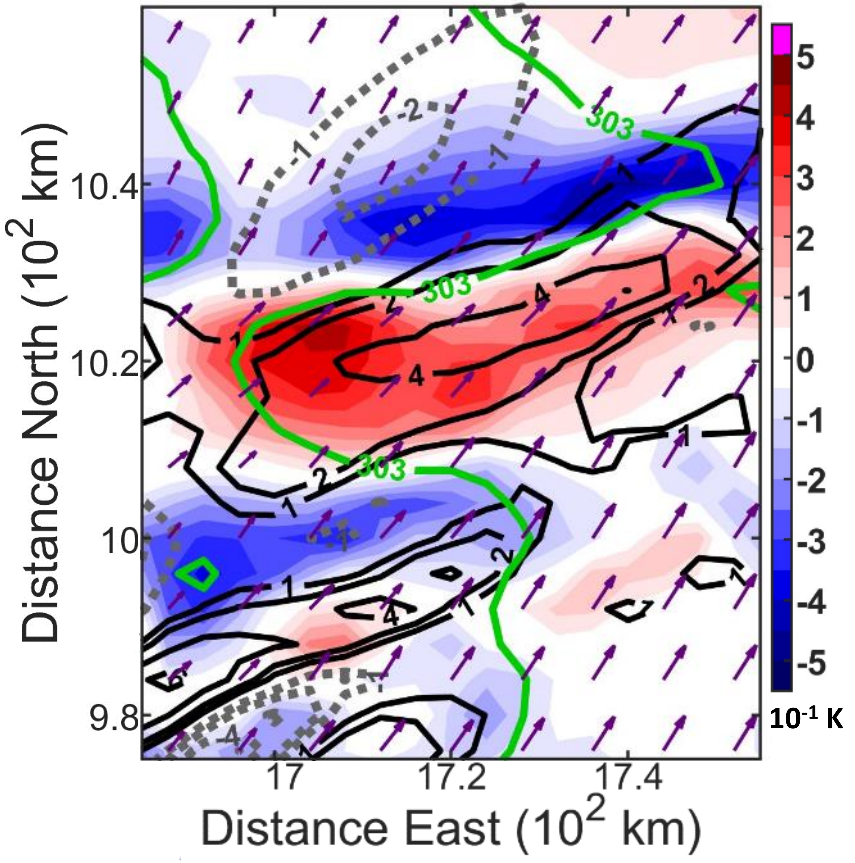

PV<0 (PVU)
PV>0 (PVU)

- Cold subsidence redistributes horizontal absolute vorticity into the vertical in a dipole opposite of the one created by latent heating and ascent-> cancels-out the negative absolute vorticity.